

This document was produced
by scanning the original publication.

Ce document est le produit d'une
numérisation par balayage
de la publication originale.

LATE QUATERNARY CLIMATIC RECONSTRUCTION
USING THE DEEP-WATER CORAL
Desmophyllum cristigalli

BY

JODIE ELLEN SMITH

OF 2950

L I C E N C E T O M c M A S T E R U N I V E R S I T Y

This thesis has been written
[Thesis, Project Report, etc.]

by Jodie Ellen Smith for
[Full Name(s)]

Undergraduate course number 4K06 at McMaster
University under the supervision/direction of Dr. M.J. Risk.

In the interest of furthering teaching and research, I/we
hereby grant to McMaster University:

1. The ownership of _____ copy(ies) of this work;
2. A non-exclusive licence to make copies of this work, (or any part thereof) the copyright of which is vested in me/us, for the full term of the copyright, or for so long as may be legally permitted. Such copies shall only be made in response to a written request from the Library or any University or similar institution.

I/we further acknowledge that this work (or a surrogate copy thereof) may be consulted without restriction by any interested person.

M. Risk
Signature of Witness,
Supervisor

Jodie Smith
Signature of Student

June 14/93
date

(This Licence to be bound with the work)

LATE QUATERNARY CLIMATIC RECONSTRUCTION
USING THE DEEP-WATER CORAL
Desmophyllum cristigalli

LATE QUATERNARY CLIMATIC RECONSTRUCTION
USING THE DEEP-WATER CORAL
Desmophyllum cristigalli

by
Jodie Ellen Smith

A thesis
Submitted to the Department of Geology
in Partial Fulfillment of the Requirements for the
Degree Honours Bachelor of Science

McMaster University

May, 1993

BACHELOR OF SCIENCE (HONOURS), 1991 McMaster University,
(Geography and Geology) Hamilton, Ontario.

TITLE: Late Quaternary Climatic Reconstruction
 Using the Deep-Water Coral
 Desmophyllum cristigalli

AUTHOR: Jodie Ellen Smith

SUPERVISOR: Dr. M.J. Risk

NUMBER OF PAGES: xi, 100

Abstract

In 1978, the Bedford Institute of Oceanography dredged dead specimens of the solitary, deep-water, ahermatypic coral *Desmophyllum cristigalli* from the top of Orphan Knoll, at a depth of 1700 m. The collection lay unstudied until last year. Dating of several individuals by uranium - thorium and ^{14}C shows that the retrieved corals ranged in age from 70,000 to 4,000 y BP. One especially large specimen lived from 12,000 to 11,000 y BP. Detailed analysis of the $\delta^{18}\text{O}$ stratigraphy of this long-lived coral shows that the Younger Dryas climatic event is preserved as an abrupt shift of >2 per mil, which suggests a profound change in the saline circulation. It also supports the theory that massive ocean-atmosphere reorganizations trigger glacial cycles - specifically, in the North Atlantic, via the shutdown of the Gulf Stream 'heat conveyor'. Estimations of coral-growth rates give a good indication of the rapidity of the Younger Dryas onset: it is possible that the transition from interglacial to glacial conditions may have occurred with 15 years. Many climatic reconstructions to date have been based on the foraminiferal record, but solitary corals are likely to be far superior recorders of paleoenvironmental conditions because of their immunity to bioturbation and large-scale transport.

Acknowledgements

I would like to thank Cherylyn Heikoop for the U-Th dates, and Martin Knyf for help in the isotope lab. The work benefited from discussions with Henry Schwarcz of McMaster, and Peta Mudie and Shelley Thibaudeau of BIO. I would like to thank Barbara Hecker for supplying the modern coral sample, as well as Page Valentine and Victor Plichota for photographs. The work was supported by an EMR Research Subvention and NSERC supplemental funds awarded to MJR, with additional funds from MJR's NSERC operating grant. Further support was provided by an NSERC summer undergraduate award to JES. Alan Ruffman never gave up his belief that these corals had a story to tell, and to him belongs much of the credit for that story coming to light. Leaving the best to last, I would like to thank Mike Risk, with whom life is better.

Table of Contents

Half-title Page	i
Title Page	ii
Information Page	iii
Abstract	iv
Acknowledgements	v
Table of Contents	vi
List of Figures	viii
List of Plates	x
List of Tables	xi
Chapter 1: Introduction	
1.1 Milankovitch Cycles and Late Quaternary Climate Changes	1
1.1.1 Milankovitch's Hypothesis	1
1.1.2 Oceanic Influences	1
1.1.3 The Younger Dryas Event	6
1.2 Corals as Environmental Indicators	13
1.3 Orphan Knoll	16
1.4 Deep-Water Coral	25
1.4.1 Overview	37
1.4.2 <i>Desmophyllum cristigalli</i>	37
1.4.3 Results of Previous Work	41
1.5 Hypothesis	46
	48
Chapter 2: Methods	
2.1 Preparation	52
2.2 U/Th Dating	52
2.3 Stable-Isotope Analyses	54
	56
Chapter 3: Results and Discussion	
3.1 Dates	59
3.2 Oxygen Isotopes	59
3.3 Carbon Isotopes	62
3.4 Comparison to the Foraminiferal Record	67
	72

Chapter 4: Conclusions	75
Appendix 1: Results of Previous Studies	77
Appendix 2: Results of This Study	
a. Dates	84
b. Isotope Data	85
References	87
	96

List of Figures

1.1-1	Climate during a full glacial cycle for the midlatitudes	1
1.1-2	Eccentricity	2
1.1-3	Precession	3
1.1-4	Tilt	3
1.1-5	Amplitude history in the $\delta^{18}\text{O}$ record	4
1.1-6	Correlation of summer-insolation curve with ocean surface temperature	5
1.1-7	The distribution of ice sheets during the last glacial maximum	7
1.1-8	Comparison of climate records and summer insolation curves	8
1.1-9	Surface currents of the North Atlantic Ocean	9
1.1-10	North-south cross section of subsurface circulation of the Atlantic	10
1.1-11	The distribution of surface water temperature for two modes of circulation	12
1.1-12	European pollen record from the end of the last glacial period	13
1.1-13	Map showing Laurentide ice sheet and routing of overflow	14
1.1-14	Timing of ocean-atmosphere reorganization events	15
1.2-1	X-radiograph positive of a coral sample	16
1.2-2	Plot of linear vertical growth as a function of depth	17
1.2-3	Fluctuations in the Barbados coral-isotope record with time	18
1.2-4	$\delta^{18}\text{O}$ values for <i>Acropora</i> plotted against water temperature	19
1.2-5	Temperature records derived from oxygen isotopes	19
1.2-6	$\delta^{13}\text{C}$ distributions with age in a Bermuda brain coral	20
1.2-7	Comparison between the rainfall record and $\delta^{18}\text{O}$ shifts in coral	21
1.2-8	Fluorescent banding on a length of coral core	22
1.2-9	Interval from Niue core	23
1.3-1	Map of the area around Orphan Knoll	25
1.3-2	Bathymetry of Orphan Knoll in corrected metres	27
1.3-3	Seismic profile and line interpretation along line G-H	28
1.3-4	Line interpretation of composite seismic profiles	29
1.3-5	Seismic profile and line interpretation along lines K-L and L-M	30
1.3-6	Distribution of mounds on top of Orphan Knoll	32
1.3-7	A reconstruction of the North Atlantic 72 million y BP	34
1.3-8	Sinking history of Orphan Knoll	35
1.4-1	Distribution of modern hermatypic and ahermatypic corals	39
1.4-2	The development of deep-water coral mounds	40
1.4-3	Principal morphological features of a solitary scleractinian coral	43
1.5-1	Simulation of the last glacial termination	49
1.5-2	Major categories of bioturbation effects	50
2.1-1	Staining procedure for identification of carbonate minerals	53
2.2-1	The radioactive decay series for ^{238}U	54
2.2-2	Relationship between $^{230}\text{Th}/^{234}\text{Th}$ and $^{234}\text{U}/^{238}\text{U}$ in closed systems	55
2.3-1	Sketch showing the first twelve sampling sites on Coral 1	56
3.1-1	Magnetic dipole and ^{14}C production over time	59
3.1-2	U/Th ages plotted against ^{14}C ages	60
3.2-1	Plot of $\delta^{18}\text{O}$ data from Corals 1, 14 and 27 versus age	62
3.2-2	Relationship between $\delta^{18}\text{O}$ of the ahermatypic skeletons and temperature	63
3.2-3	Plot of $\delta^{18}\text{O}$ versus salinity for water samples from the North Atlantic	64
3.3-1	Plot of $\delta^{13}\text{C}$ from Corals 1, 14 and 27 versus age	67

3.3-2 Correlation of carbon- and oxygen-isotopic composition	68
3.3-3 Distribution of $\delta^{13}\text{C}$ and $\delta^{18}\text{O}$ in ahermatypic scleractinian corals	69
3.3-4 Oxygen- and carbon-isotopic disequilibria in two corals	70
3.3-5 Major carbon components and their $\delta^{13}\text{C}$ ranges	71
3.4-1 Planktonic foram oxygen-isotope record	73

List of Plates

Plate 1 Large pseudocolony of <i>Desmophyllum cristigalli</i>	42
Plate 2 Two individual corallites of <i>D. cristigalli</i>	42
Plate 3 <i>D. cristigalli</i> attached to the lower surface of talus blocks	44
Plate 4 <i>D. cristigalli</i> attached to the lower surface of talus blocks	44

List of Tables

Table 1 Hudson 78-020 Rock Dredge Stations	36
Table 2 Isotope ratios of twelve sites on Coral 1	57

1 Introduction

1.1 Milankovitch Cycles and Late Quaternary Climate Changes

1.1.1 Milankovitch's Hypothesis

About two million years ago a worldwide cooling trend began, initiating the last Great Ice Age. Recent studies of deep-sea cores from the Atlantic Ocean indicate that about 20 warm-cold cycles have occurred since then. Each major cycle is roughly 100,000 years long, with numerous minor oscillations superimposed on the major trends (Figure 1.1-1).

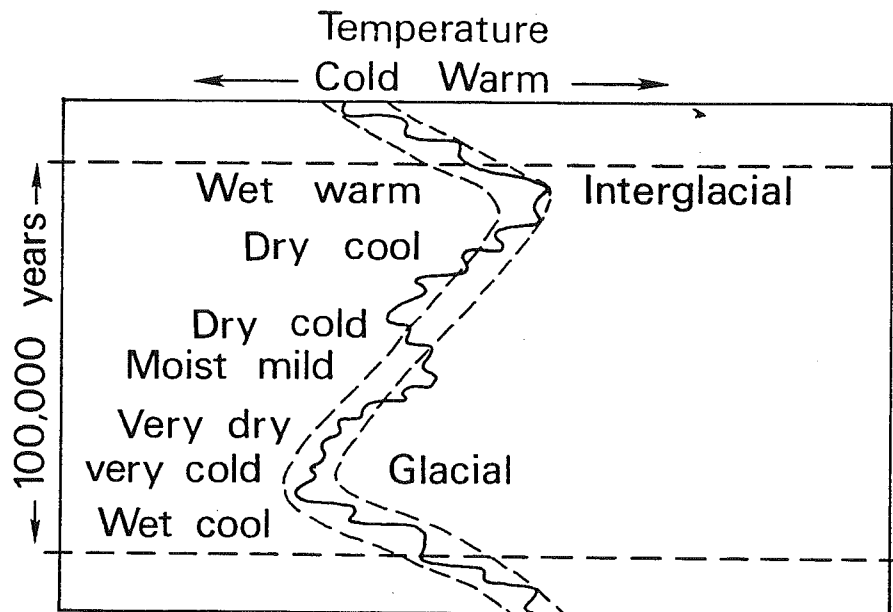


Figure 1.1-1: Climate during a full glacial cycle for the midlatitudes (from Matsch, 1976).

Several theories have been presented to explain these glacial fluctuations. Perhaps the most convincing, with a growing amount of experimental verification, is that perturbations of the orbital motions of the Earth, with concurrent changes in the incoming solar radiation (insolation), are the driving forces for Quaternary ice sheets

and climate cycles (Broecker, 1966). This theory, named the Milankovitch hypothesis after the Yugoslavian astronomer who first proposed it, assumes that glaciations correspond to periods during which the high latitudes receive a minimum of summertime insolation. Three elements of astronomical variations are considered. The first is the orbital eccentricity of the elliptical path taken by the Earth around the sun - varying from zero to 5.3 percent, with a period of about 100,000 years. A circular orbit would mean that the amount of insolation is the same throughout the year; at maximum eccentricity, the Earth is closer to the sun during one season, making it warmer, and further away during the opposite season, making it cooler (Figure 1.1-2).

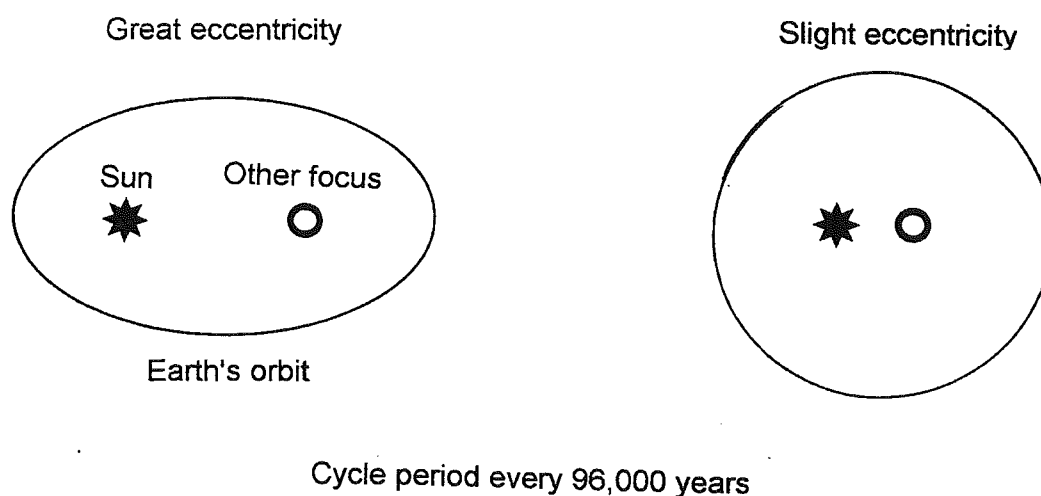


Figure 1.1-2: Eccentricity

The second factor is the precession of the equinoxes. The Earth's spin axis is tilted in relation to the plane of its orbit; gravitational influences exerted by the Sun and Moon on the spinning Earth cause the axis to trace a cone in the heavens. The clockwise 'wobble' or precession takes 21,000 years to complete one cycle, effectively reversing the seasons every 10,000 years (Figure 1.1-3). Thirdly, the tilt of the Earth's axis has varied from 22 to 24.5 degrees, which substantially shifted the position of the sun during the seasons. During periods of steep tilt, the Earth experiences large

temperature variations from one season to the next. One full tilt cycle is completed every 41,000 years (Figure 1.1-4).

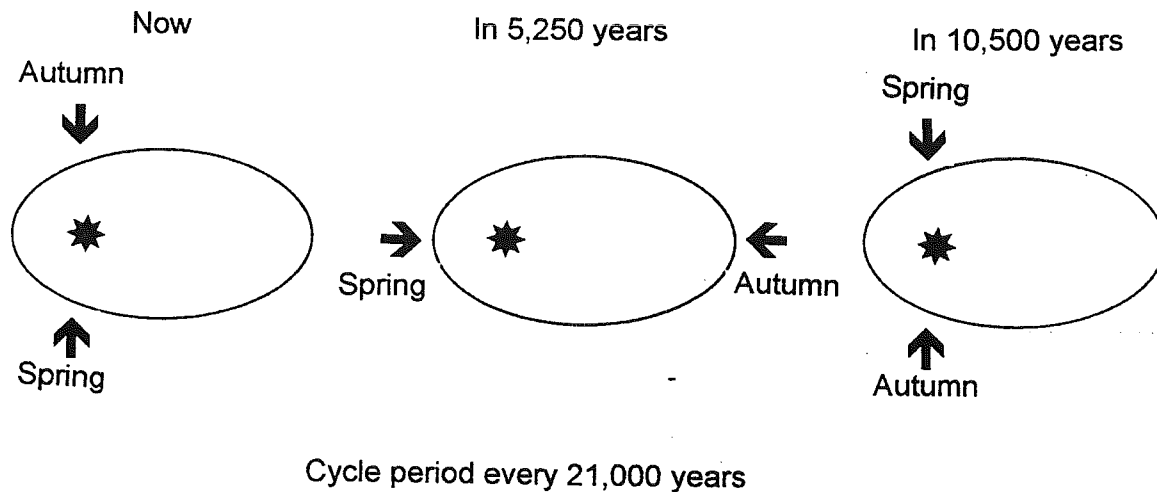


Figure 1.1-3: Precession

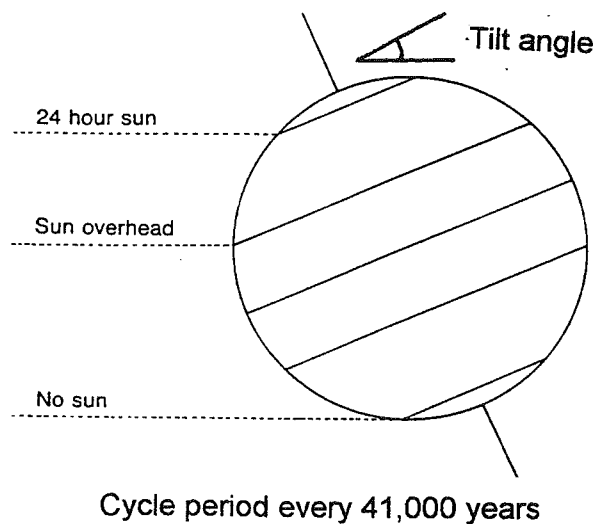


Figure 1.1-4: Tilt

Seasonal and geographical distribution of insolation received by the Earth, then, depends on the interactions of these three types of orbital parameters i.e., the geometry of the orbit, the precession of the equinoxes and the tilt of the spin axis.

Global ice growth is favoured during periods when summer insolation is low (leading to decreased ice ablation) and winter insolation is high (leading to increased moisture evaporation from oceans and increased snow supply to adjacent continents) (Ruddiman and McIntyre, 1981).

Perhaps the best evidence substantiating Milankovitch's hypothesis is provided by oxygen-isotope studies of benthic foraminifera from deep-sea sediments. Shackleton (1987) calculated that seven-tenths of the total amplitude of marine oxygen-isotope variations in deep Pacific cores can be attributed to changes in ice volume, while the remaining thirty percent reflects temperature fluctuations. Although it is not a simple proportional relationship, higher heavy-isotope values can be taken as a proxy for larger ice volume. Imbrie et al. (1984) compared the amplitude history of the variability in the isotope record with those of tilt- and precession-induced changes in seasonality and demonstrated a close correlation in both frequency and magnitude (Figure 1.1-5).

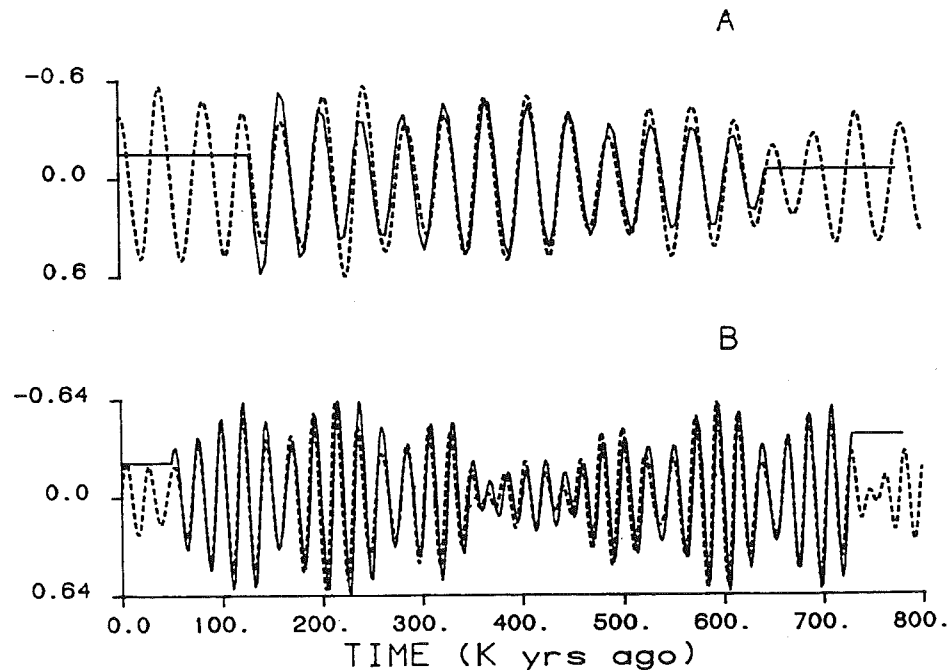


Figure 1.1-5: Amplitude history in the $\delta^{18}\text{O}$ record (solid lines) compared with a: tilt-induced changes in seasonality and b: precession-induced changes (dashed lines) (from Imbrie et al., 1984).

Broecker et al. (1968) have also lent support to the Milankovitch hypothesis by their studies on dated, elevated coral-reef tracts on Barbados which were formed at successive high stands of the sea during interglacial times. Their results indicated that the last four sea level maxima correspond to the last four prominent warm peaks in the summer-insolation curve predicted from cycles in the tilt and precession of Earth's axis (Figure 1.1-6).

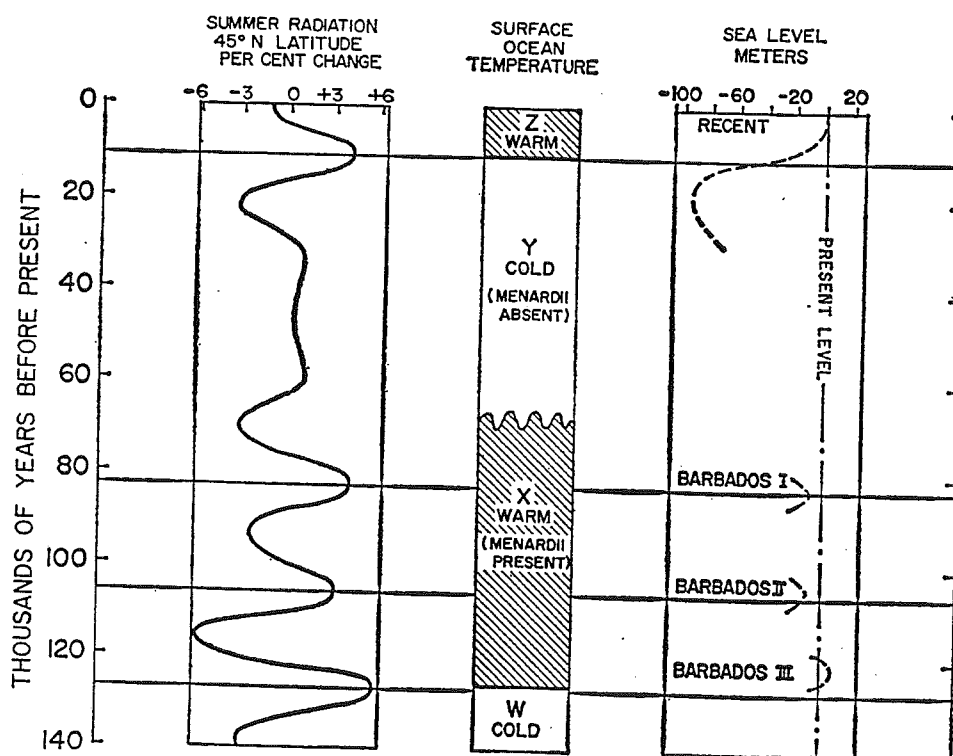


Figure 1.1-6: Correlation of summer-insolation curve for the northern hemisphere with the ocean's surface temperature and sea level records (from Broecker et al., 1968).

1.1.2 Oceanic Influences

Whereas many climatic researchers accept Milankovitch's hypothesis as the underlying cause of climate cycles, the nature of the link between seasonal insolation and global climate is debated. Workers investigating the problem have tried to interpret evidence of synchronous climate changes of similar severity in both polar hemispheres, as well as indications of a rapid transition from full glacial to interglacial conditions: phenomena for which a direct linkage between orbital cycles and Earth's climate cannot account. Evidence from mountain glaciers, for example, implies that the last glacial termination began simultaneously and abruptly in both polar hemispheres. Several sites studied along a north-south transect, across virtually all of the Earth's climatic zones, show mountain snowline depression caused by high-mountain temperature lowering of nearly equal magnitude at the last glacial maximum (Figure 1.1-7).

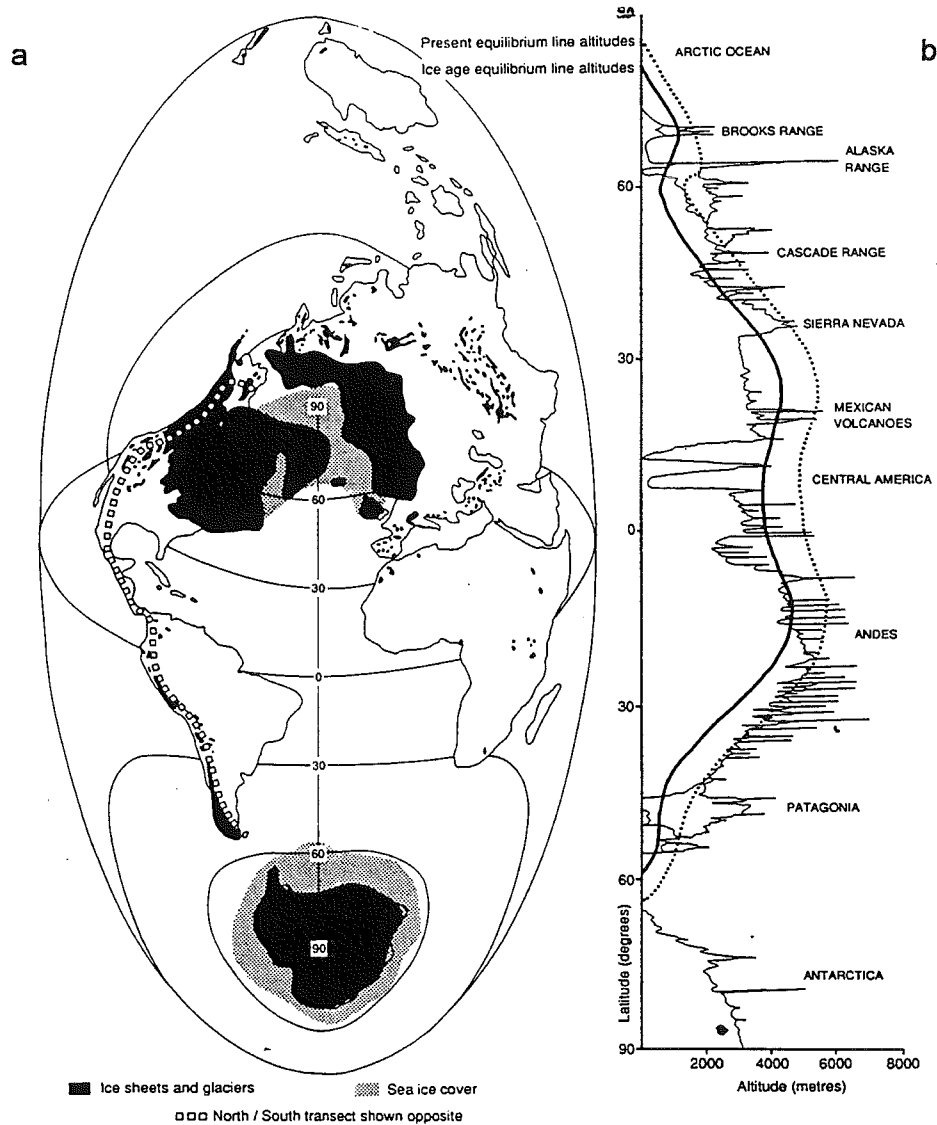


Figure 1.1-7a: The distribution of ice sheets and mountain glaciers during the last glacial maximum.

b: the position of the present day mountain snowline is shown as a dotted line, the depressed snowline at the last glacial maximum is depicted by the heavy line along a transect of the cordillera of North and South America (from Dawson, 1992).

From an analysis of ice in the Yukon Territory's St. Elias Mountains, Denton (1974) concluded that an abrupt background climate event ended full glacial conditions at approximately 14,000 y BP (Figure 1.1-8a). A similar conclusion was reached by Porter (1981) after studying ice caps and mountain snowlines in the Southern Andes

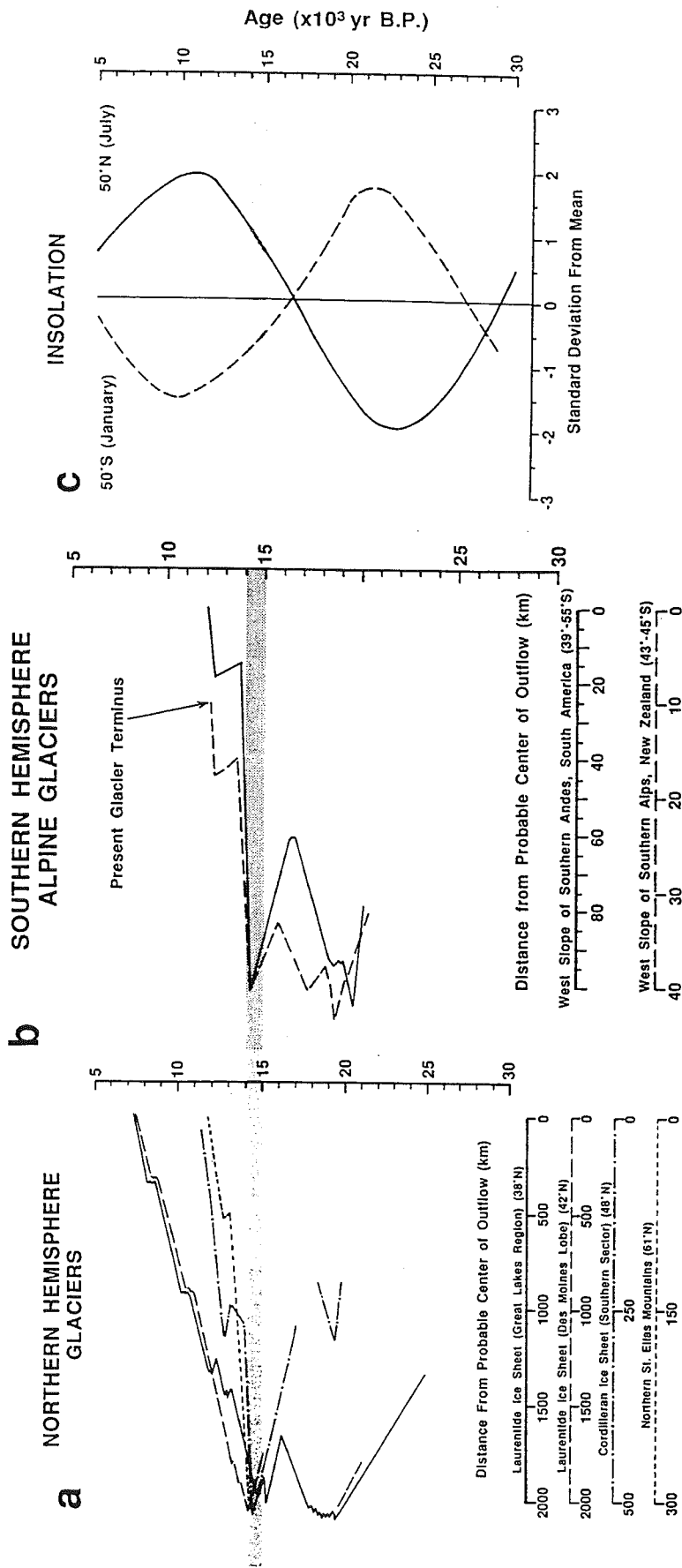


Figure 1.1-8: Comparison of climate records and summer insolation curves in both polar hemispheres. a: Fluctuations in Northern Hemisphere glaciers b: Fluctuations in Southern Hemisphere glaciers c: Summer insolation curves for mid-latitudes of the Northern and Southern Hemispheres. The grey bar marks the time of an abrupt global event that ended full-glacial conditions. (from Broecker and Denton, 1989)

(Figure 1.1-8b). Interestingly, these synchronous changes occurred despite the fact that the summer insolation signals were out of phase at the latitudes of the key glacial records (Figure 1.1-8c).

Many recent studies of the mechanism by which periodic changes in Earth's orbital elements affect the timing of glacial cycles have proposed that the key may be a massive ocean-atmosphere reorganization. Ocean circulation patterns have a profound impact on global climate, as ocean currents pick up heat in low latitudes and release it in high latitudes. This is especially evident in the North Atlantic, where the northward flowing warm surface waters of the Gulf Stream gradually give up heat to the atmosphere (Figure 1.1-9). In so doing, the water becomes cooler and more saline, causing it to sink and form a southward-flowing mass (i.e., North Atlantic Deep Water - Figure 1.1-10).

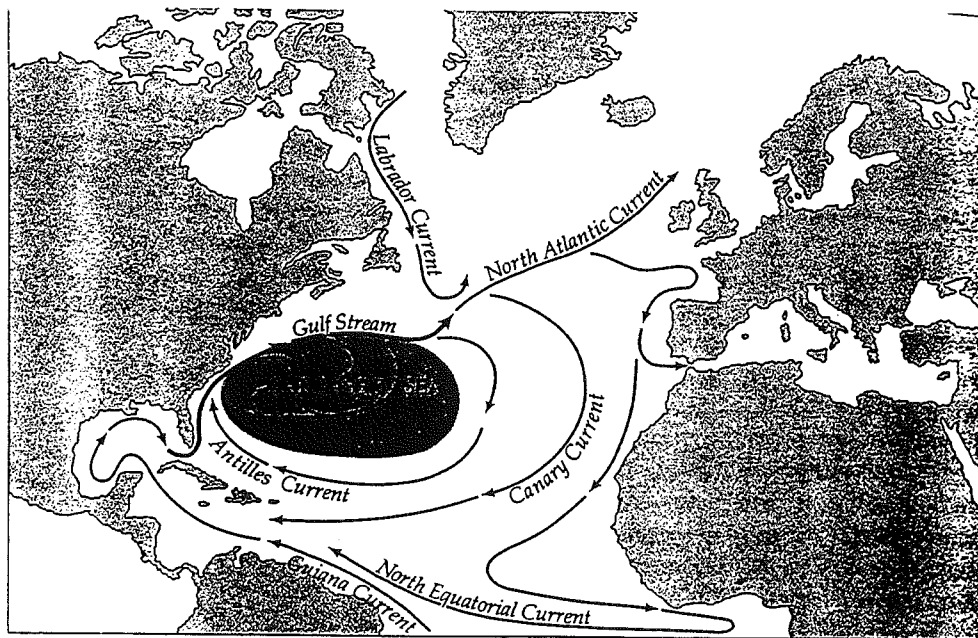


Figure 1.1-9: Surface currents of the North Atlantic Ocean (from Ingmanson and Wallace, 1989).

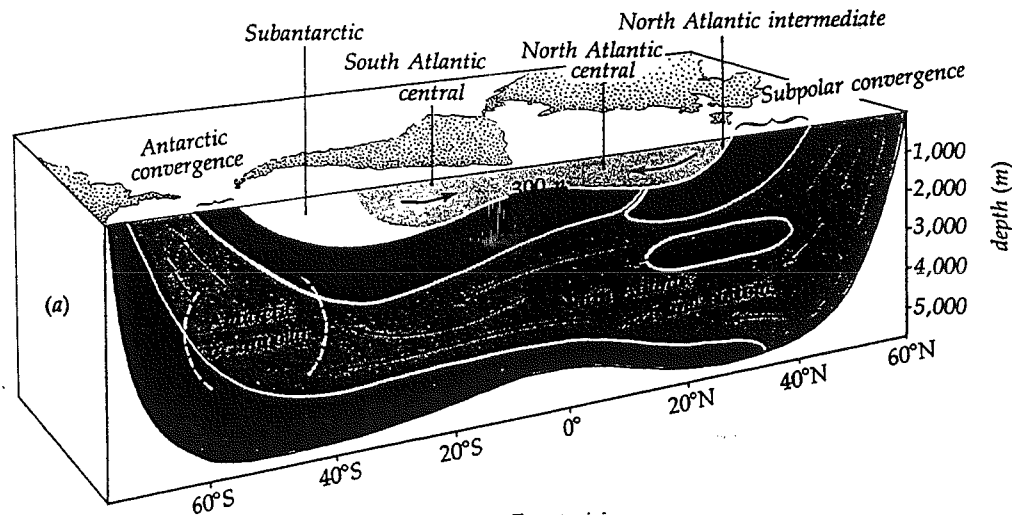


Figure 1.1-10: North-south cross section of subsurface circulation of the Atlantic (from Ingmanson and Wallace, 1989).

This system is a substantial 'conveyor belt' of heat: the northward-flowing water averages about 10°C, while the return flow is approximately 2°C, meaning that 8 calories are released for every cubic centimeter of deep water formed. The yearly total is 5×10^{21} calories, supplementing yearly insolation by 25%. The released heat is then carried by winds onto the adjacent continents. Mounting experimental evidence (e.g., Boyle and Keigwin's (1987) work on cadmium measurements; the report from Duplessy et al. on carbon isotope measurements of benthic Foraminifera; Schnitker's (1979) faunal evidence, etc.) has led many researchers to believe that this conveyor belt was not operating during glacial times, but was replaced by an alternate mode of operation in which the high latitudes did not receive this bonus of heat.

It is postulated by Broecker and Denton (1989) that the mode of ocean circulation employed may be based on the nature of the link between water transport through the atmosphere and salt transport in the sea. When water vapour is transported from one major drainage basin to another, the salt is left behind, which eventually must be compensated for by the influx of fresh water. Since an increase in salinity corresponds to denser seawater, any changes in water export can lead to

dramatic differences in the rates and patterns of ocean circulation. In the North Atlantic, the excess salt is transported by the lower limb of the conveyor (i.e., North Atlantic Deep Water), and is balanced by returning waters with lower salinity.

This conveyor belt is finely balanced: poleward transport of less-saline water works against deep-water formation by diluting the salt content and reducing the density of the surface waters. A slight change, therefore, in the extent of this dilution (which depends on the ratio of water vapour transport to ocean transport) could disrupt the conveyor belt by preventing deep water formation. Once the system is disturbed, a layer of low-salinity water would form at the surface of the North Atlantic, thereby perpetuating the disruption.

Manabe and Stauffer (1988), using a coupled air-sea model, experimented with Atlantic circulation modes by balancing water vapour loss from the Atlantic by net transport of salt from the Atlantic to the Southern Ocean. They demonstrated that one of two patterns could emerge: the first was the expected Gulf Stream circulation system, but the second was a nonconveyor mode with a totally different pattern of currents. It was noted that in the mode without thermohaline circulation the surface waters of the North Atlantic were colder and fresher than in today's ocean, implying that less heat would be delivered to the high latitudes (Figure 1.1-11). These modeling results support the contention that a nonconveyor mode was the circulation pattern operating in the oceans during glacial times.

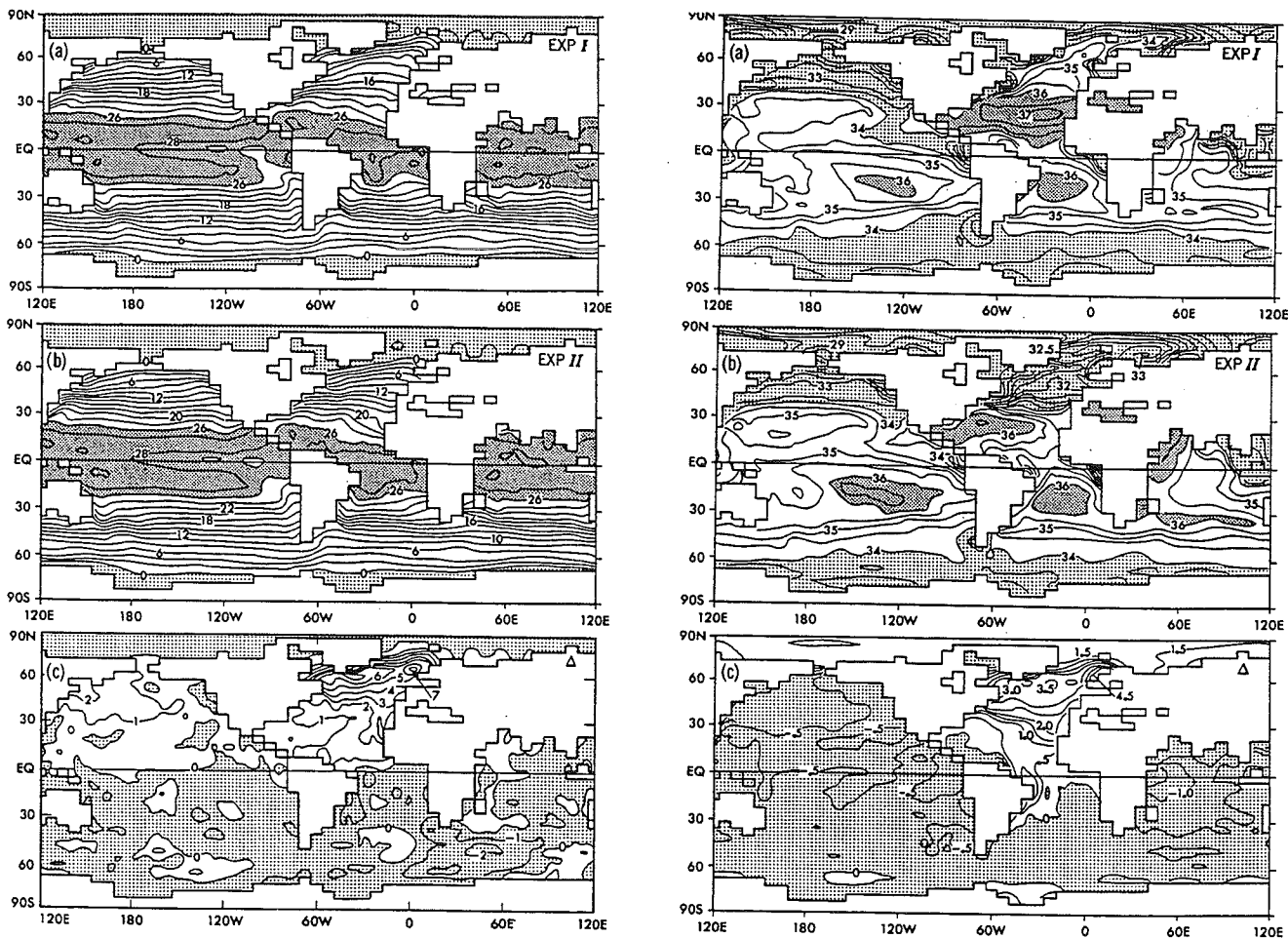


Figure 1.1-11: The distribution of surface water temperature for two modes of ocean circulation is shown on the left; the salinity distributions on the right. The top maps show the mode with strong thermohaline distribution; the middle maps are without. The bottom maps show that significant differences between the two modes exist only in the North Atlantic (from Manabe and Stauffer, 1988)

1.1.3 The Younger Dryas Event

Perhaps the most convincing evidence of a change in the mode of operation of the oceans is the Younger Dryas event. This extraordinary episode was a sudden, brief and intense climatic deterioration which punctuated the transition from the last glacial to the present interglacial periods. This reversion to cold conditions from about 11,000 to 10,000 y BP, resulting in major ice advances, was especially evident in the North Atlantic (Dawson, 1992). Evidence for this was first gathered by European palynologists who were attempting to reconstruct vegetation changes over the past several thousand years. As expected, the ameliorating climate was reflected in the gradual increase in the abundance of tree pollen as compared with tundra-type grasses and herbs in lake sediment cores. At depths corresponding to the 11,000 to 10,000 y BP range, however, there was an abrupt decline in the percentage of tree pollen found, suggesting a sudden change in climate (Figure 1.1-12).

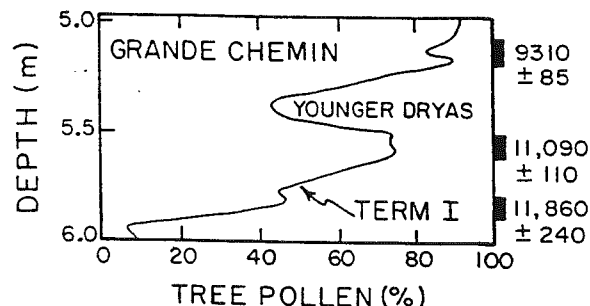


Figure 1.1-12: European pollen record from the end of the last glacial period (from Broecker et al., 1988).

Rooth (1982) proposed that the Younger Dryas resulted from a diversion of water from proglacial Lake Agassiz, which collected runoff from a large area along the southwestern side of the Laurentide ice sheet. Prior to 11,000 y BP, the Lake Agassiz meltwater overflowed into the Gulf of Mexico through the Mississippi River drainage system. By approximately 11,000 y BP, the Laurentide ice sheet had retreated back

sufficiently to allow a series of channels to open into the Lake Superior basin, allowing meltwater to flow through the St. Lawrence Valley into the North Atlantic. This influx of fresh water reduced the salinity of the surface waters in the region where the North Atlantic Deep Water now forms. As discussed earlier, this would render the formation of deep water improbable and may have resulted in the turnoff of the North Atlantic's conveyor belt circulation system thereby reducing the amount of heat delivered to the region (Figure 1.1-13).

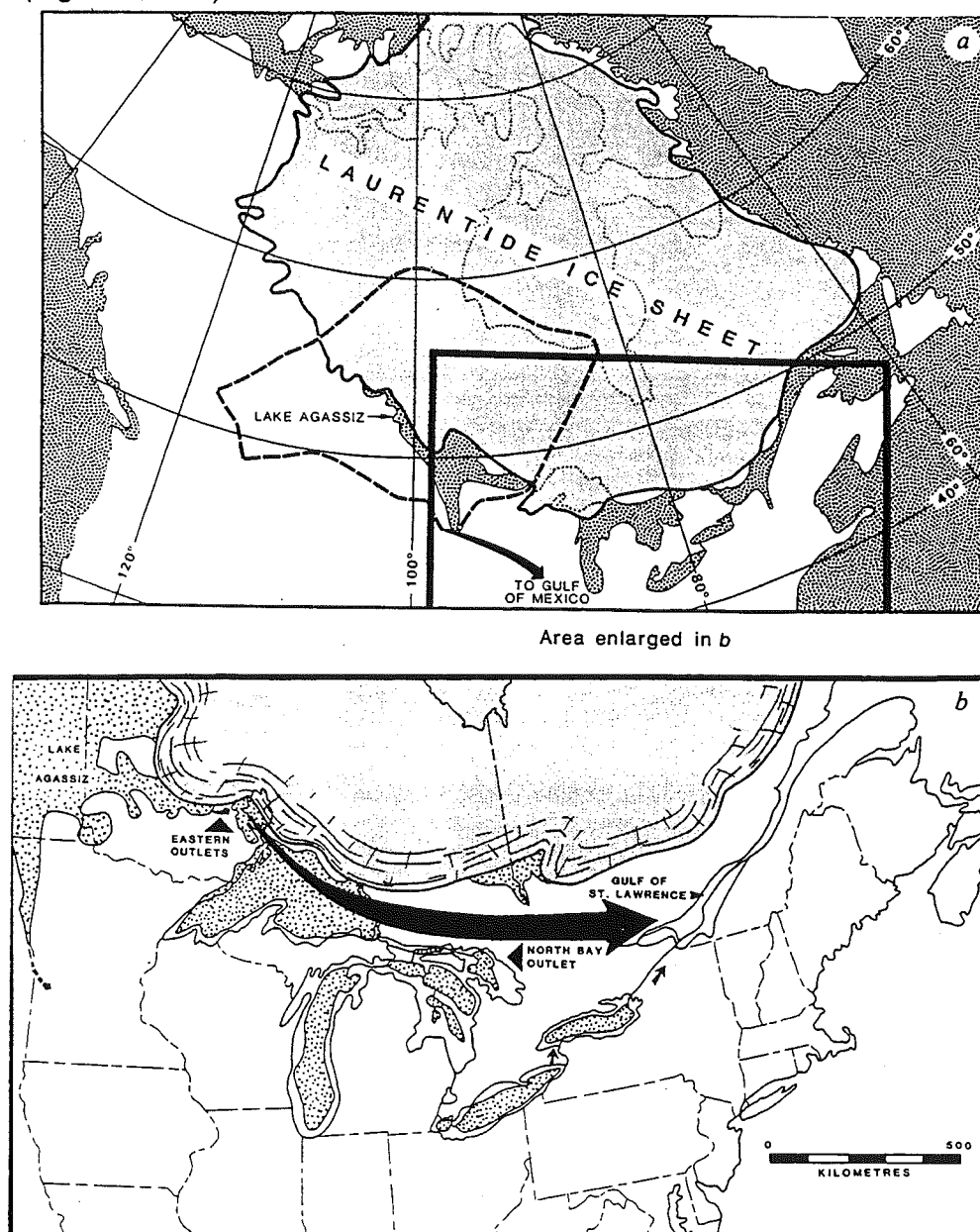


Figure 1.1-13a: Map showing Laurentide ice sheet and routing of overflow from the Lake Agassiz basin (dashed outline) to the Gulf of Mexico just before the Younger Dryas. b: Routing of overflow from Lake Agassiz to the St. Lawrence and North Atlantic during the Younger Dryas (from Broecker et al., 1989).

Once the conveyor stopped, salt began to accumulate in the North Atlantic. While there was still a net export of water vapour, the excess salt was no longer transported southwards: increased ice volume also raised salinity. Eventually the density of the seawater built to a level which permitted the conveyor to reinitiate (Broecker, 1992). The abrupt end to the Younger Dryas was probably triggered by the readvance of the Marquette lobe of the Laurentide ice sheet which dammed the eastern outflow channels and routed drainage back into the Mississippi River and the Gulf of Mexico beginning about 10,000 y BP. The reestablishment of the conveyor mode of circulation facilitated heat transfer to the northern latitudes. Figure 1.1-14 summarizes the timing of events which occurred during the ocean-atmosphere reorganization at the last glacial termination.

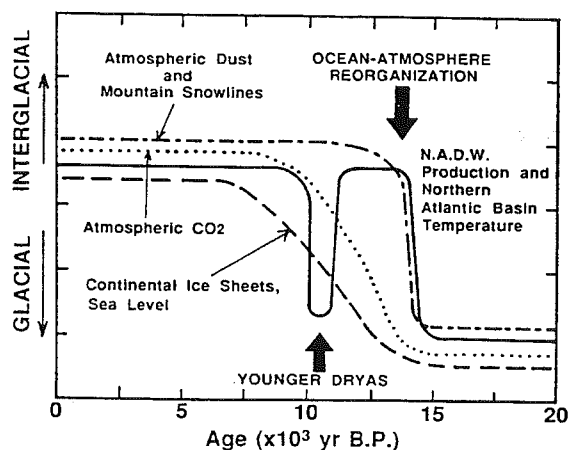


Figure 1.1-14: Timing of ocean-atmosphere reorganization events (Broecker and Denton, 1989).

1.2 Corals as Environmental Indicators

Charles Darwin (1842, cited by Aharon, 1991) was among the first to recognize that reef corals are reliable monitors of environmental variations of surface ocean conditions: geologists have subsequently utilized this phenomenon as a means to reconstruct paleoecological patterns. Many reef corals exhibit regular annual cycles in the density of aragonite deposited (e.g. Knutson et al., 1972 and Figure 1.2-1).

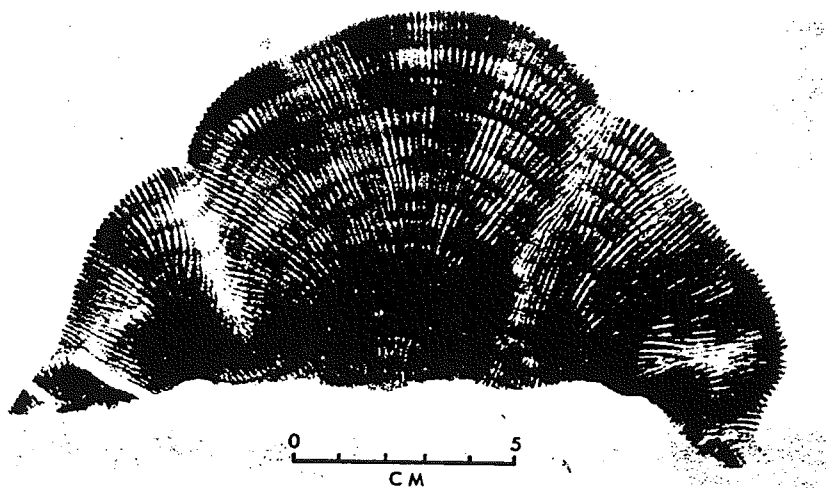


Figure 1.2-1: X-radiograph positive of a coral sample (*Porites lobata*) - dark images correspond to high skeletal density, light images to low density (from Buddemeier et al., 1974).

Density and growth rate variation data, retrieved from these periodic growth patterns, can be used to document fluctuations in the ambient conditions on a coral reef. As corals depend on their zooxanthellae for skeletogenesis, available light, or changes in the level of available light, have been found to be the underlying control on the rate of skeletal mass deposition (Figure 1.2-2). For instance, Goreau (1959) reported calcification rates in sunny weather to be twice those under cloudy conditions.

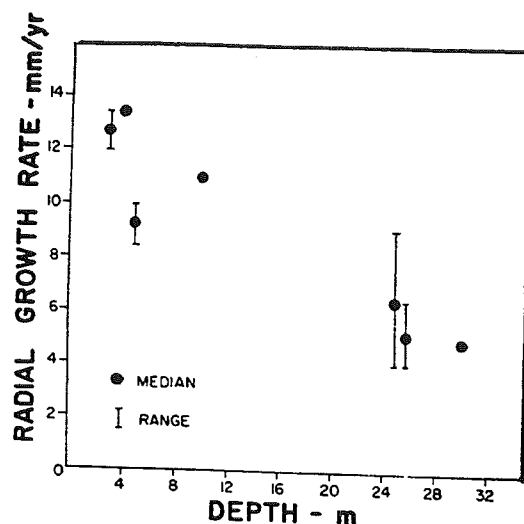


Figure 1.2-2: Plot of linear vertical growth as a function of depth (i.e., an attenuation of light) for *Porites lutea*, Eniwetok Atoll (from Buddemeier et al., 1974).

Cores with records exceeding 400 years have been extracted from contemporary reefs (Hudson et al., 1976), allowing sclerochronology to be used as a tool for a long-term reconstruction of paleoecologic patterns in coral-bearing accumulations.

Stable isotopes have recently been used as recorders of reef environment histories: the isotopic compositions of biologically-precipitated carbonates are governed by thermodynamic isotope fractionation factors and the isotopic makeup of the ambient fluid (McCrea, 1950).

Fairbanks and Matthews (1978), using oxygen-isotope records from Pleistocene corals in Barbados, have attempted temperature estimates of the late Quaternary ocean. The researchers made use of the fact that, although corals do not deposit skeletal aragonite in precise isotopic equilibrium with sea water, the $\delta^{18}\text{O}$ values are nevertheless temperature dependent and can be used as 'paleothermometers'. Several samples of the genus *Acropora* from a modern reef and fossil reefs of varying ages were analyzed for their oxygen-isotope composition, thereby giving an account of

variations through time (Figure 1.2-3). The $\delta^{18}\text{O}$ fluctuations were converted into estimations of temperature change - the degree of offset of *Acropora* from the calcite-water isotope equilibrium scale had been derived during previous research (Figure 1.2-4).

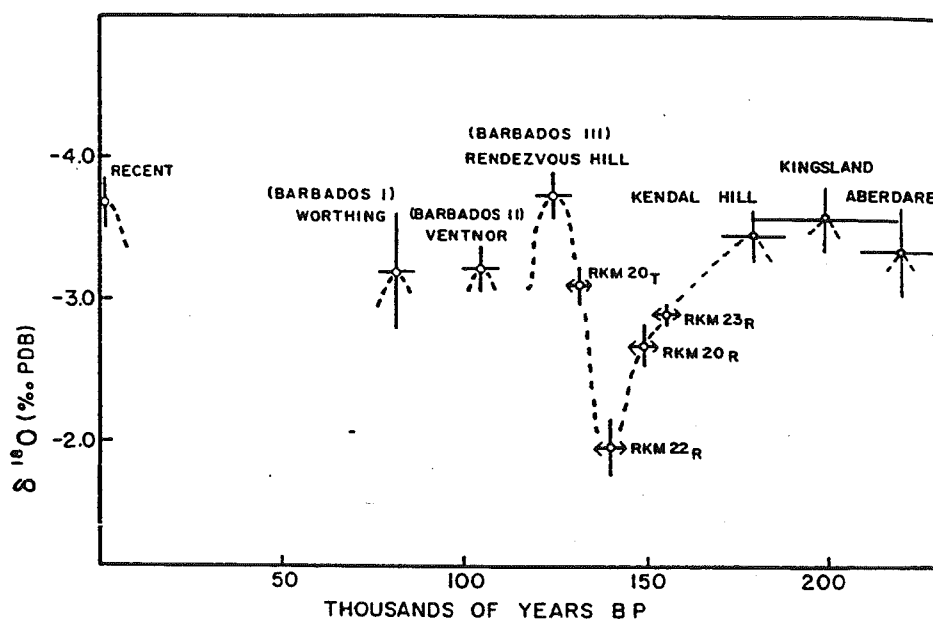


Figure 1.2-3: Fluctuations in the Barbados coral-isotope record with time (from Fairbanks and Matthews, 1978).

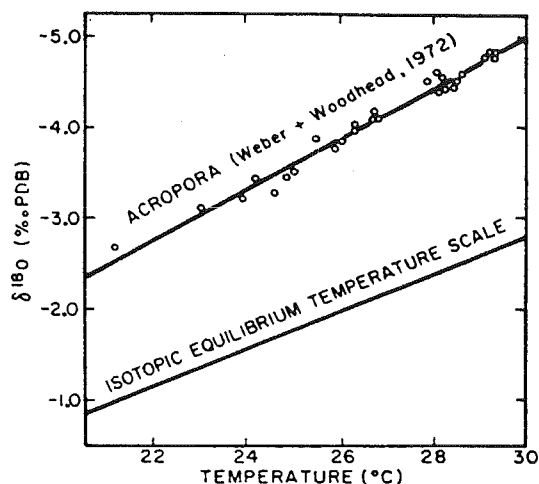


Figure 1.2-4: $\delta^{18}\text{O}$ values for *Acropora* plotted against ocean-water temperature, with calcite-water isotopic equilibrium line (from Fairbanks and Matthews, 1978).

Temperature histories associated with El Niño events have also been documented using oxygen-isotope records from banded Costa Rican reef corals. Carriquiry et al. (1988), were able to establish firmly the magnitude, duration and timing of the 1982-83 El Niño warming event (Figure 1.2-5). In so doing, they have also suggested a means whereby similar occurrences may be recognized in the geologic record.

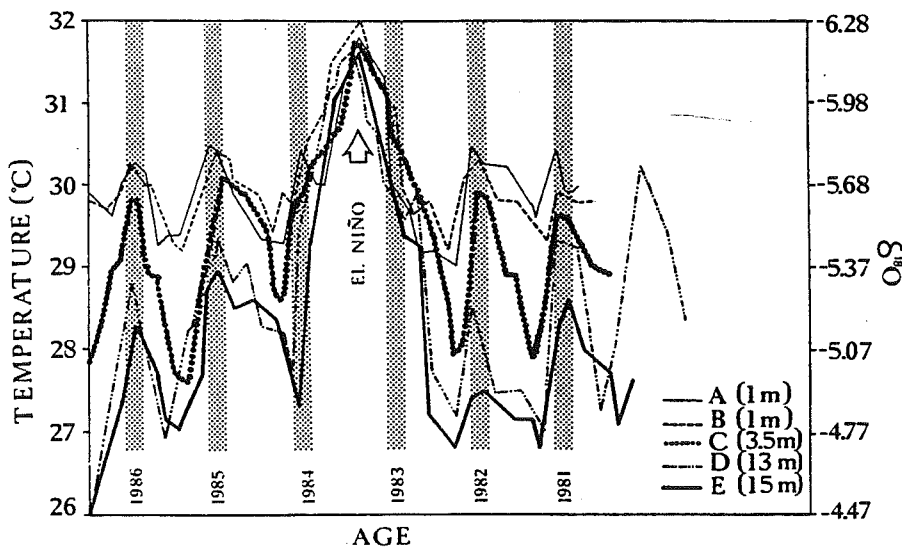


Figure 1.2-5: Temperature records derived from oxygen isotopes for five coral heads at different depths, plotted against time (from Carriquiry et al., 1988).

Stable carbon isotopes in Bermuda corals were measured by Nozaki et al. (1978) and used to recount the recent history of fossil fuel CO_2 uptake by the ocean. During the past two centuries, there has been a dilution in both carbon-14 and carbon-13 in the atmosphere due first to increased human burning of trees and then to fossil-fuel burning. The continuous growth of a 200-year-old *Diploria labyrinthiformis* was used to track atmospheric variations in carbon isotopes over time (Figure 1.2-6).

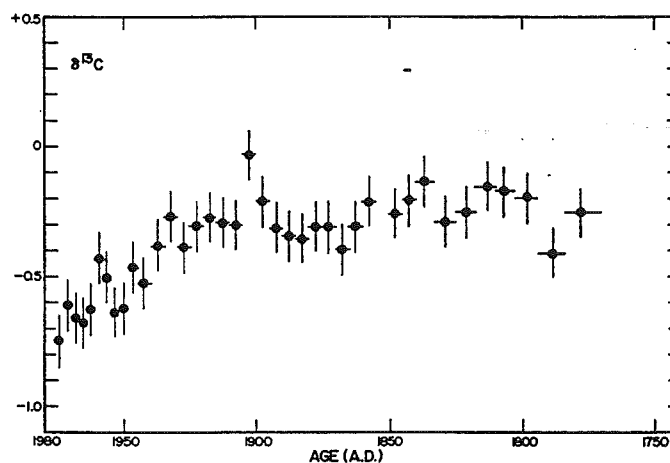


Figure 1.2-6: $\delta^{13}\text{C}$ distributions with age in a Bermuda brain coral (from Nozaki et al., 1978).

Although difficult to separate from temperature effects, the $\delta^{18}\text{O}$ in corals also varies with salinity changes (Rye and Sommer, 1980). The salinity of normal sea water is about 35‰, but is increased during evaporation processes. Evaporation also affects the isotopic composition of the sea water, as there is a preferential depletion of the lighter isotopes of oxygen. Generally speaking, near-shore ecosystems subjected to fresh- and melt-water dilutions are of relatively low salinities and low $\delta^{18}\text{O}$ values, while mid-oceanic water tends to be more saline with higher $\delta^{18}\text{O}$ ratios.

Aharon (1991) demonstrated that freshwater incursions into the reef environment can leave an imprint on the isotopic compositions of the coral. He compared a thirteen-year rainfall record at Great Palm Island of the Great Barrier Reef with $\delta^{18}\text{O}$ shifts from the coral mean, and found a good match in periodicity and magnitude (Figure 1.2-7).

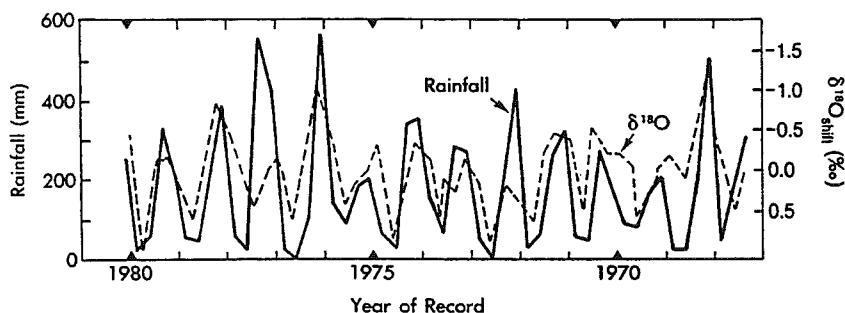


Figure 1.2-7: Comparison between the rainfall record and $\delta^{18}\text{O}$ shifts in coral skeletons, Great Barrier Reef, 1967 - 1980 (from Aharon, 1991).

Aharon, however, offered a caveat: because the region experiences a monsoon climate, the freshwater signal overlaps with the temperature signal, and he therefore suggested that only reef skeletal material of relatively-high longevity be used as 'paleo rain gauges'.

Fluorometric analysis of banding in scleractinian skeletons has been shown to be useful as a means to estimate historical rainfall. Isdale (1984) demonstrated that yellow-green fluorescent bands appear in the skeletons of massive corals under longwave UV light. The timing, width and intensity of the bands correlate strongly with the volume and timing of terrestrial runoff into the coastal environment. As large coral colonies may be several centuries old, long records of nearshore fluvial history may be recorded within them (Figure 1.2-8).

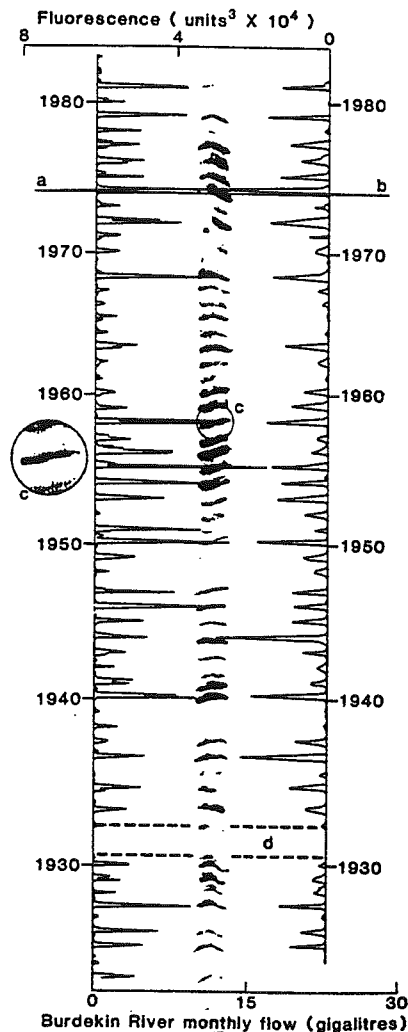


Figure 1.2-8: Fluorescent banding on a 885-mm length of coral core from Pandora Reef, Australia. Points a, b and c show episodes of strong rainfall and runoff, while d represents a period of drought (from Isdale, 1984).

Corals, because of their light requirements, are limited in distribution by the concurrent sea level; this allows coral reefs to be used as oceanic 'dipsticks' (Wheeler and Aharon, 1991). If a eustatic sea level fall exceeds the rate of tectonic subsidence, the upper portion of a reef may experience subaerial exposure, with the subsequent creation of a meteoric ground-water system. Meteoric diagenesis imparts a distinct

isotopic fingerprint on biologically-precipitated carbonate: oxygen and carbon stable-isotope analyses can reveal the location of both the exposure surface and the paleo-water table. A strontium-isotope technique can also be used to date disconformities associated with sea level low stands. Island carbonate platforms, which have developed on mid-plate seamounts, are most amenable to paleo-sea-level determinations because their water tables approximate contemporaneous sea level and their tectonic histories are relatively simple. Figure 1.2-9 shows isotopic detection of two archaic exposure-surface / water-table couplets from Niue, a carbonate platform in the south Pacific, near Samoa. Apparent ages estimated from $^{87}\text{Sr}/^{86}\text{Sr}$ ratios are also shown.

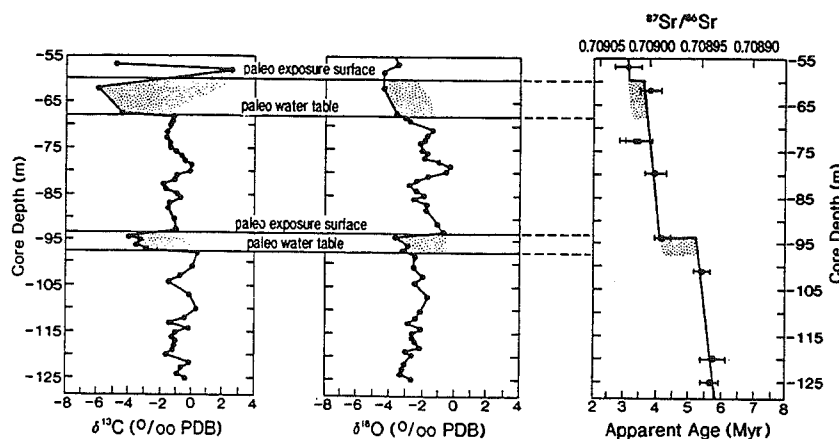


Figure 1.2-9: Interval from Niue core showing effects of exposure surface and water on oxygen and carbon isotopes and strontium isotopes (from Wheeler and Aharon, 1991).

The timing of sea level high stands may also be ascertained by isotopic dating; in this case the procedure is performed on exposed coral-reef tracts. For example, precise uranium / thorium dating of elevated coral terraces on Barbados allowed Broecker et al. (1968) to chronicle sea level rises and infer paleo-climatic conditions.

McConnaughey (1989) presented the interesting suggestion that a CO_2 'greenhouse' effect may be inferred from isotopic analyses of coral skeletons. If the

concentration of carbon dioxide in the atmosphere is indeed increasing, it should be reflected in a reduced carbonate $\delta^{13}\text{C}$ over a long period of time, due to isotopically-light CO_2 additions. Extending the atmospheric carbon-dioxide record back over centuries may allow climatic researchers to understand better present-day trends.

Given the proven effectiveness of coral as environmental indicators, it is perhaps surprising that all research to date has focused on the shallow-sea record. It seems feasible that deep-water coral could be equally useful as recorders of ecological fluctuations at depth as hermatypic corals have been near the ocean surface.

1.3 Orphan Knoll

An opportunity for studying deep-water coral arose serendipitously as a result of unrelated research, after several specimens were retrieved during a rock dredge of Orphan Knoll by a geophysics vessel. Orphan Knoll is a pronounced submarine feature which lies at the edge of the continental rise 550 km northeast of Newfoundland and 350 km north of Flemish Cap. Its exact position, as determined by satellite navigation, is $50^{\circ} 25.57' N$, $46^{\circ} 22.05' W$ (Figure 1.3-1).

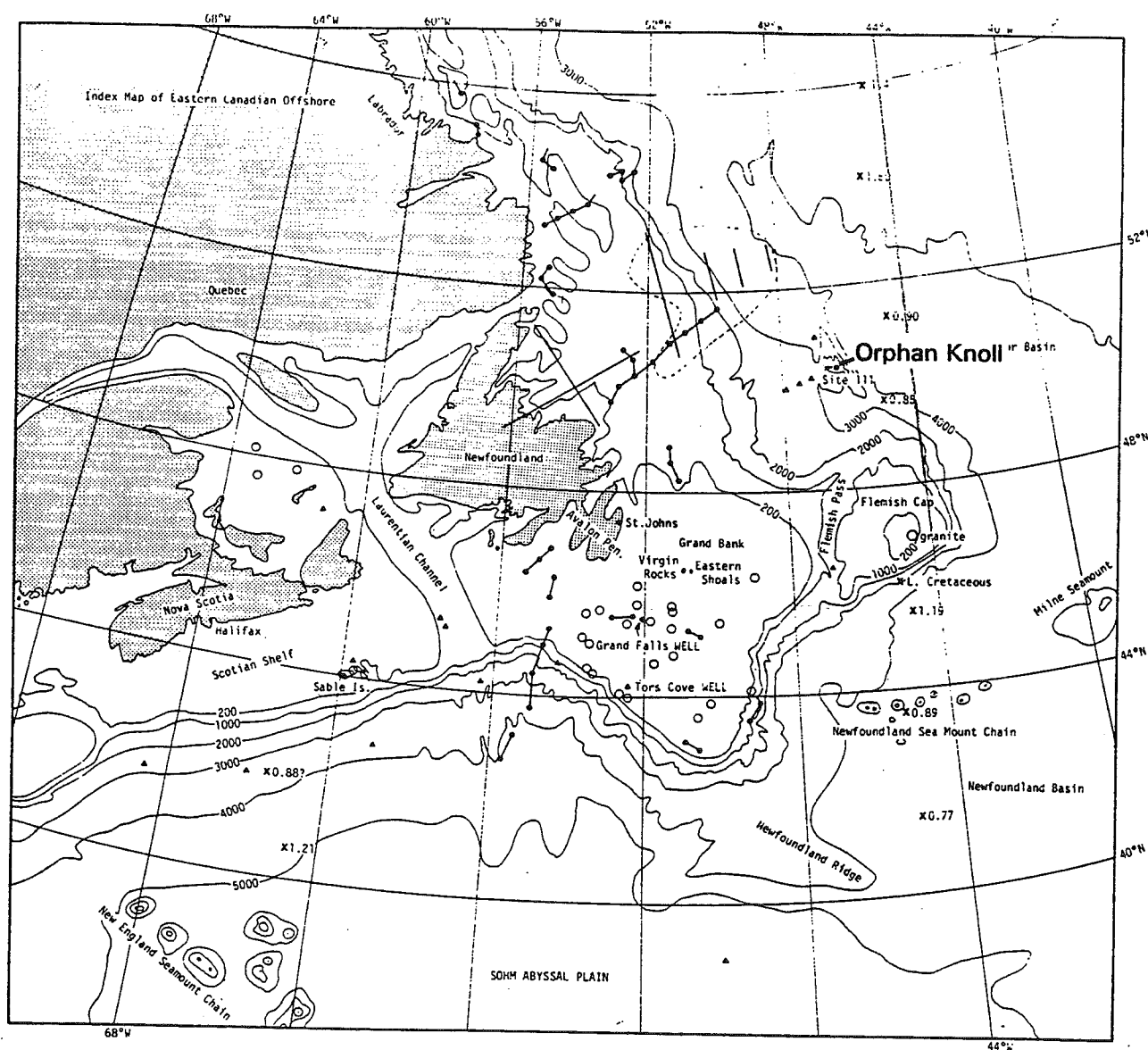


Figure 1.3-1: Map of the area around Orphan Knoll, showing general bathymetry (from Laughton et al., 1972).

The knoll, which is elongated in a northwest-southeast direction, is separated into two parts connected by a ridge. The larger, southern section rises to depths of less than 1800 m, while the smaller, northern extension lies under more than 2400 m of water (Figure 1.3-2). Orphan Knoll is quite isolated - its northeast side is bounded by the 4000-meter-deep abyssal plain of the Labrador Basin, and it is separated from the Labrador and Flemish Cap shelves by water 2800 to 3400 m in depth.

Detailed bathymetry of Orphan Knoll has been inferred from results of seismic-refraction work performed by D/V Glomar Challenger on Leg 12 of the Deep Sea Drilling Project and sponsored by Joint Oceanographic Institutions for Deep Earth Sampling (JOIDES) in June, 1970 (Figures 1.3-3, 1.3-4 and 1.3-5).

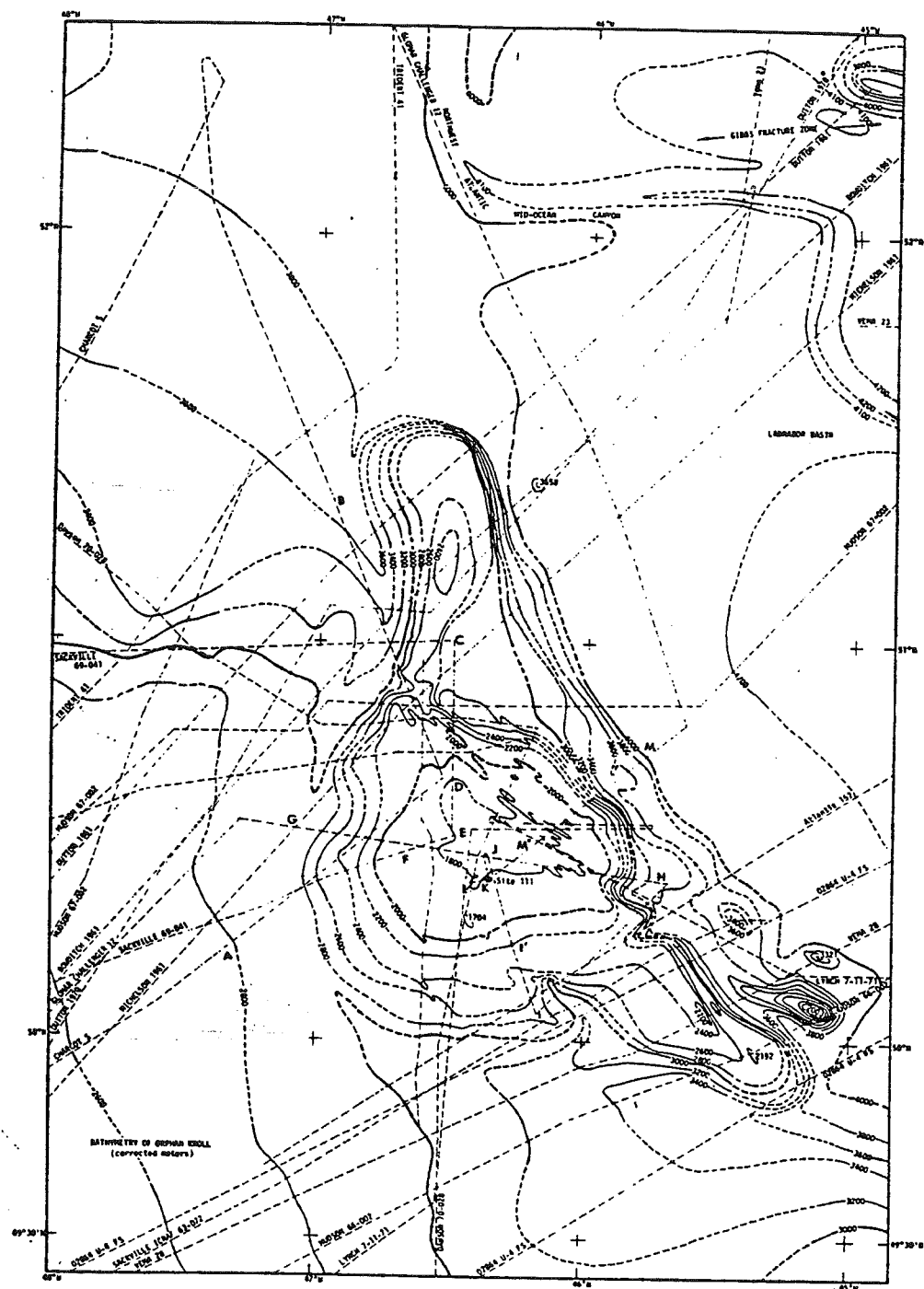
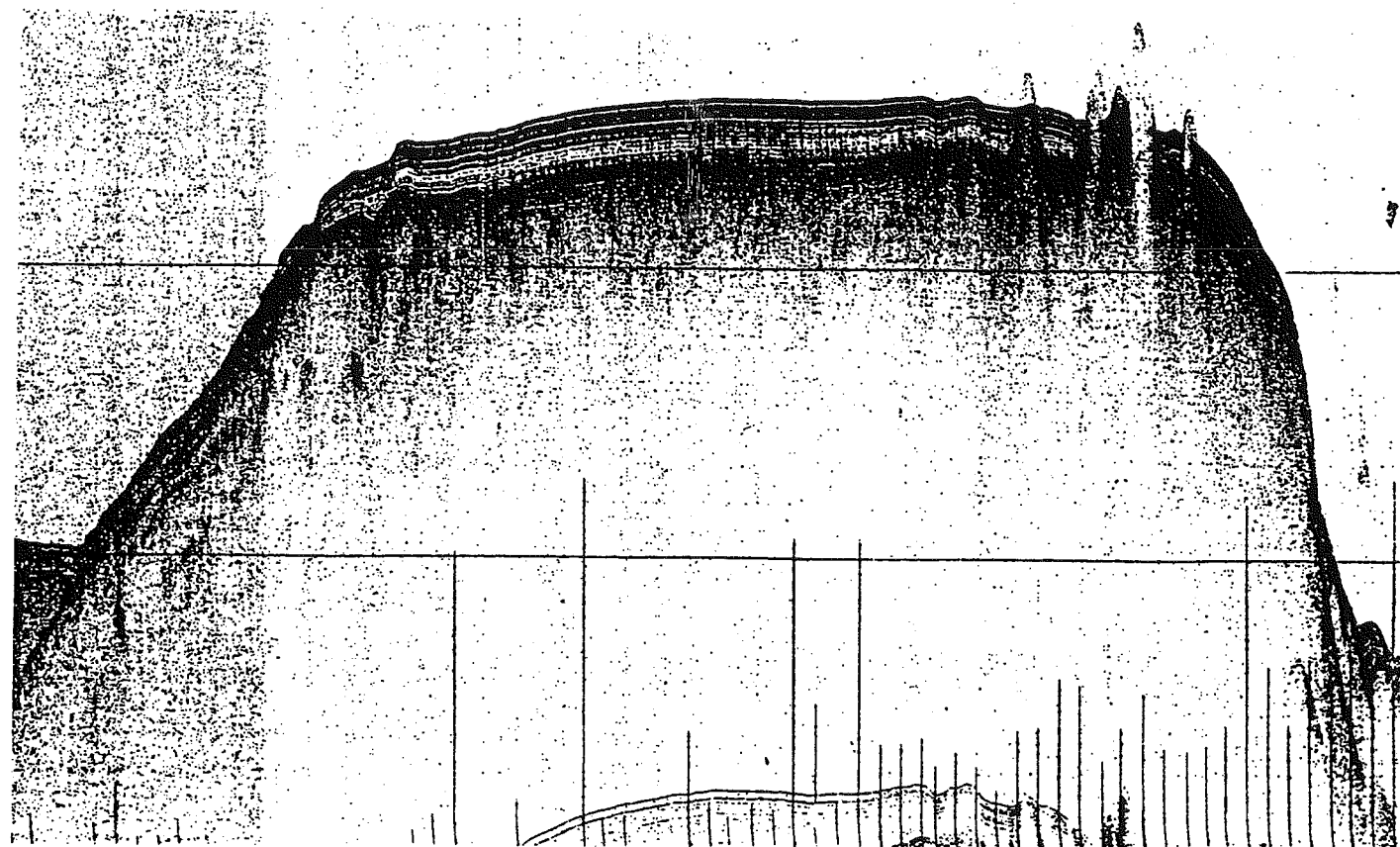


Figure 1.3-2: Bathymetry of Orphan Knoll in corrected metres; letters shown refer to profiles referenced in later figures (from Laughton et al., 1972).



LOCAL TIME, JUNE 24, 1970 - GLOMAR CHALLENGER 12

1700

1900

2100

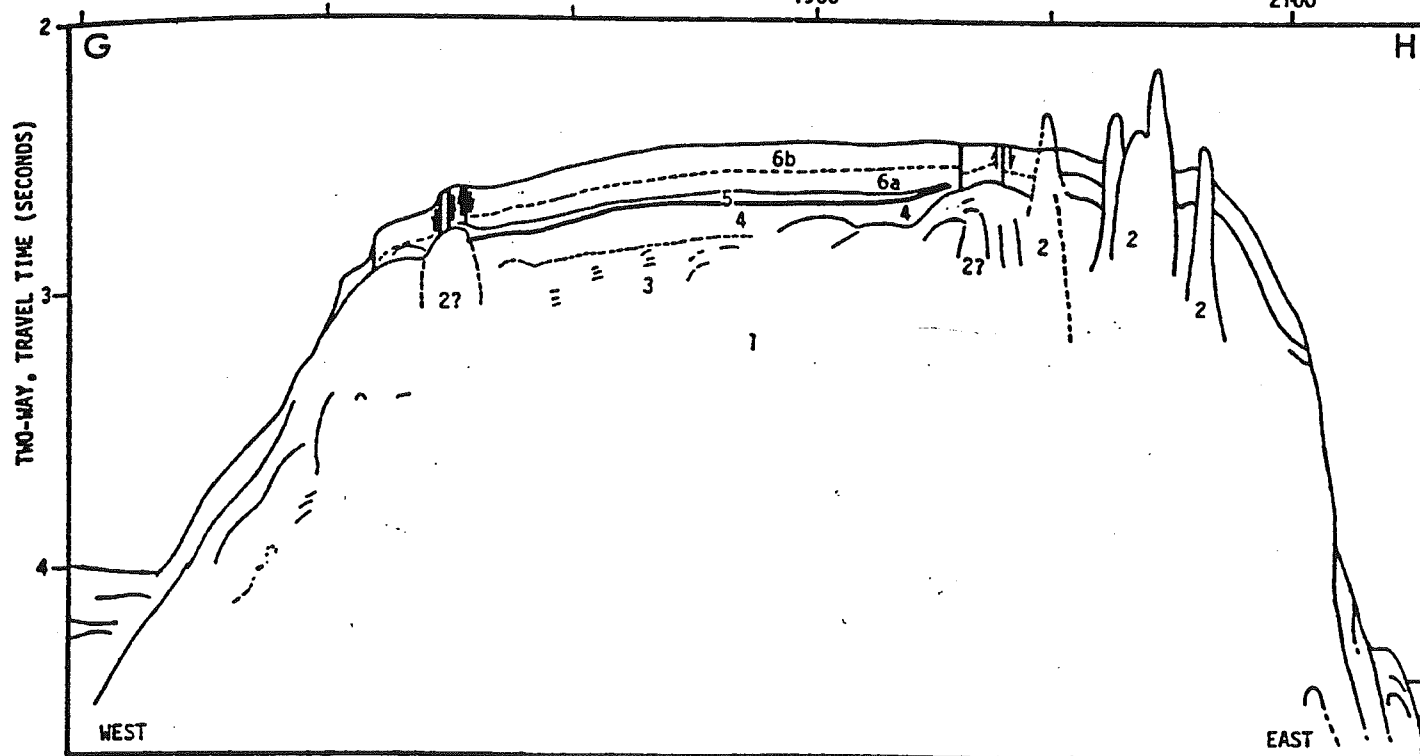


Figure 1.3-3a: The seismic profile across Orphan Knoll along line G-H
b: Line interpretation of same profile (from Laughton et al., 1972).

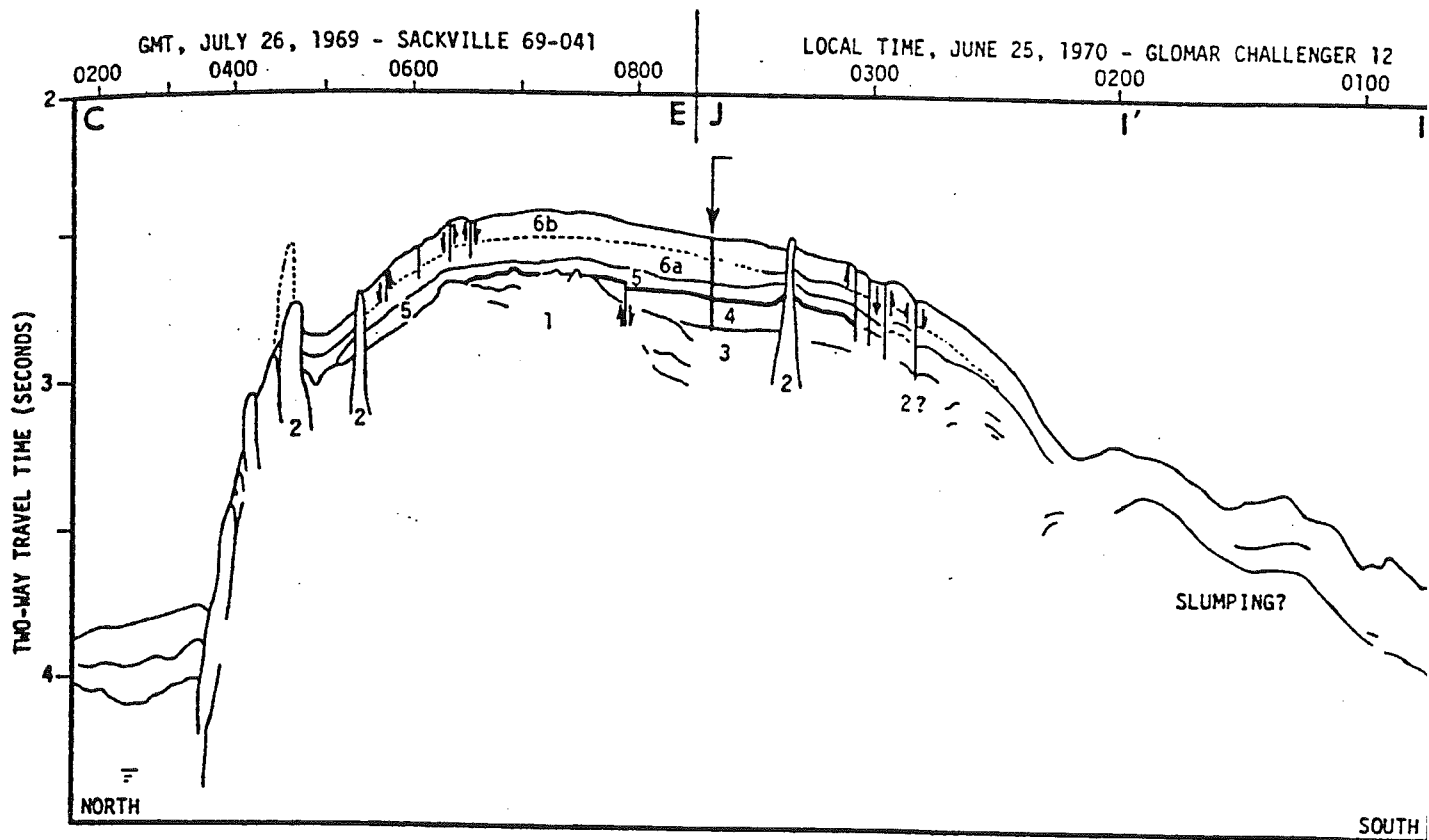


Figure 1.3-4: Line interpretation of the composite seismic profiles along lines C-E and J-I (from Laughton et al., 1972).

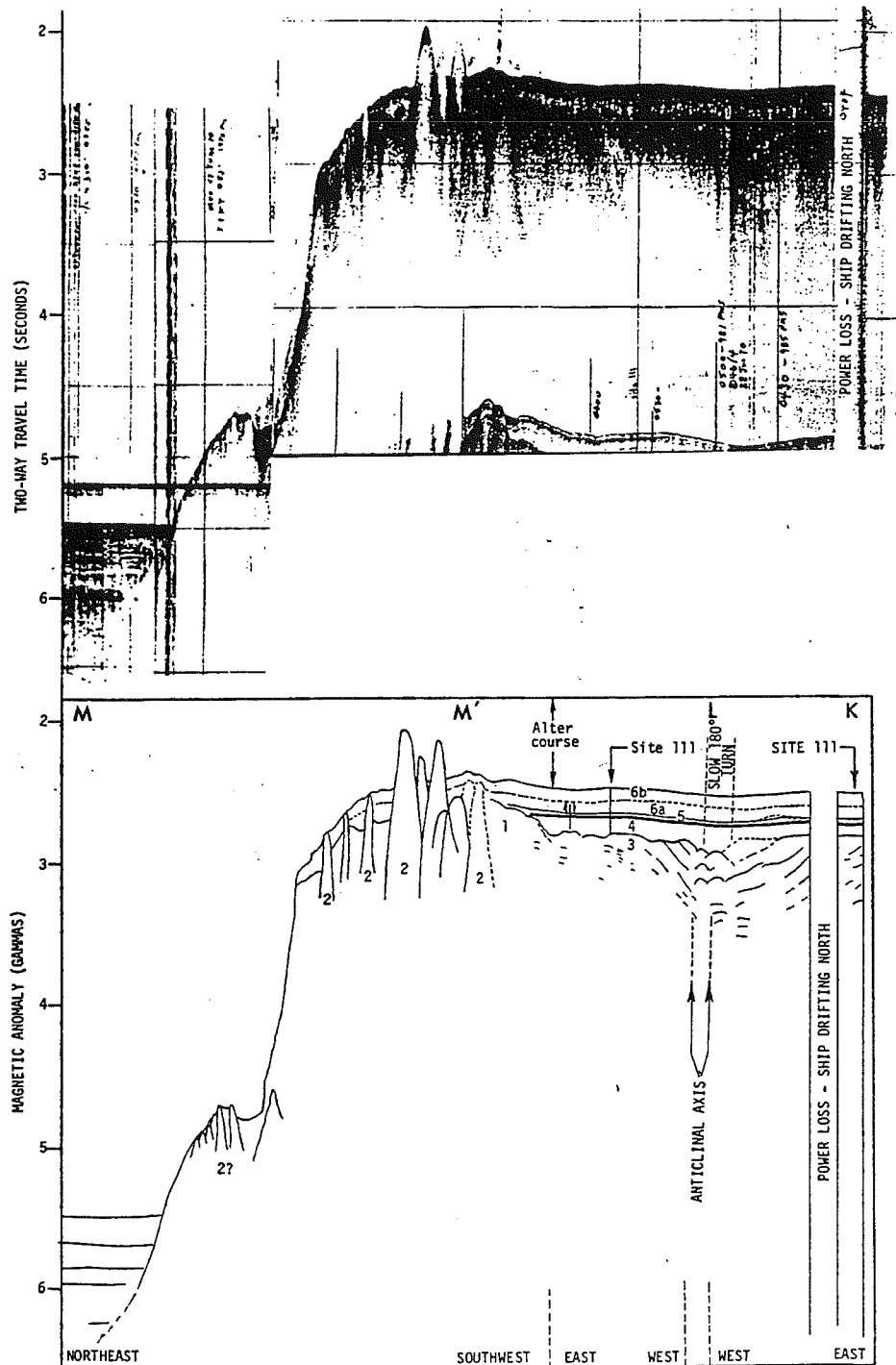


Figure 1.3-5a: A continuous seismic profile along lines K-L and L-M
 b: Line interpretation of same profile (from Laughton et al., 1972).

Most seismic transects show a series of bathymetric heights rising 200 - 300 m above the relatively flat upper surface of the knoll, puncturing the cover of younger sediments (labeled 2 on the line interpretations). These mounds have been interpreted as erosional remnants of a patch reef environment or mature Karst topography (e.g., Ruffman and van Hinte, 1989). Figure 1.3-6 shows the distribution of mounds on top of Orphan Knoll, superimposed on a simplified bathymetry. A biological dredge performed on the knoll in 1971 by the USNS Lynch cruise of the U.S. Naval Oceanographic Office, contained talus material which identified these mounds as Devonian-aged, shallow-marine limestone outcrop (Ruffman and van Hinte, *op. cit.*).

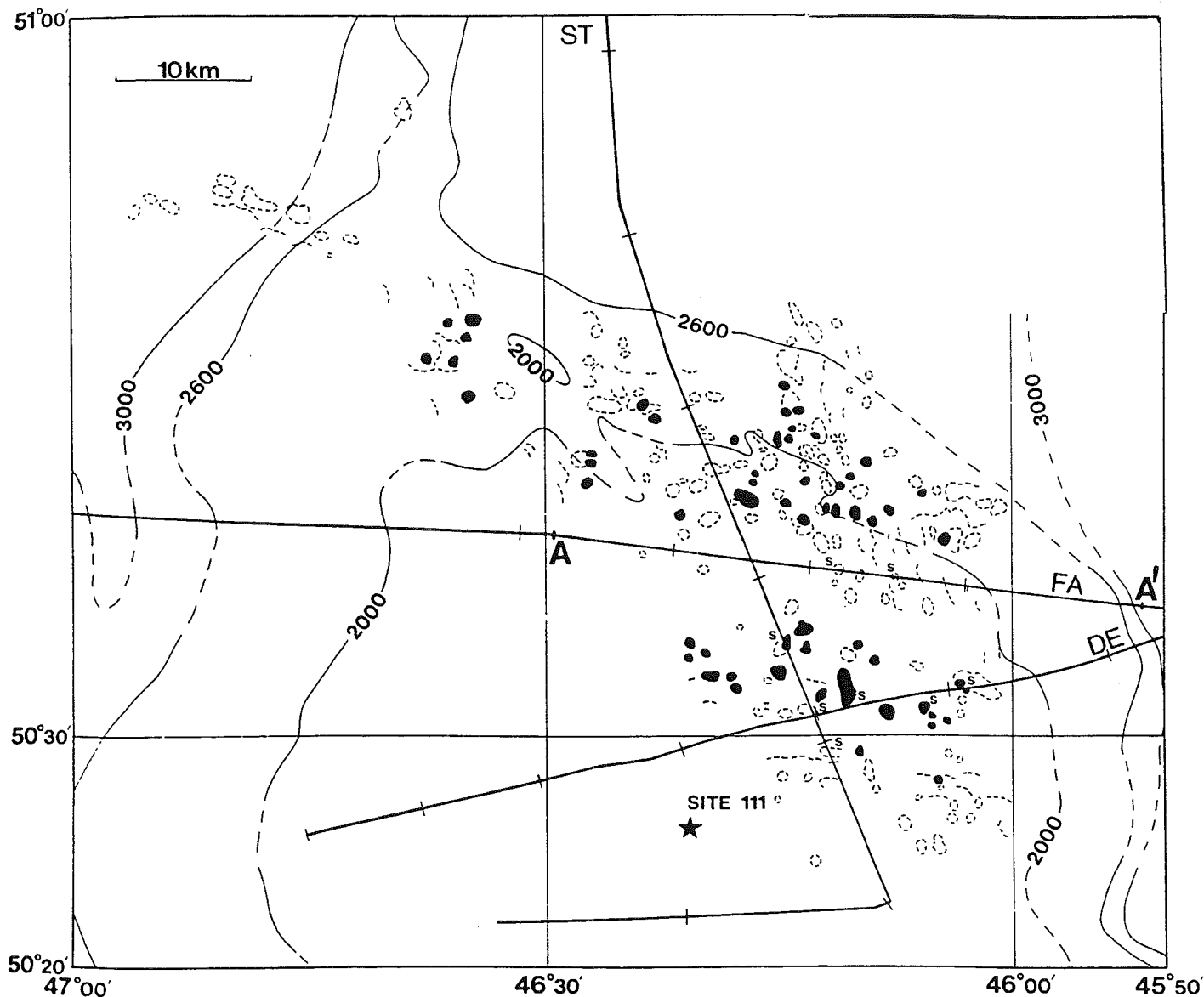


Figure 1.3-6: Distribution of mounds on top of Orphan Knoll. The black shaded features are mounds definitely located from perpendicular seismic tracks, the unshaded features were observed from only one direction (from Parson et al., 1984).

The discovery of Devonian limestone bedrock confirmed that Orphan Knoll is actually a piece of continental crust; it has been a relatively positive element throughout much of its history, lying close to sea level since at least the Devonian.

Reconstructions of the paleo North Atlantic show Orphan Knoll as originally part of the supercontinent Laurasia. At some point during the late Triassic - Early Jurassic, a thermal upwarping occurred in the Newfoundland / Labrador coast area as a precursor to continental rifting. Because of this tectonic activity, Orphan Knoll experienced subaerial exposure while it was situated at a paleolatitude of about 15 degrees south of the equator. Presumably, development of Karst topography followed as the knoll was subjected to erosional processes in a warm, wet, tropical climate.

In the lower Cretaceous Orphan Knoll began to subside, with concurrent deposition of shallow-water limestones - probably as a result of the first marine separation between Europe and North America (Figure 1.3-7).

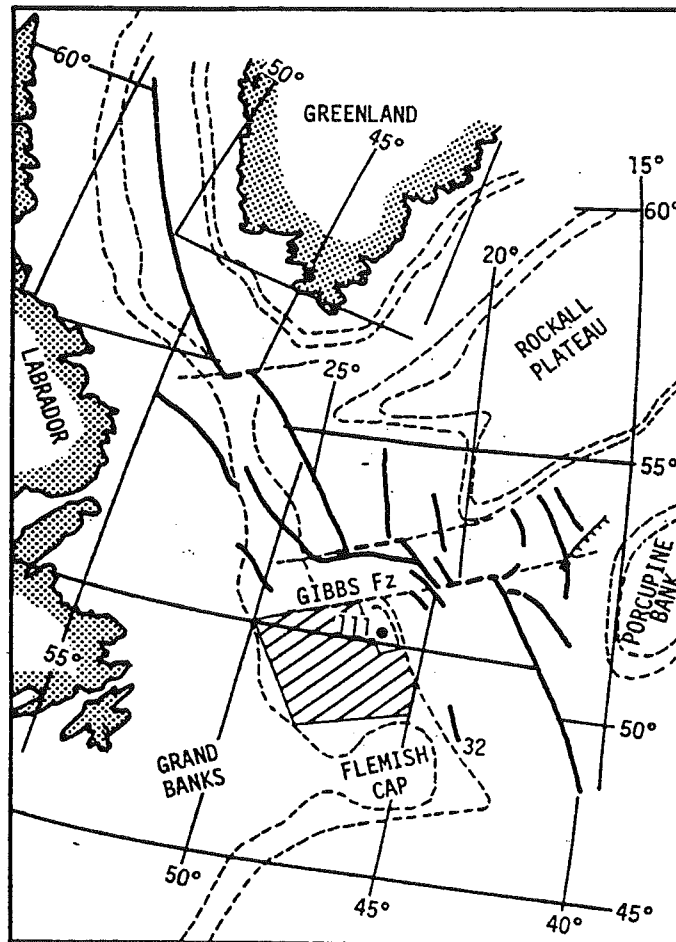


Figure 1.3-7: A reconstruction of the North Atlantic 72 million years BP. The shaded area of Orphan Knoll and environs is an area of continental crust which subsided early in sea-floor spreading. Black lines are magnetic anomalies, transform faults are heavy dashed lines, shelf edges are dashed lines paralleling continental margins (from Laughton, et al., 1972).

The knoll continued to sink until the early Tertiary; its maximum depth was reached by Eocene times. Subsequently, sediment accumulating on the upper surface caused Orphan Knoll to become progressively shallower from the Eocene to the present. Throughout its sinking history, the sedimentation rate has fluctuated: for the last 3 million years sediment with a high glacial content has been added to the knoll at the relatively-high average rate of 6.2 cm / 1000 yrs. (Figure 1.3-8).

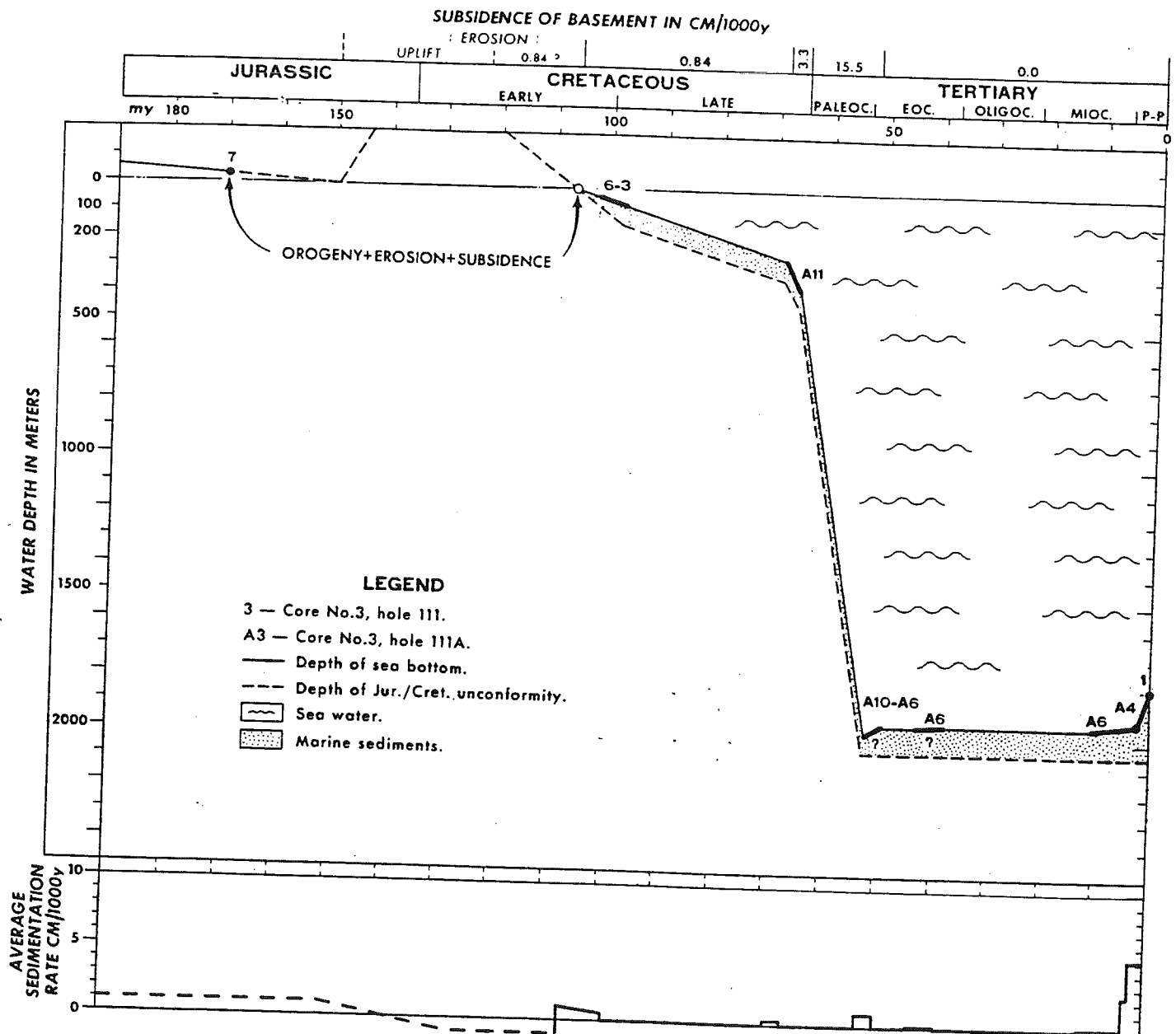


Figure 1.3-8: Sinking history of Orphan Knoll with sedimentation rates through time (from Laughton, et al., 1972).

Further study of Orphan Knoll was undertaken in June, 1978 by the Atlantic Geoscience Centre of the Bedford Institute of Oceanography on the Hudson 78-020

cruise. Two rock dredges were carried out and are listed in Table 1; these were the sources of the unexpectedly-exhumed, deep-water corals mentioned earlier.

<u>Rock Dredge Station No.</u>	<u>Day/Time of Bottom Contact</u>	<u>Latitude</u>	<u>Longitude</u>	<u>Uncorrected Depth</u>
001	192/0705 GMT	50°33.00'N	46°11.60'W	890 fm (1628 m)
002	192/1335 GMT	50°33.33'N	46°10.05'W	980 fm (1792 m)

Table 1: Hudson 78-020 Rock Dredge Stations

The dredge stations recovered 23.4 kg of dead, manganese-coated corals, as well as a small number of Gorgonian octocorals and lithistid sponges. Many of the specimens are quite complete; one pseudocolony is 3.0 kg in weight and 28 cm long, inevitably becoming nicknamed 'The Bouquet'. Most of the 189 pieces of coral retrieved displayed at least some evidence of bioerosion, while many possessed adhering bryozoan growths, serpulid and sabellid worm tubes, *etc.*

The corals were initially identified as *Cyathoceras diomedae*, and were subsequently stored at the Bedford Institute of Oceanography for the next several years. At some point more than 50% of the coral specimens were discarded because of space problems. Alan Ruffman (one of the scientific party aboard the dredging vessel) maintained an interest in these corals, however, and his persistence eventually ensured their serious assessment. He garnered the interest of Dr. Michael Risk; together they were awarded a research agreement to undertake an investigation on the archived deep-water corals.

1.4 Deep-Water Coral

1.4.1 Overview

The word coral usually elicits an image of palm trees, tropical breezes and the crashing surf, but in defiance to this stereotype, there are many cold- and/or deep-water species. As a further contrast, these taxa are usually solitary (non-colonial), azooxanthellate (without symbiotic algae inhabiting their tissues) and ahermatypic (non-reef building).

Throughout the geological column, it appears that most successful reef builders have had a symbiotic relationship with algae (Cowen, 1983). The fossil record from the early Mesozoic shows little evidence of shallow-water coral-reef development. The algal symbiosis necessary for reef building is thought to have evolved in the late Triassic, thereby initiating the ecologic differentiation of the two groups of corals (Stanley, 1981). Benton (1986) suggested that the impetus for this change was a profound mass-extinction event: certainly the fossils of the Jurassic and succeeding geological periods reveal ahermatypic coral communities as distinctly separate from the hermatypic taxa (Wells, 1956). This is usually explained in terms of competition - when zooxanthellate species are excluded from an environment due to restrictive conditions, azooxanthellates can flourish in relatively-shallow water. In less-than-optimum, non-reef settings, azooxanthellates can coexist with zooxanthellates, however, they are generally outcompeted and relegated to cryptic habitats on shallow-water reefs.

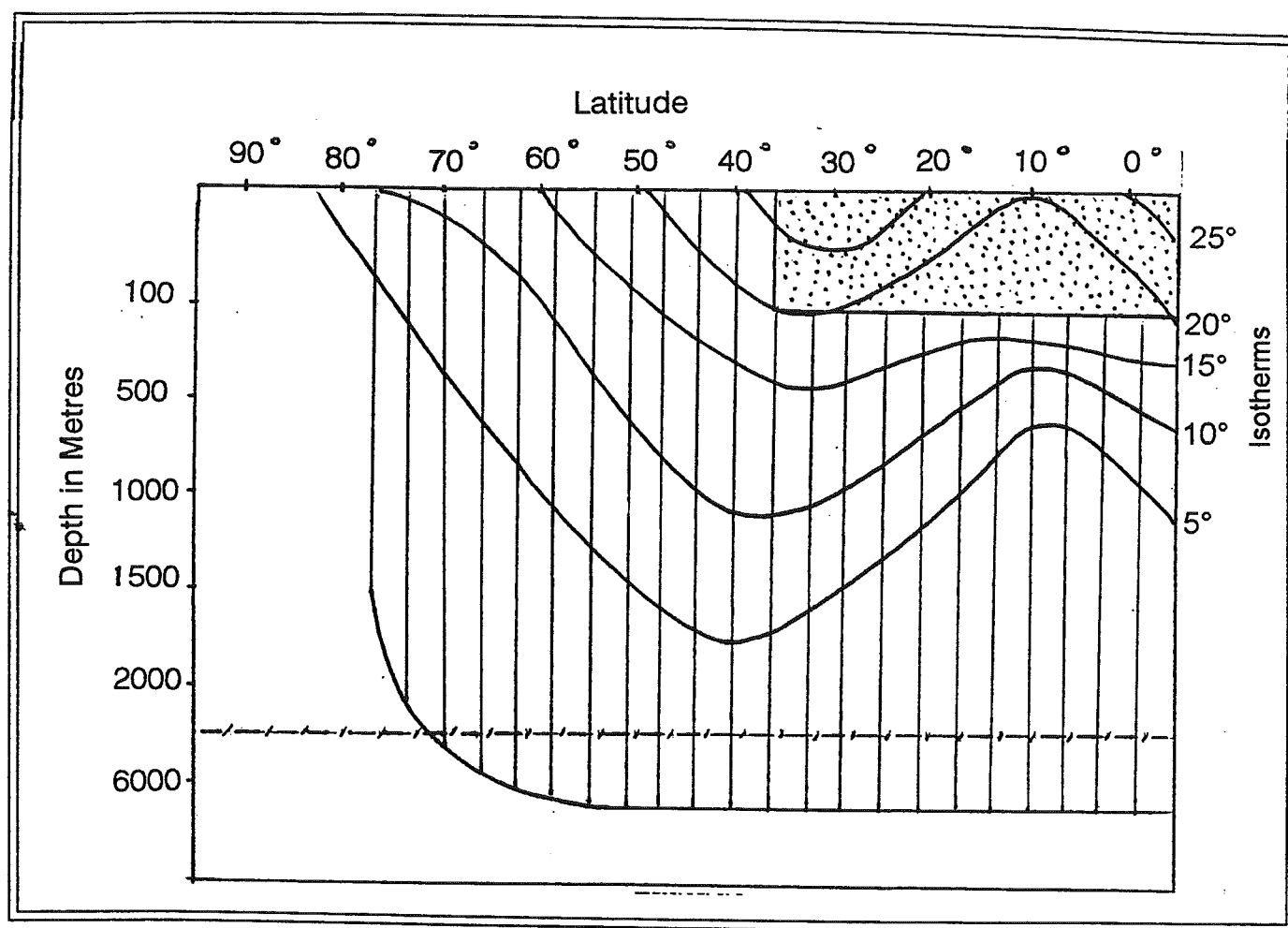
Azooxanthellates comprise a significant fraction of Holocene scleractinia - 90 of the 190 genera and about 560 of the 1500 species belong to this group. Character may be ecologically influenced, however, as some species can exist in either condition (apozooxanthellate). For example, in shallow water *Oculina varicosa* grows as golden-brown, wave-resistant colonies with stout branches and a base that firmly encrusts onto

rocks. In deep water it forms colonies 1 to 1.5 m in height, with fragile, tapering branches that are pure white in colour, since they lack zooxanthellae (Reed and Jones, 1982).

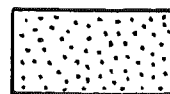
Factors essential to ahermatypic coral establishment appear to include hard substrates accompanied by sufficient submarine topography, vigorous current activity with an abundance of nutrients carried in the currents and cool water temperatures (Stanley and Cairns, 1988). Zooxanthellate coral are restricted, geographically and bathymetrically, to shallow, tropical waters by their algal symbionts. Azooxanthellates experience no such restrictions, so can attain wider distributions. They occur in all major oceans, from 0 - 6200 m, -1 to 29°C and from the Norwegian Sea (70° N) to the Ross Sea, Antarctica (78° 24' S) (Figure 1.4-1).

Under favourable conditions, ahermatypic corals can produce constructional frameworks i.e., slow-growing mounds which trap sediment and skeletal debris and provide niches for other organisms. Usually, one or two species predominate as framework builders, but harbour a rich diversity of other invertebrates and fish. The composition and abundance of scleractinians varies for coral banks of different geographic localities: for example, *Lophelia prolifera* is a prime constructor of framework in the western Atlantic, while south Pacific structures are dominated by *Solenosmilia variabilis* (Stanley and Cairns, 1988).

A deep-water coral structure can produce a pronounced topographical feature, which can be classified according to a 'colony - thicket - coppice - bank' scheme (Squires, 1964) depending upon its stage of development (Figure 1.4-2).



Ahermatypic Coral



Hermatypic Coral

Figure 1.4-1: Distribution of modern hermatypic and ahermatypic corals (modified from Stanley and Cairns, 1988.)

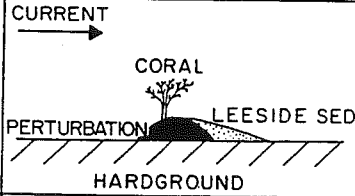
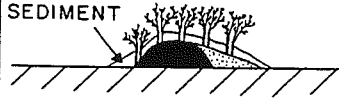
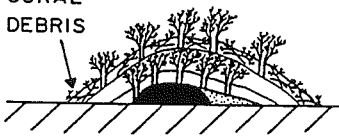
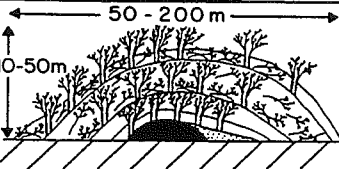
STAGE	DESCRIPTION	
COLONY		COLONIZATION OF A SEA-FLOOR PERTURBATION BY ISOLATED COLONIES. MODIFICATION OF BOTTOM CURRENTS BEGINS.
THICKET		AGGREGATION OF COLONIES. ECOLOGIC COMPLEXITY AND DIVERSITY INCREASES. BAFFLING/ TRAPPING ACTIVITY BEGINS.
COPPICE		ADDITION OF <u>IN SITU</u> SKELETAL DEBRIS PLUS TRAPPED SEDIMENT. DIVERSE BENTHIC FAUNA SUPPORTED BY CORAL DEBRIS.
BANK		SEDIMENTATION CONTINUES. STRUCTURE GROWS UP AND OUT. CAP OF LIVING CORAL. CIRCULAR TO ELLIPTICAL IN PLAN VIEW

Figure 1.4-2: The development of deep-water coral mounds (from Mullins et al., 1981).

The first recorded discovery of a deep-water coral bank was in 1865 off the coast of Norway. Since then, continued exploration of the sea has shown these structures to be widely distributed in a variety of physical and biological settings throughout the world's oceans.

1.4.2 *Desmophyllum cristigalli*

The coral dredged by the research vessel Hudson was identified as *Desmophyllum cristigalli* by Dr. Stephen Cairns of the National Museum of Natural History, Smithsonian Institution in Washington, D.C. (Plates 1 and 2). Complete taxonomy is as follows:

Phylum Cnidaria
Class Anthozoa
Subclass Zoantharia
Order Scleractinia (Bourne, 1900)
Suborder Caryophylliina (Vaughan and Wells, 1943)
Superfamily Caryophylliica (Gray, 1847)
Family Caryophylliidae (Gray, 1847)
Subfamily Desmophylliinae (Vaughan and Wells, 1943)
Genus *Desmophyllum* (Ehrenberg, 1834)
D. cristigalli (Milne, Edwards and Haime, 1848)

D. cristigalli is a large, robust solitary species of trochoid form that fixes itself to suitable hard substrates. It often attaches to others of the same species, forming pseudocolonial clumps, and implying rather long-lived individuals (Dr. Helmut Zibrowius, Université d'Aix-Marseille, personal communication to A.S. Ruffman, 1990). Cairns (1982) described the corallum of *D. cristigalli* as variable in shape, from cylindrical to hornlike, and often quite flared. A salient feature of this species is the thick pedicel for firm attachment to a substrate. The theca is thick, covered by low, fine, rounded granules and features ridged costae. Septa are thick, widely spaced and hexamerally arranged in five cycles - the first two cycles are equal in size and exsert, whereas septa of the remaining cycles become progressively smaller and less protruding. The septa have straight edges and smooth faces, which are also covered by low, rounded



Plate 1: Large pseudocolony of *Desmophyllum cristigalli*, called Coral 1 or 'The Bouquet'

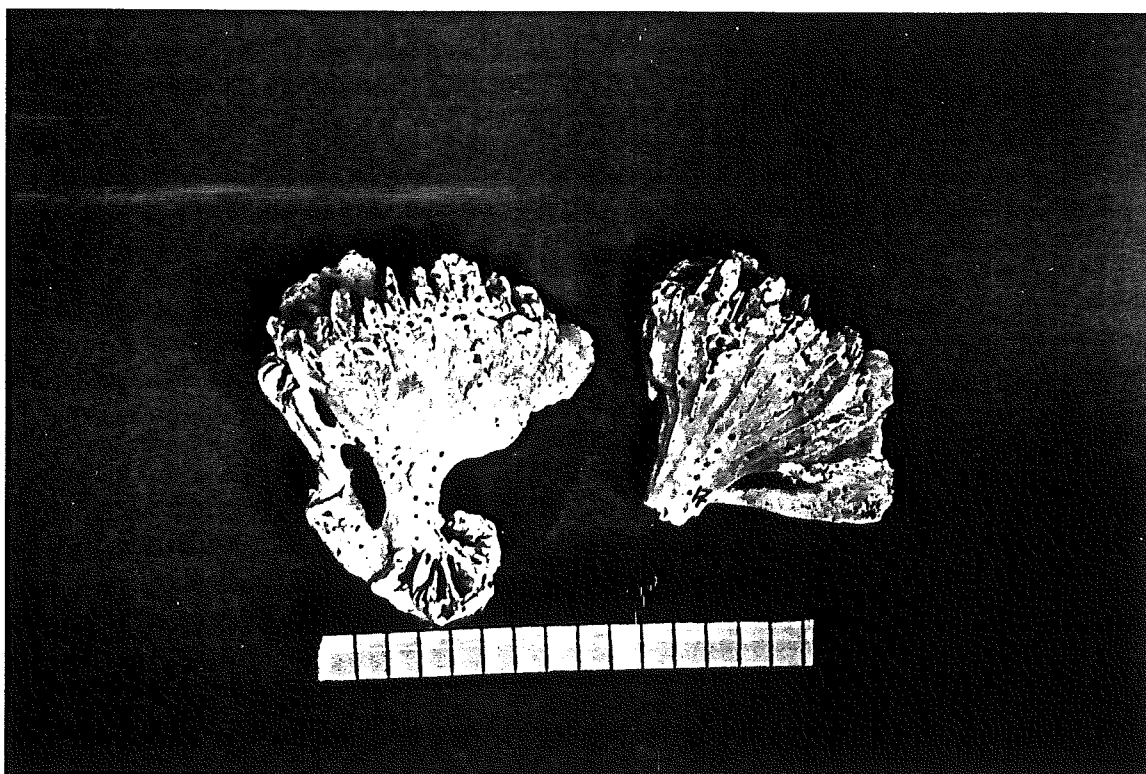


Plate 2: Two individual corallites of *D. cristigalli*

Photographs courtesy of Victor Plichota, Antares Tech.

granules. The fossa is relatively deep; dissepiments and columella are sometimes present (Figure 1.4-3).

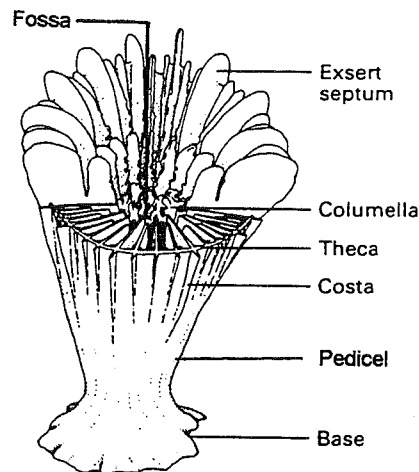


Figure 1.4-3: Principal morphological features of a solitary scleractinian coral (from Oliver and Coates, 1987).

D. cristigalli is one of the few cosmopolitan species of Scleractinia, being widely distributed in the Atlantic, Pacific and Indian Oceans, at depths ranging from 35 - 2460 m. For instance, it is known to be the framework coral of a deep-water (334 m) coral bank on the Campbell Plateau, New Zealand and is thought to form a Chilean structure at depths of 300 - 800 m.

Generally, *D. cristigalli* prefers to inhabit vertical rock faces and the underside of ledges, but has been observed to flourish on other objects affording a hard surface for attachment, such as telephone cables and airplane wrecks (Dr. Barbara Hecker, Columbia University, personal communication to A.S. Ruffman). Its orientation is frequently downward facing, presumably to minimize sediment loading (Plates 3 and 4). Individuals or pseudocolonies may break off from the substrate when they become too large, are knocked by fish or are caught in rockslides. As a result of these processes,

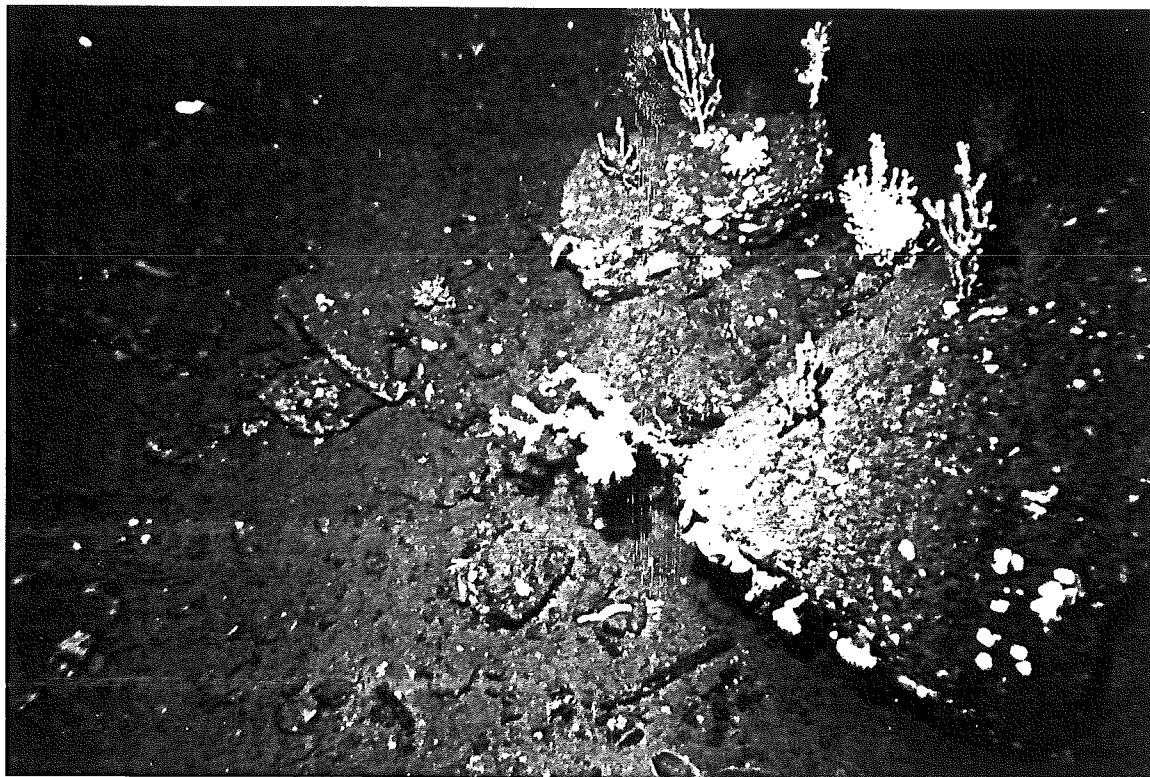


Plate 3

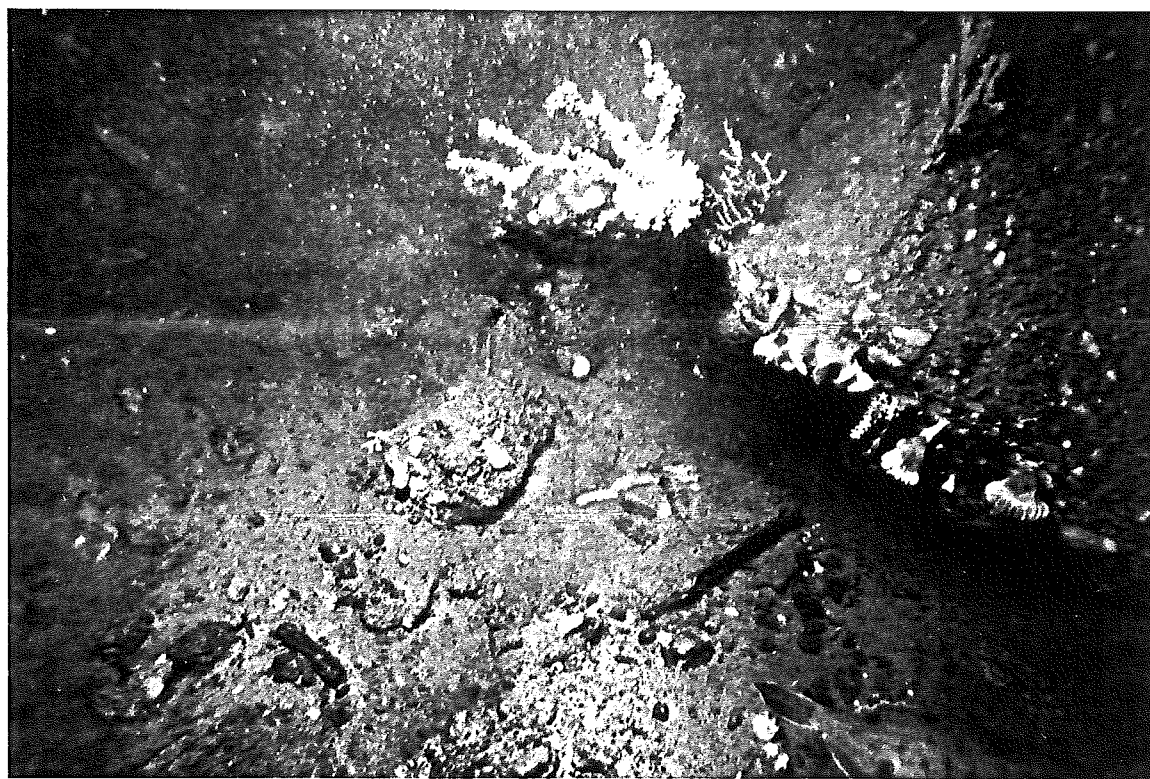


Plate 4

Desmophyllum cristigalli attached to the lower surfaces of talus blocks from the east wall of Oceanographer Canyon (723m), obtained on Alvin dive 1035 in 1980. Also present are erect sponges, a variety of soft corals and a four-spot flounder. One of the photographs is murky due to the resuspension of sediment by the movement of Alvin. (Photographs courtesy of Page Valentine, U.S. Geological Survey).

large quantities of dead corals are frequently found amongst the talus at the bases of cliffs. Given *D. cristigalli*'s habitat selection, one would not expect the Hudson dredge bucket to sample members of a living community, but rather to retrieve dead corals from the talus piles. It is likely that this early burial prevented excessive skeletal breakdown, thereby contributing to the excellent preservation of most of the dredged specimens.

1.4.3 Results of Previous Work

After a visit to the Bedford Institute of Oceanography in October, 1989, Dr. John Andrews of the Department of Geological Sciences at the University of Colorado at Boulder, voluntarily arranged radiocarbon age determination for one of the archived coral samples. Geochron Laboratories of Krueger Enterprises, Cambridge, Massachusetts was chosen to perform the analysis, and on March 3, 1990 reported an age of $29,270 \pm 960$ C-14 yr BP (C-13 corrected). A $\delta^{13}\text{C}$ PDB value of -2.9‰ was also returned.

Dr. Andrews was subsequently sent another piece of coral, designated by the A.G.C. as sample '78020-001 Bucket 112'. He submitted one fragment to the Center for Geochronological Research, INSTAAR, University of Colorado at Boulder for Uranium / Thorium dating, amino acid racemization dating and stable-isotope analysis. The remainder of the specimen was sent to the NSF-Arizona AMS facility at the University of Arizona, Tucson for an accelerator radiocarbon date. The Center for Geochronological Research reported a final U/Th disequilibrium date of $13,600 \pm 300$ yr BP on January 14, 1992. The Amino Acid Geochronology Laboratory returned a mean D-alloisoleucine to L-isoleucine ratio of 0.085 ± 0.011 , placing the age of the sample to within the late Pleistocene (10 - 125 ka). Results of stable-isotope analysis were reported on May 7, 1992 as $\delta^{13}\text{C} = -5.32\text{‰}$ and $\delta^{18}\text{O} = 2.16\text{‰}$ relative to PDB. On April 9, 1992, the University of Arizona disclosed that the accelerator radiocarbon date was $11,525 \pm 105$ yr BP.

Finally, a third coral - the largest pseudocolony in the collection - was dated at the request of Dr. P.J. Mudie at the Atlantic Geoscience Centre (Coral 1 of this study). One sample was taken from the bottom of the lowest pedicel base and another was extracted from a septum at the top. Three small, immature buds from the uppermost

collected. All three samples were submitted to the Isotrace Laboratory at the University of Toronto: the first two for high-precision radiocarbon analysis, and the buds for a normal precision procedure. Isotrace returned ages (corrected for a 410 yr reservoir effect) of $12,370 \pm 90$ yr BP for the base of the colony, $11,130 \pm 80$ yr BP for the septal sample, and 50 ± 70 yr BP for the buds.

See Appendix 1 for copies of original notifications.

1.5 Hypothesis

The first three coral specimens returned a variety of dates, suggesting that the collection could represent an entire suite of late Quaternary ages. As noted earlier, stable-isotope data can yield information regarding the isotopic composition of the ambient seawater, and can subsequently allow assessment of paleoclimatic / paleoceanographic conditions. It was hypothesized that stable-isotope analyses of individual corals of different ages could be used as a tool for the long-term reconstruction of paleoecologic patterns - specifically, those relating to glacial events.

To date, reconstructions of oceanic conditions have generally been based on the foraminiferal record from sediment cores: deep-water coral, while not as ubiquitous as Foraminifera, may be superior recorders of ocean-bottom conditions. In areas where sedimentation rates are relatively low (such as Orphan Knoll throughout much of its history), it may prove difficult to obtain records of isotope stratigraphy from deep-sea cores. Even where sedimentation rates are high, bioturbation can greatly reduce age accuracy of the data. Dawson (1992) estimated that the most precise time resolution one might hope to obtain from a core is approximately 1000 years. Fairbanks (1989) commented that the effects of bioturbation must be considered as significant in an investigation of a chronozone as condensed as the Younger Dryas, and stressed that subtle shifts in age assignments can alter the interpretations of deep-ocean response to glacial cycles. To ascertain the magnitude of bioturbation effects, Bard et al. (1987) created a computer model to simulate the last deglaciation. They plotted abundance patterns and $\delta^{18}\text{O}$ records of cool- and cold-water Foraminifera and found that 'following' bioturbation, substantial leads and lags occurred in the paleoclimatic record (Figure 1.5-1).

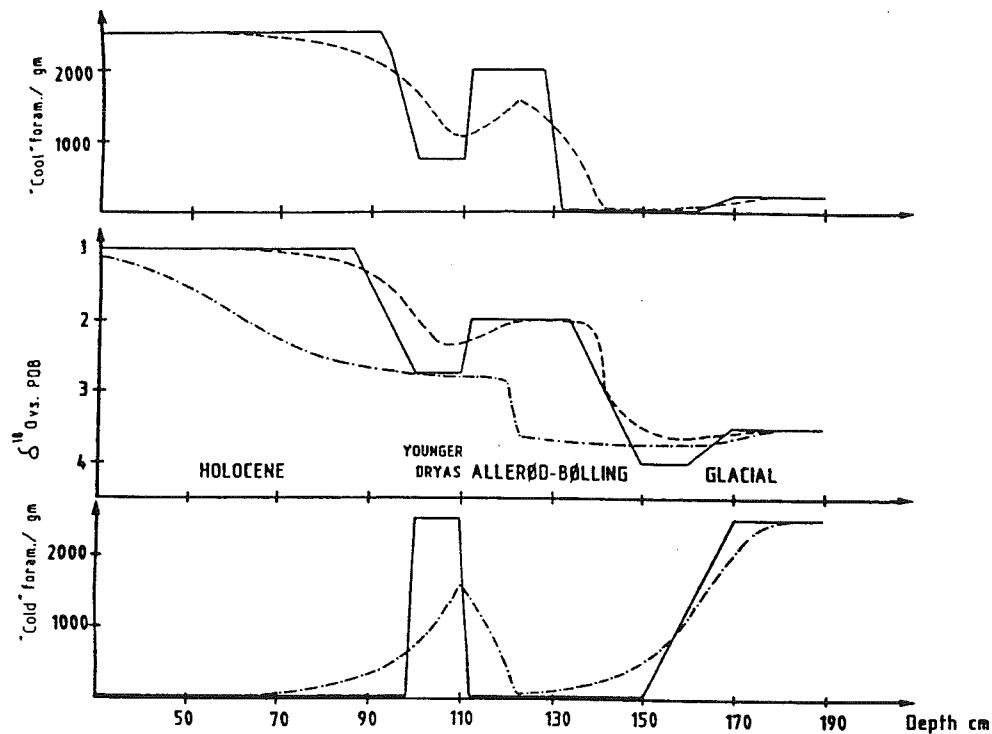


Figure 1.5-1: Simulation of the last glacial termination. Solid lines = assumed input signal without bioturbation, short dashes = bioturbated record for cool-water Foraminifera, dash-dot = bioturbated record for cold-water Foraminifera (from Bard et al., 1987).

Ruddiman et al. (1984) also discussed the effects of bioturbational mixing on climatic records and concluded that the most serious consequences are amplitude suppression, gradient reduction and translational offsets (Figure 1.5-2). These three effects act as filters which smooth original paleoclimatic curves. Since the magnitude of the mixing processes is usually unknown, it is virtually impossible to remove the smoothing effects from the data and restore the actual climatic record.

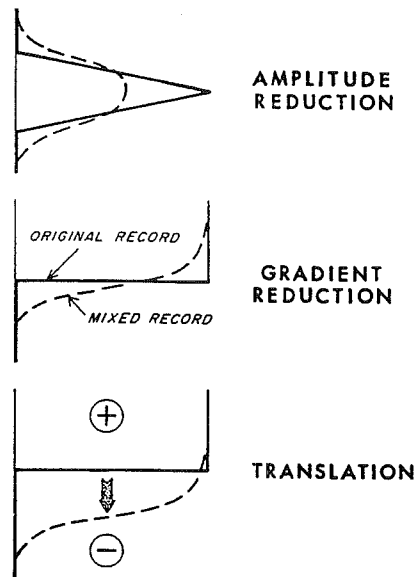


Figure 1.5-2: Major categories of bioturbation effects typical in deep-sea paleoclimatic records (from Ruddiman et al., 1984).

Isotope data are only useful if the isotopic composition of foraminiferal tests is a function of the surrounding ocean waters; this is not the case for all species.

Calculations of isotope ratios are often performed on mixed species of Foraminifera, which compounds the problem and leads to ratios of dubious accuracy. Correlation problems may be exacerbated by certain foraminiferal species that secrete carbonate only during specific months of the year and those that migrate through the water column during secretion. Furthermore, it is unlikely that corals have been transported, in contrast to the conceivably large displacements experienced by Foraminifera.

Submarine landslides, turbidity flows and bottom currents have the potential to significantly alter the spatial and temporal distribution of microfossils: erosional gaps are left in some records, while other sequences are thickened with redeposited sediments.

The immunity of corals to the confounding effects of fluctuating sedimentation rates, bioturbation, inconsistent calcification, taphonomic transport, etc., suggests that

accurate chronicling of isotopic fluctuations is possible. Even if the coral account should not prove to be superior to the foraminiferal record, it should serve to supplement existing paleoclimatic data.

2 Methods

2.1 Preparation

In June 1992, 55 of the archived coral specimens were brought to McMaster University from the Bedford Institute of Oceanography. From this population, 14 pieces of *D. cristigalli*, each at least 50 g in weight, were selected essentially at random. In order to facilitate laboratory analyses, the manganese coating was removed using the procedure described by Fitzgerald et al. (1987). This method, which involved soaking the samples in 1 M hydroxylamine hydrochloride, was chosen because it left the underlying calcium-carbonate skeleton virtually undamaged.

A basic assumption of most geochemical analyses is that the test material was undisturbed by such influences as diagenesis, dissolution or recrystallization after its initial deposition, i.e., a closed system. For example, an indication that a piece of coral has been 'opened' by a post-depositional processes would be calcic replacement of the original aragonite. Prior to their analyses of Sample 78020-001-112, the Center for Geochronological Research produced an X-ray diffractogram of the specimen which showed it to be between 95 and 100% aragonite and suitable for further testing.

For this study, a portion of Friedman's (1959) procedure for the identification of carbonate materials was employed, namely Feigl's test (Figure 2.1-1). Feigl's test is quite sensitive, depending upon the slightly different solubilities of aragonite and calcite in water.

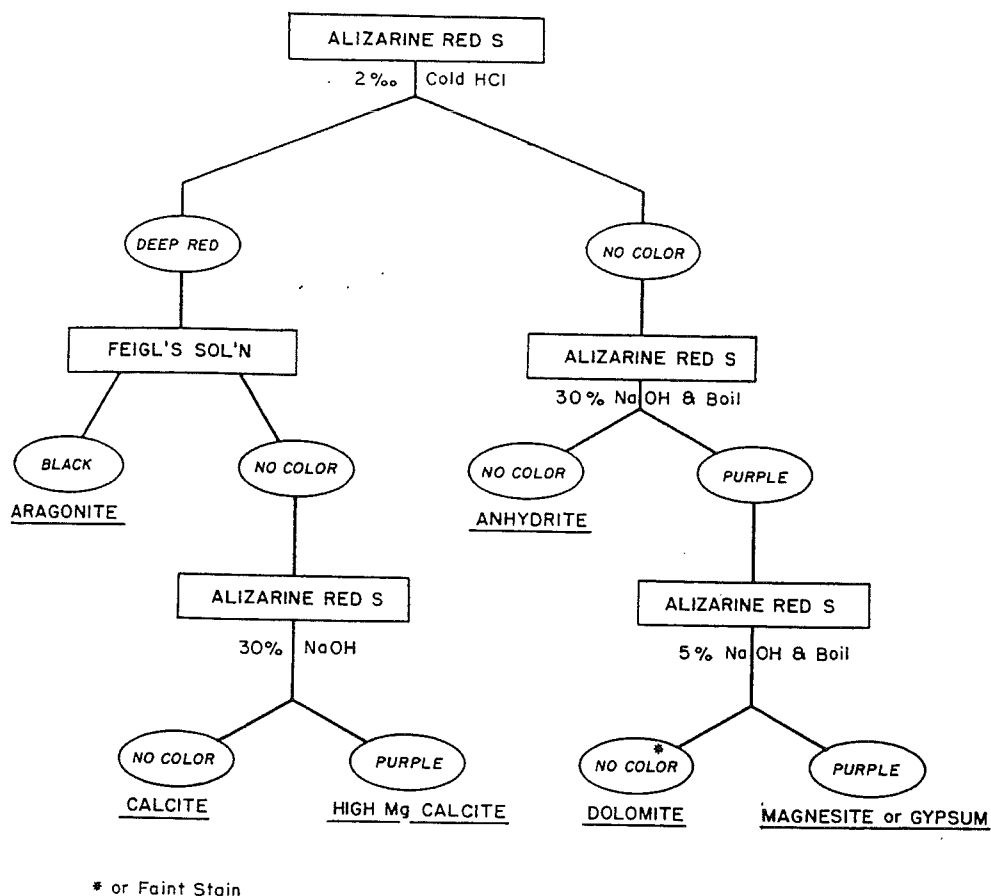


Figure 2.1-1: Staining procedure for identification of carbonate minerals (from Friedman, 1959).

The required reagent was prepared using the method described by Friedman (*op. cit.*) and pieces of cleaned, acid-etched coral were placed into it. The carbonate samples were stained black, which indicated an aragonitic composition free from significant recrystallization and suitable for use in further analyses.

2.2 Dating

Based on the results of Feigl's procedure, the corals were assumed to be 'closed systems', which permitted the use of a uranium-series dating procedure. U-series disequilibrium dating is based on the growth of an initially-deficient daughter (thorium-230) into equilibrium with the parent (uranium-234) (Figure 2.2-1).

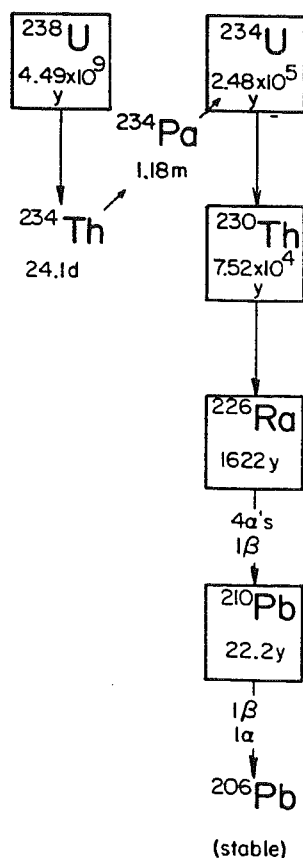


Figure 2.2-1: The radioactive decay series for ^{238}U . The longer-lived isotopes, typically used for dating, are outlined in boxes (from Schwarcz and Blackwell, 1985).

The procedure was feasible because uranium dissolves in seawater to form soluble UO_2^{2+} ions, while thorium is adsorbed onto the surfaces of clay or co-precipitated with hydroxides. When coral polyps precipitate CaCO_3 from the water, the uranium is co-

precipitated. ^{234}U concentrations in the carbonate precipitate may initially be several parts per million, with virtually no ^{230}Th present: over time, ^{230}Th will grow into equilibrium with ^{234}U . The relationship between $^{230}\text{Th}/^{234}\text{U}$ and $^{234}\text{U}/^{238}\text{U}$ ratios determines the age of the material tested (Figure 2.2-2)

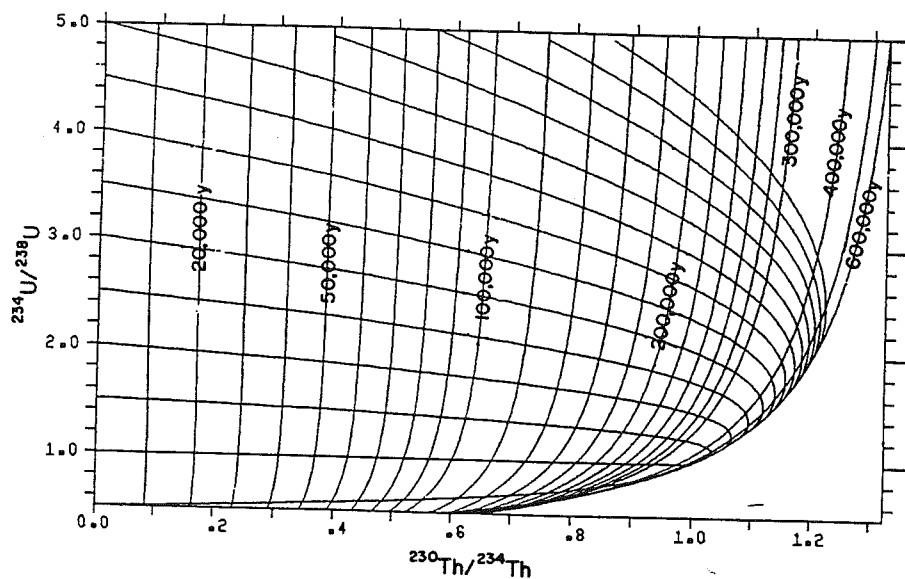


Figure 2.2-2: Relationship between $^{230}\text{Th}/^{234}\text{U}$ and $^{234}\text{U}/^{238}\text{U}$ ratios of closed systems. The subhorizontal curves are decay paths for samples initially free from ^{230}Th ; the steep curves are isochrons (from Schwarcz and Blackwell, 1985).

For this study, approximately 10g of skeletal material was removed from each of the 14 corals. The large pseudocolony, Coral 1, had portions extracted from both the bottom of the lowest pedicel base and a septum at the top - close to the areas previously sampled for ^{14}C -dating. The pieces were dissolved separately in nitric acid; anion-exchange techniques were then employed to separate uranium and thorium from the matrix. The amount of each retrieved element was ascertained using Thermal Ionization Mass Spectrometry. Dates were calculated by iterative solution of an age equation using a computer program written by Joyce Lundberg, Department of Geography, McMaster University in 1990.

2.3 Stable Isotopes

The first set of samples retrieved for isotopic analysis was from different morphological parts of a single skeleton, to ascertain if the distribution of carbon-13 and oxygen-18 varied throughout a coral. Approximately 8 mg of powdered material was collected from each of twelve sites on Coral 1, using a dental carbide burr. Of these, four samples were taken from the outer wall of the theca, four along a septum and the remainder from a cross-section of a broken pedicel (Figure 2.3-1).

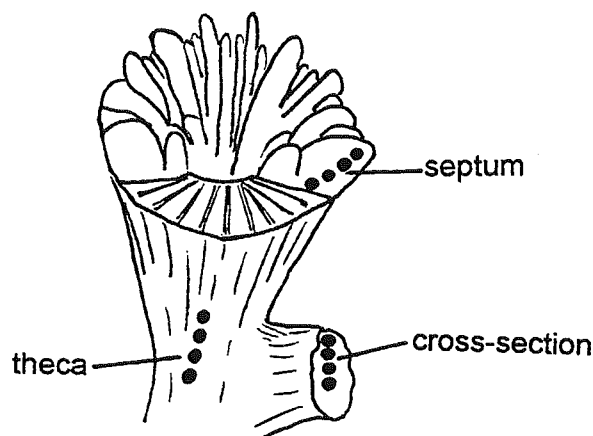


Figure 2.3-1: Sketch showing the first twelve sampling sites on Coral 1.

The coral powder was reacted at 25°C with 100% phosphoric acid, using a vacuum extraction line. The liberated CO₂ was subsequently extracted and purified under vacuum, using a dry-ice/isopropanol bath and liquid nitrogen. The resulting gas was analyzed in a SIRA Series II Isotope-Ratio Gas-Source Mass Spectrometer. Based on multiple analyses of the laboratory standard GCS, precision (reproducibility) of the chemistry and mass spectrometry was determined and is expressed by a standard deviation of 0.017 per mil for ¹³C and 0.208 per mil for ¹⁸O.

Data are expressed in delta notation, defined as the deviation in per mil of the isotopic ratios of the oxygen and carbon of the analyzed sample from that of a standard. In the case of oxygen:

$$\delta^{18}\text{O} = \left[\frac{(^{18}\text{O}/^{16}\text{O})_{\text{sample}} - (^{18}\text{O}/^{16}\text{O})_{\text{standard}}}{(^{18}\text{O}/^{16}\text{O})_{\text{standard}}} \right] \times 1000$$

A similar equation is used for carbon ratios. The standard in this study is the PDB standard from a Cretaceous belemnite from the PeeDee formation of South Carolina.

The results of the initial twelve samples are displayed in Table 2.

	Sample	$\delta^{13}\text{C}$	$\delta^{18}\text{O}$
Cross-section	A1	-5.493	0.547
	A2	-6.077	0.256
	A3	-5.231	0.931
	A4	-5.218	1.010
Septum	A5	-1.063	3.038
	A6	-1.126	3.144
	A7	-1.390	3.143
	A8	-1.147	3.035
Theca	A9	-0.924	2.711
	A10	-2.098	2.194
	A11	-2.056	2.247
	A12	-1.983	2.484

Table 2: Isotope ratios of twelve sites on Coral 1.

Large differences between isotope ratios from structurally-distinct areas of the same corallite demonstrated the need for consistency in subsequent samplings. The outer surface of the theca was selected as the anatomical feature best reflecting

the isotopic composition of the ambient seawater. Each sample from the theca represents a single episode of carbonate deposition, which occurred in physical contact with the surrounding water. In contrast, septa are in contact with the organic tissues of the coral polyp, so potentially are more affected by metabolic processes; the cross-section showed 'growth rings', implying nonconcurrent CaCO_3 precipitation.

Coral 1 was sampled along what appeared to be a line of continuous growth, from the lowest pedicel base to the uppermost calice. In total, 70 samples were collected, each about 3 mm apart (Plate 5). Another large specimen, Coral 10, had 22 samples extracted in a similar manner. The remaining thirteen corals were also sampled: 4 to 8 portions were taken from each, depending on its size. This suite of samples was subsequently analyzed for its isotopic composition, utilizing the procedure described earlier.

3. Results and Discussion

3.1 Dates

Of the fifteen samples submitted for mass-spectrometric uranium / thorium dating, twelve were successfully completed. The returned ages ranged from 4093 ± 22 to $76,628^{+422}_{-417}$ years old. Full data are presented in Appendix 2.

Most paleoclimatic reconstructions to date have been based on the foraminiferal record, and have most commonly used radiocarbon dating for their chronologies. It is now known that the ^{14}C timescale is not totally accurate, as the atmospheric reference level has changed through time. The disparity between true age and the carbon-14 age becomes increasingly problematic before 9,000 years BP: radiocarbon ages are consistently younger than true ages. The $\Delta^{14}\text{C}$ fluctuations have been correlated with variations in the Earth's magnetic dipole, which are inversely related to the production of ^{14}C by cosmic rays (Figure 3.1-1); short term oscillations result from changes of the solar wind's magnetic properties.

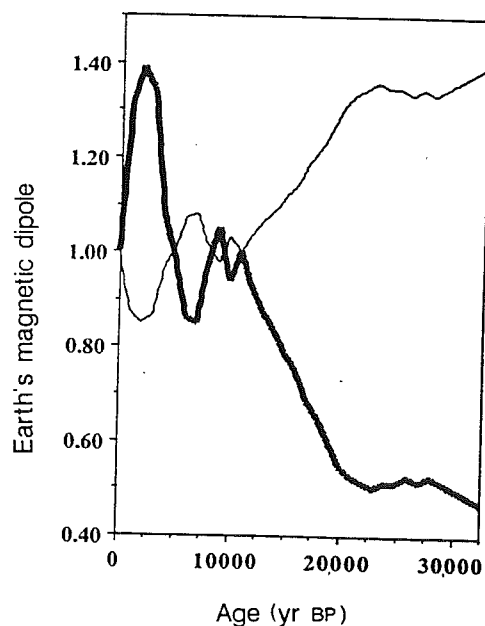


Figure 3.1-1: Magnetic dipole and ^{14}C production over time. Thick line = intensity of magnetic dipole, thin line = cosmogenic nuclide production (from Bard et al., 1990)

Current techniques for U/Th dating have proven to be very precise; extreme accuracy, by way of comparison with the dendrochronological calibration, has also been noted (Bard et al., 1990). Allowance must therefore be made for the age discrepancies inherent in any comparison between ^{14}C and U/Th dates. In this study, uranium-series disequilibrium ages older than 9,000 y BP were adjusted slightly to permit more accurate correlation with previously-attempted ^{14}C paleoclimatic reconstructions. Where necessary, adjustments were made using Figure 3.1-2, a plot comparing U/Th and carbon-14 dates from numerous coral specimens of varying ages.

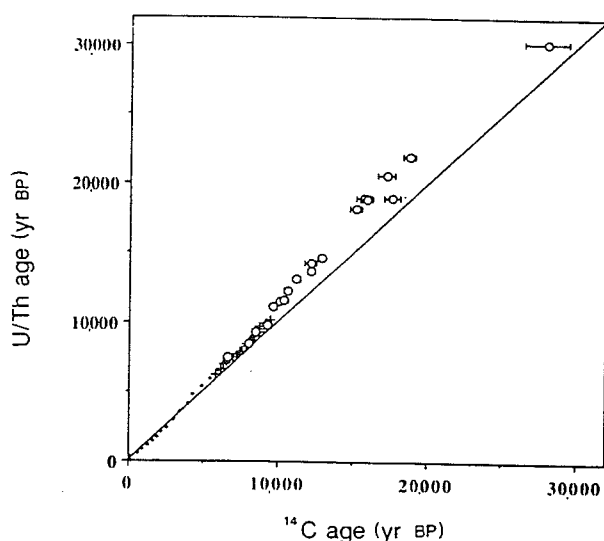


Figure 3.1-2: U/Th ages plotted against ^{14}C ages (open symbols). Small crosses = dendrochronological calibration, large crosses = varved sediment correlation (from Bard et al., 1990).

Thus, Coral 14, with a U/Th age of $14,095 \pm 104$ y BP was 'assigned' a ^{14}C -equivalent age of approximately 12,500 y BP. Coral 1 proved these date alterations to be justified: the top of the pseudocolony was dated by Isotrace, using high-precision

radiocarbon techniques, at $11,130 \pm 80$ y BP. In contrast, the U/Th date produced at McMaster was $13,822 \pm 49$ y BP, agreeing well with Bard et al.'s (*op. cit.*) predicted degree of dissimilarity for specimens of this general age. Unfortunately, the sample collected from the base of Coral 1 was not able to be U/Th dated - a further comparison with a ^{14}C age would have been interesting. Specimen 78020-001-112, sent to the Center for Geochronological Research in Colorado, showed a similar trend: it was dated by the uranium-disequilibrium technique at $13,600 \pm 300$ y BP, compared with a reported radiocarbon age of $11,525 \pm 105$ y BP.

3.2 Oxygen Isotopes

The complete set of oxygen-isotope data is presented in Appendix 2. The $\delta^{18}\text{O}$ results from three specimens, Corals 1, 14 and 27, were plotted against age (Figure 3.2-1). These specific corals were chosen because their ages correspond to immediate pre- and post-Younger Dryas times; it was hoped that the results would elucidate some of the details concerning this climatic episode.

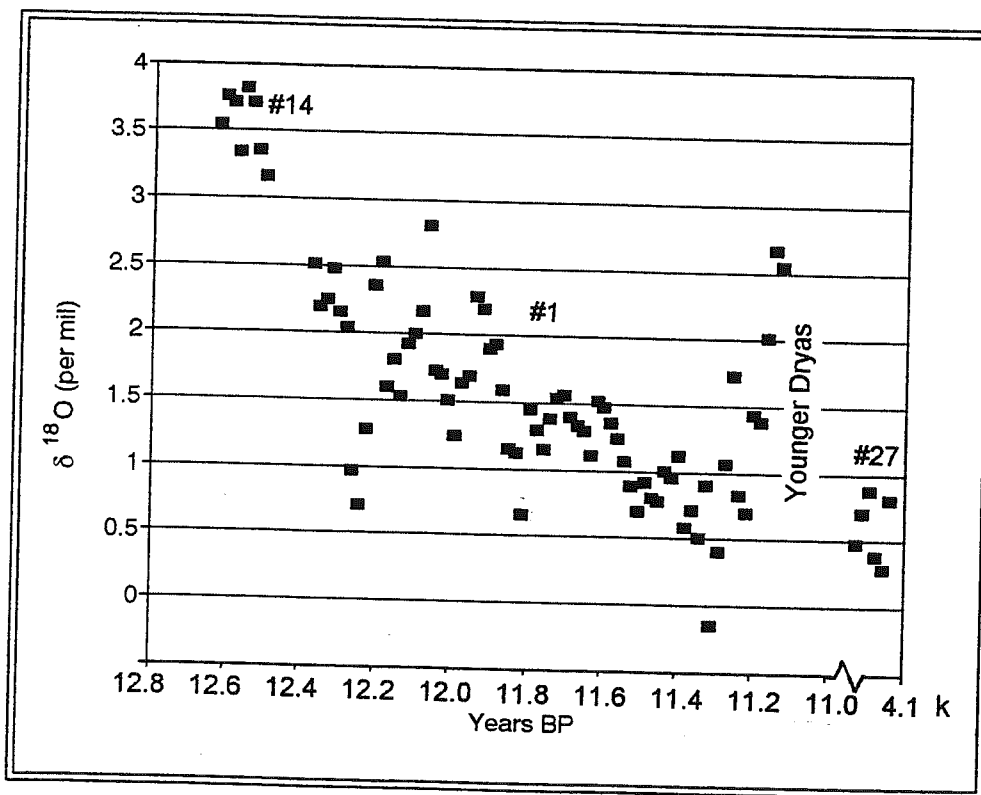
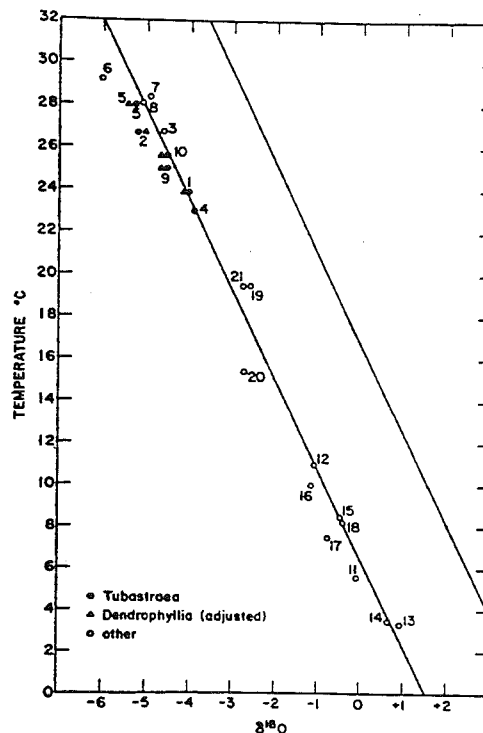


Figure 3.2-1: Plot of $\delta^{18}\text{O}$ data from Corals 1, 14 and 27 *versus* age.

In order to furnish data for paleoenvironmental interpretations, Weber (1973) measured $^{18}\text{O}/^{16}\text{O}$ ratios of numerous ahermatypic scleractinian corals and found, despite an apparent isotopic disequilibrium, that there were systematic relationships

between isotopic values and some environmental parameters. Skeletal $\delta^{18}\text{O}$ and water temperature were found to be closely related for ahermatypes over the entire temperature range of modern oceans (ca. 0 - 30°C). The relationship is linear and inverse, i.e., $\delta^{18}\text{O}$ values increase with decreasing water temperatures (Figure 3.2-2).



positively related in a linear fashion: increasing degrees of saltiness are coupled with elevated $\delta^{18}\text{O}$ per mil.

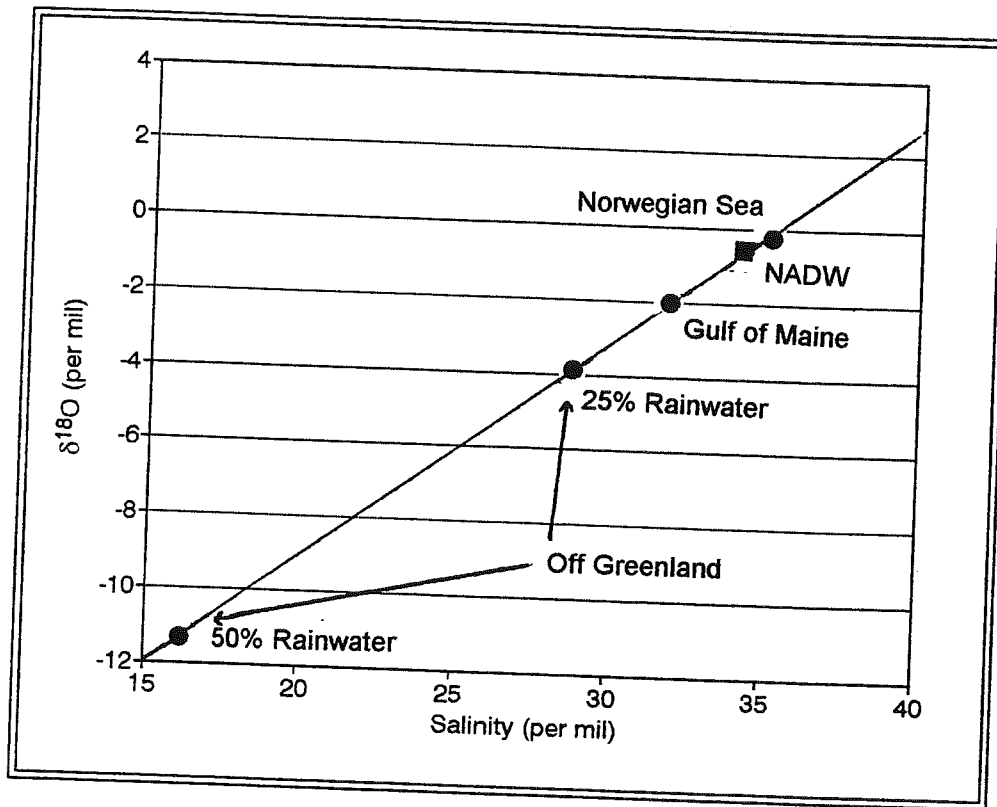


Figure 3.2-3: Plot of $\delta^{18}\text{O}$ versus salinity for water samples from the North Atlantic Ocean. North Atlantic Deep Water has a composition falling on the line because it consists dominantly of sinking water (from Broecker, 1974).

Specific interglacial and glacial characteristics of North Atlantic Deep Water were examined in an attempt to separate the effects of temperature and salinity. At the depth from which the corals were retrieved (ca. 1700 m), variations of water temperature appear to have been minimal. Estimates of the magnitude of bottom-water temperature drop during glacial times range from essentially nil (Broecker, 1982)

Observatory, Columbia University, provided a specimen of *D. cristigalli* which had been collected alive in the axis of Baltimore Canyon, at a depth of 1024 m. The coral was recovered in July, 1981 from the tail strut of a WW II Grumman 'Hellcat' airplane in use between 1943 - 1947. The supplied sample measured about 37 mm: assuming larval settlement shortly after emplacement of the airplane allows calculation of the growth rate to have been approximately 1 mm/yr. If this computed growth rate is also accurate for the Coral 1 data points, the timing of the Younger Dryas onset would be reduced to less than 30 years. Theories concerning the mechanism of abrupt climatic change that do not involve ocean-atmosphere reorganizations cannot generally account for extremely rapid interglacial to glacial transitions, such as the one observed in this study.

3.3 Carbon Isotopes

Carbon-isotope data are presented in Appendix 2; results from Corals 1, 14 and 27, were plotted against age and are displayed in Figure 3.3-1.

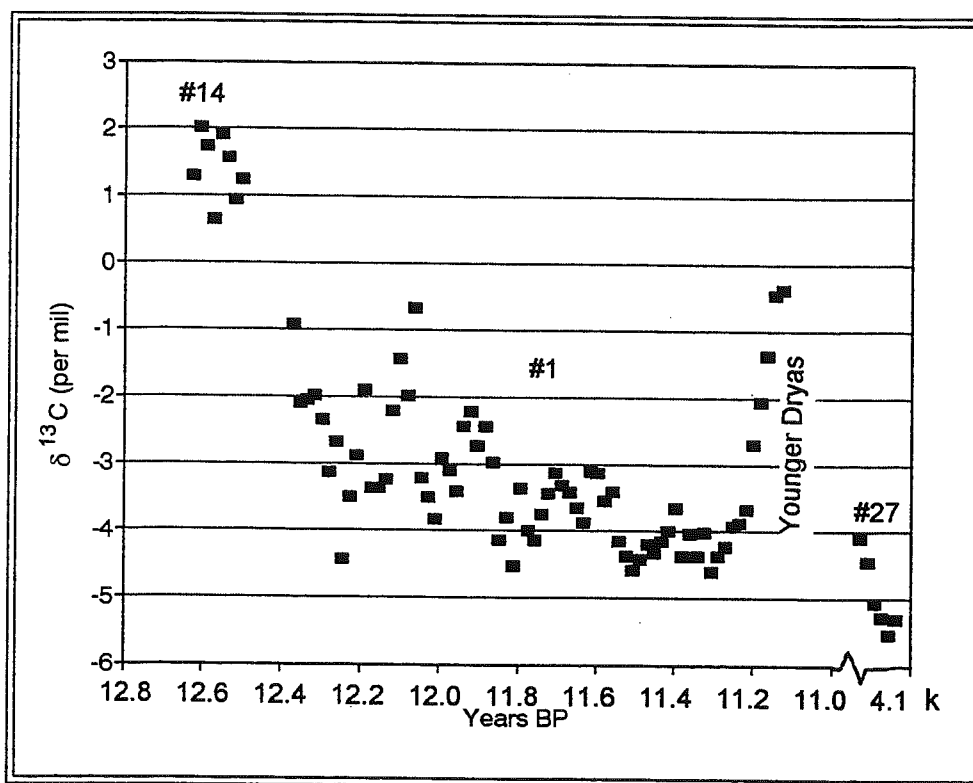


Figure 3.3-1: Plot of $\delta^{13}\text{C}$ data from Corals 1, 14 and 27 *versus* age.

The plotted ratios appear to follow closely the trend displayed by the oxygen-isotope data: a steady decline in $\delta^{13}\text{C}$ during initial deglaciation, a profound, abrupt rise at the beginning of the Younger Dryas with a subsequent decline to modern values. In order to ascertain the relationship, if any, between isotope ratios in the corals, a regression of $\delta^{13}\text{C}$ against $\delta^{18}\text{O}$ was performed. The regression yielded the equation

$$\delta^{13}\text{C} = 1.45 \delta^{18}\text{O} - 5.34 \quad (r = 0.872)$$

demonstrating a high degree of linear correlation between the two heavy isotopes and implying a functional linkage (Figure 3.3-2).

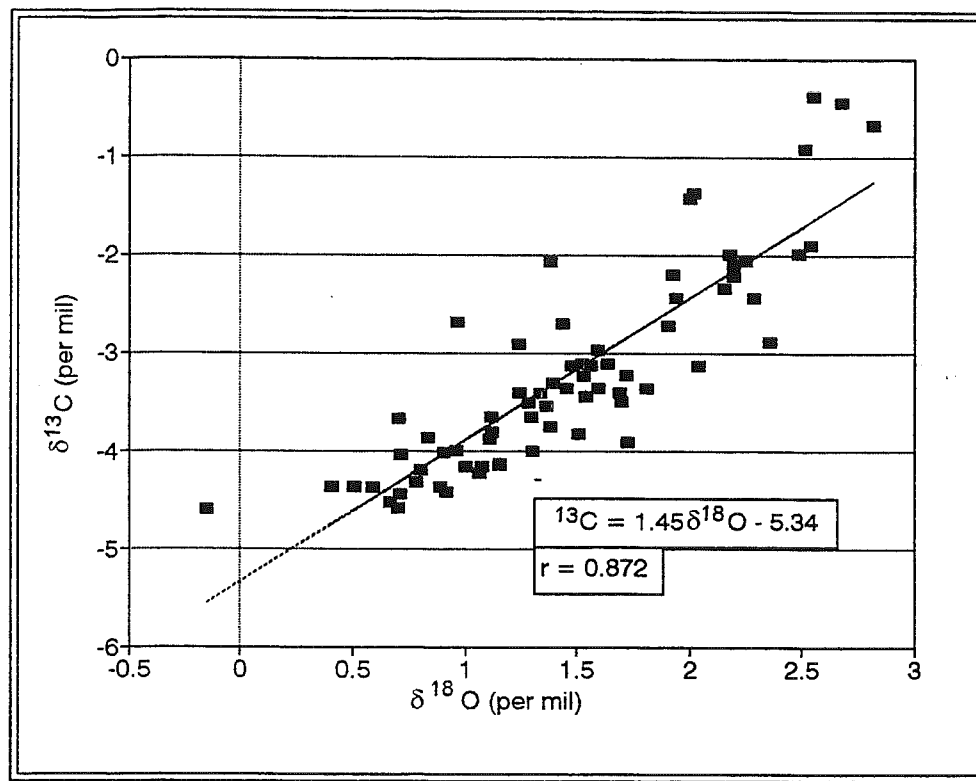


Figure 3.3-2: Correlation of carbon and oxygen isotopic composition.

The tendency of skeletal $\delta^{13}\text{C}$ and $\delta^{18}\text{O}$ to be strongly correlated in ahermatypic corals was first noted by Keith and Weber (1965). Weber (1973) reaffirmed this relationship and demonstrated that different genera of deep-sea corals had varying fields of distribution of carbon- and oxygen-isotopic ratios (Figure 3.3-3)

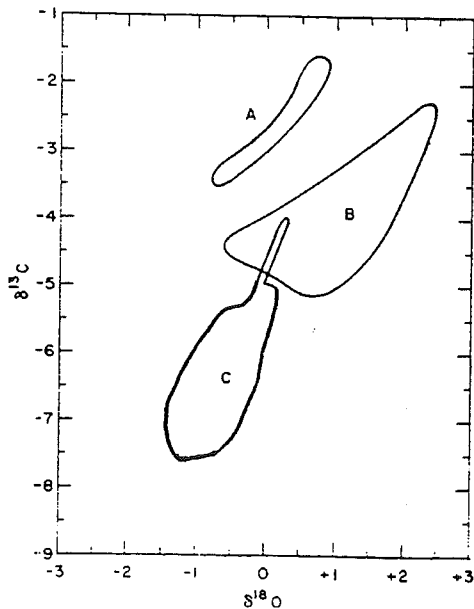


Figure 3.3-3: Distribution of $\delta^{13}\text{C}$ and $\delta^{18}\text{O}$ in ahermatypic scleractinian corals. A. *Caryophyllia* B. *Solenosmilia* C. *Lophelia* (from Weber, 1973).

The details of this correlation are still being investigated. McConnaughey (1989a) identified two types of equilibrium isotope partitioning when CaCO_3 is precipitated from solution. The isotope pattern exhibited by *D. cristigalli* in this study is likely the result of a 'kinetic' isotopic effect - it occurs because the different reaction kinetics of molecules containing ^{18}O and ^{13}C cause the heavy isotopes to be discriminated against during the hydration and hydroxylation of CO_2 . Hermatypic corals do not typically display a linear correlation of heavy isotopes: their isotopic patterns can be accounted for by the superposition of 'metabolic' and kinetic effects. Metabolic isotopic effects involve changes of isotope composition in the neighbourhood of precipitating carbonate, caused primarily by photosynthesis and respiration (Figure 3.3-4).

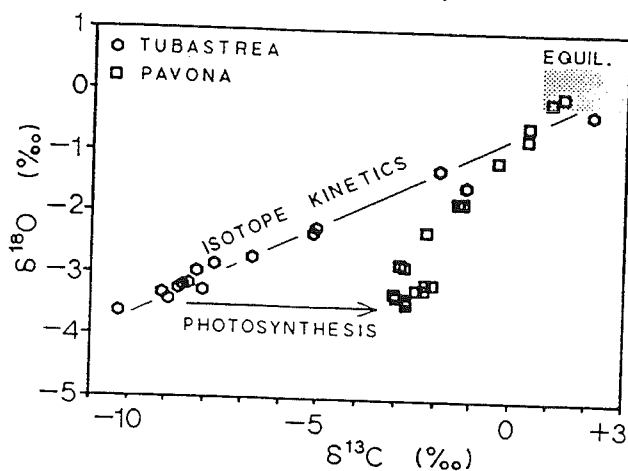


Figure 3.3-4: Oxygen- and carbon-isotopic disequilibria in two corals. Non-photosynthetic *Tubastrea* illustrates kinetic isotopic disequilibrium behaviour, while the photosynthetic *Pavona* shows additional metabolic behaviour (from McConnaughey, 1989b).

Some of the fluctuations in $\delta^{13}\text{C}$ may reflect changes in the ultimate source of skeletal building material: azooxanthellate corals derive carbon for skeletogenesis from both seawater bicarbonate and metabolically-produced carbon dioxide (from food and respiration). The $\delta^{13}\text{C}$ in biogenic carbonate can change as the proportions of carbon from various sources change, because terrestrial-produced nutrients are significantly depleted in the heavier isotopes compared with marine sources (Figure 3.3-5).

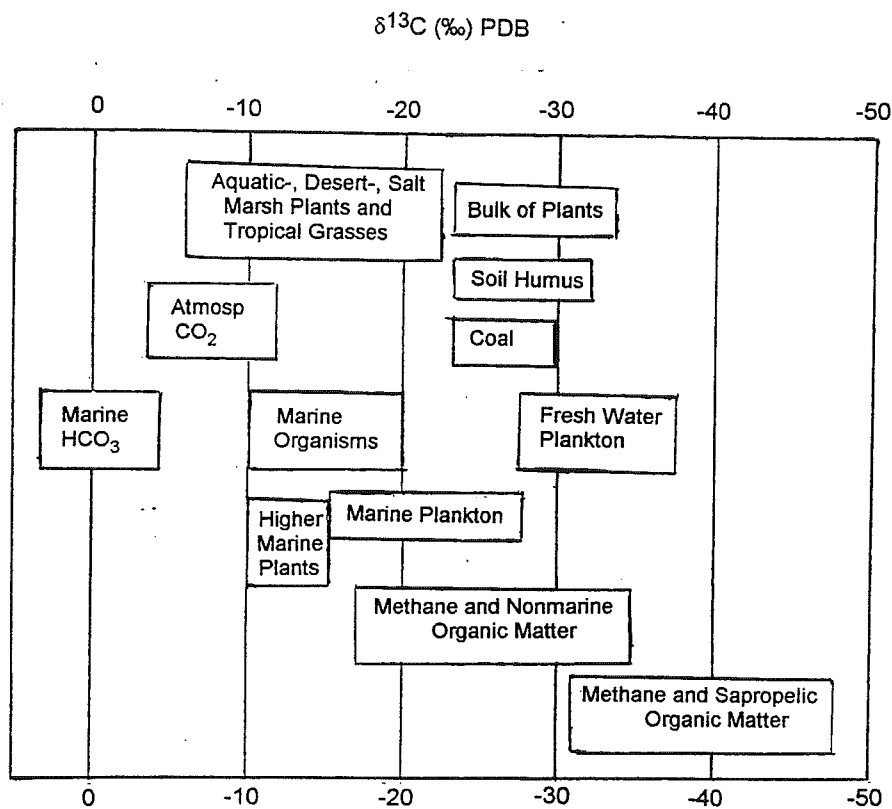


Figure 3.3-5: Major carbon components and their $\delta^{13}\text{C}$ ranges (modified from (Anderson and Arthur, 1983).

The high degree of correlation between $\delta^{13}\text{C}$ and $\delta^{18}\text{O}$, however, suggests that most of the fluctuations observed in the ^{13}C ratios occurred as a result of kinetic isotopic effects, due to a functional linkage of the heavy isotopes.

3.4 Comparison to the Foraminiferal Record

The Younger Dryas climatic event was 'discovered' by European palynologists studying the continental climatic record - the name of the chronozone was derived from the remains of arctic flower *Dryas octopetala*, found in periglacial deposits near Alleröd, Denmark. The interpretation of vegetation changes is not obvious, however, as pollution by modern or 'dead' carbon has to be qualitatively evaluated for each sample. Additionally, the non-instantaneous response of plants to climate change, coupled with the low speed of floral propagation introduces time-lags and reduces the validity of continental chronologies.

To avoid these problems, most climatic reconstructions have been based on the isotopic analysis of planktonic Foraminifera. Surface water conditions vary within and between glacial cycles, significantly influencing the oxygen-isotope ratios of foram tests: most North Atlantic deep-sea cores show an unmistakable response of planktonic forams to the Younger Dryas cold spell. A typical example is Figure 3.4-1, which shows the ^{14}C -dated isotope record of *Globigerina bulloides* from a core extracted offshore of Portugal.

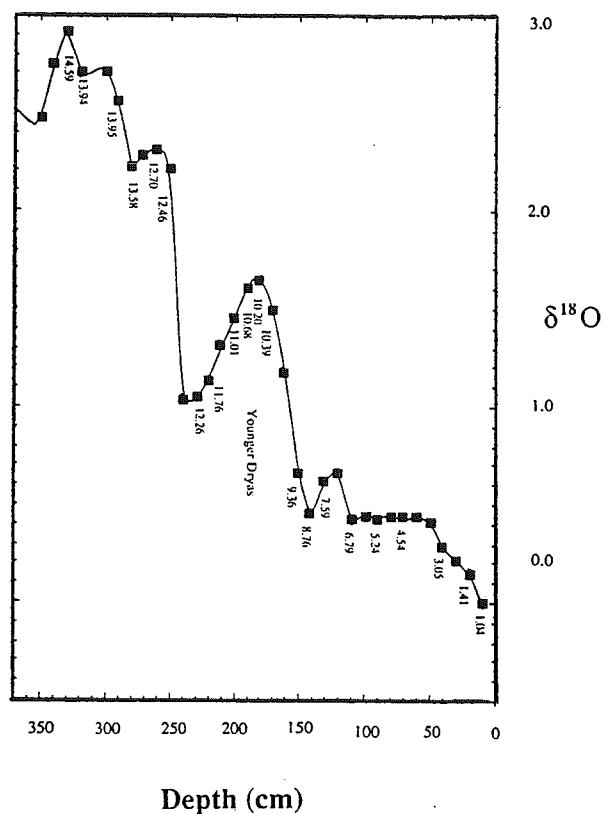


Figure 3.4-1: Planktonic foram oxygen-isotope record (from Fairbanks, 1989).

The shape of this plot mirrors that of the coral $\delta^{18}\text{O}$ results: values steadily decline during initial deglaciation (implying warmer, fresher water) and increase abruptly near the lower boundary of the Younger Dryas. Ratios fall suddenly at the end of the glacial episode, and then gradually decline toward modern values.

The results of the two studies contrast, however, in the timing of the Younger Dryas and the magnitude of oceanic response to the event. The coral samples document that the Younger Dryas was fully established within two hundred years, whereas the foram response seems to indicate that the transition from interglacial to glacial conditions required a period of time an order of magnitude larger. As mentioned earlier, deep-sea cores are vulnerable to bioturbation, one effect of which is to reduce

the amplitude of plotted curves (Figure 1.5-2). As coral skeletons are unlikely to have been subjected to this 'smoothing', the timing of events, as chronicled by the corals, is probably more realistic than the bioturbated foram record.

The $\delta^{18}\text{O}$ variations exhibited by the corals have been interpreted as primarily representing changes in ocean salinity, since bottom temperatures change little from one glacial episode to the next. Planktonic forams inhabit surface waters which experience large fluctuations in both temperature and salinity, hence the relative contribution of each variable on the isotopic composition of tests is virtually impossible to assess. Nevertheless, the oxygen-isotope records for the corals clearly demonstrate an increase of ca. 2‰ during the transition from interglacial to glacial conditions; the change of isotopic composition of foram tests is less than 1 per mil. Since plots of bioturbated cores often suffer from curve gradient reduction, it is likely that the timing of the Younger Dryas onset, as suggested by coral analyses, are more accurate than chronicles based on planktonic-Foraminiferal studies.

To date, both the magnitude and timing of oceanic response to the Younger Dryas may have been significantly underestimated: with their immunity to the confounding effects of bioturbation, corals may more accurately record the degree of salinity change in the North Atlantic during the Younger Dryas and possibly allow more precise timing of this event.

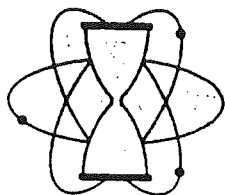
4 Conclusions

1. The hypothesis of this study, i.e., that stable-isotope analyses of deep-water corals of different ages could be used as tools for paleoclimatic reconstructions, has been validated. Deep-water corals appear to be sensitive, accurate recorders of benthic conditions, shown especially by the capturing of the Younger Dryas climatic episode.
2. Combined ^{14}C and U/Th dating of two coral specimens have supported Bard et al.'s (1990) contention that in biogenic carbonate samples older than 9,000 y BP, ^{14}C dates are systematically younger than the corresponding U/Th ages. The magnitude of this disparity (ca. 2,000 to 2,500 years) coincides with the predicted value for samples of this general antiquity.
3. The abrupt increase in ocean salinity shown by the $\delta^{18}\text{O}$ record suggests that the Gulf Stream conveyor was not operating during the time of the Younger Dryas event. This implication supports the hypothesis that ocean-atmosphere reorganizations trigger glacial cycles.
4. The carbon- and oxygen-isotope data give a good indication of the rapidity of the Younger Dryas onset. Assuming an approximately constant coral-growth rate, the shift from interglacial to glacial conditions occurred entirely within 150 years and possibly in less than 30 years.
5. During the Younger Dryas episode, $\delta^{18}\text{O}$ increased by about 2 per mil. In contrast, both the benthic and planktonic foraminiferal records show typical increases of less than 1 per mil. Since common effects of bioturbation in deep-sea cores include

amplitude and gradient reduction of paleoclimatic records, the magnitude of isotopic change reflected in the coral data is more likely to be correct.

6. There is a linear correlation between skeletal $\delta^{13}\text{C}$ and $\delta^{18}\text{O}$, indicating that any isotopic disequilibria between *D. cristigalli* and the ambient seawater are due to 'kinetic' effects - the discrimination against the heavy isotopes of carbon and oxygen during the hydration and hydroxylation of CO_2 . This is in contrast to 'metabolic' effects shown by hermatypic corals, whereby carbon and oxygen isotopes are decoupled as a result of photosynthesis and respiration.

Appendix 1:
Results of Previous Work



KRUEGER ENTERPRISES, INC.

GEOCHRON LABORATORIES DIVISION

24 BLACKSTONE STREET • CAMBRIDGE, MASSACHUSETTS 02139 • (617) 876-3691

RADIOCARBON AGE DETERMINATION

REPORT OF ANALYTICAL WORK

Our Sample No. GX-15548

Date Received: 01/18/90

Your Reference: SPO #BS0023032

Date Reported: 03/03/90

Submitted by: John T. Andrews & Susan Short
INSTAAR, Box 450
University of Colorado
Boulder, CO 80309-0450

Sample Name: Bucket 1182.
Coral.

AGE = 29,270 +/- 960 C-14 years BP (C-13 corrected).

Description: Sample of coral.

Pretreatment: The coral was cleaned thoroughly in an ultrasonic cleaner. It was then leached thoroughly with dilute HCl to remove additional surficial material which may have been altered, and to be sure only fresh carbonate material was used. The cleaned coral was then hydrolyzed with HCl, under vacuum, and the carbon dioxide was recovered for analysis.

Comment: Age is significant at the 2 standard deviation level.

$\delta^{13}\text{C}_{\text{PDB}} = -2.9\text{‰}$

Notes: This date is based upon the Libby half life (5570 years) for ^{14}C . The error stated is $\pm 1\sigma$ as judged by the analytical data alone. Our modern standard is 95% of the activity of N.B.S. Oxalic Acid. The age is referenced to the year A.D. 1950.



United States Department of the Interior

GEOLOGICAL SURVEY
BOX 25046 M.S. _____
DENVER FEDERAL CENTER
DENVER, COLORADO 80225



IN REPLY REFER TO:

To: Giff Miller

26 April 1991

From: Dan Muhs

Subject: Final results of U-series analysis of Canadian coral sample 78020-001. Bucket #112
(*Desmophyllum cristagalli*)

U (ppm) = 4.35 ± 0.05

$^{234}\text{U}/^{238}\text{U} = 1.14 \pm 0.01$

$^{230}\text{Th}/^{232}\text{Th} = 40 \pm 5$

$^{230}\text{Th}/^{234}\text{U} = 0.118 \pm 0.003$

Age = 13.6 ± 0.3 ka

Interpretation: the U concentration is somewhat higher than what is typical for tropical colonial corals, but is similar to what we find for solitary corals from the west coast and what other workers have found for solitary corals from Japan and Australia. The $^{234}\text{U}/^{238}\text{U}$ value is analytically indistinguishable from modern sea water values, and this is consistent with the 13.6 ka age. The $^{230}\text{Th}/^{232}\text{Th}$ value is high, indicating no "inherited" ^{230}Th . Collectively, these data indicate that the age is probably reasonable. We X-rayed this sample and although I don't have the diffractogram in front of me, I do remember that it was somewhere between 95 and 100% aragonite, which is satisfactory.

Center for Geochronological Research

INSTAAR, University of Colorado
Boulder, Colorado 80309-0450
Telephone: 303- 492-6962
Fax: 303-492-6388

AMINO ACID GEOCHRONOLOGY LABORATORY REPORT OF RESULTS

January 14, 1992

Sample 78020-001, Bucket 112
Coral from Orphan Knoll, Canada
Submitted by Alan Ruffman, Geomarine Associates

Lab-ID	D/L ^a	Age	Possible Age Range ^b
AAL-6538	0.085 ± 0.011	Late Pleistocene	30-90 ka

^a D/L is the mean and standard deviation of D-alloisoleucine to L-isoleucine measured in the acid hydrolysate fraction of five separate preparations, two analyses of each preparation. The analyses were performed on a high-pressure ion-exchange liquid chromatographer with a fluorescence detection system. The samples were cleaned prior to analysis by mechanical grinding of the outer layer, then dissolution of 1/3 by weight in 2N HCl. Hydrolysis was performed in 6N HCl under N₂ at 110°C for 22 hours.

^b The amino acid data place the age of this sample within the late Pleistocene (10-125 ka). The age range can be narrowed provided the following assumptions are correct: (1) The effective diagenetic temperature of the sample was 1.5°C, or 2° lower than the present mean annual water temperature. (2) The rate of epimerization in the coral *Desmophyllum Cristagalli* is equivalent to the rate in the mollusc *Mya truncata*. (3) The uncertainty in the age estimate is approximately 50%. Any violation of any one of these assumptions seriously alters the estimated age range. And, any report of this possible age estimate must be accompanied both by an explicate statement of the assumptions and by an appraisal how violations of these assumptions will alter the estimated age range.

Center for Geochronological Research

INSTAAR, University of Colorado

Boulder, Colorado 80309-0450

Telephone: 303- 492-6962

Fax: 303-492-6388

REPORT OF RESULTS: STABLE ISOTOPE ANALYSIS

May 7, 1992

Sample 78020-001, Bucket 112

Coral (*Desmophyllum cristagalli*) from Orphan Knoll, Canada

Submitted by Alan Ruffman, Geomarine Associates

Lab-ID	$\delta^{13}\text{C}$ (‰)	$\delta^{18}\text{O}$ (‰)
AAL-6538	-5.32	2.16

Results reported to D.S. Kaufman by J.W. White on May 6, 1992

The sample was pretreated by removing the outer layer by mechanical grinding then acid leaching in 2 N HCl to remove an additional 33% by weight. A powdered subsample was dissolved in 100% phosphoric acid at 80°C to evolve CO₂. Isotopic analyses were performed at the INSTAAR stable-isotope laboratory on a VG mass spectrometer. The analytical uncertainty based on replicate measurements of a carbonate standard is no greater than 0.1‰. Results are reported relative to PDB.

Center for Geochronological Research

INSTAAR, University of Colorado

Boulder, Colorado 80309-0450

Telephone: 303- 492-6962

Fax: 303-492-6388

REPORT OF RESULTS: ACCELERATOR RADIOCARBON DATE**NSF-ARIZONA AMS FACILITY****PAS Building 81****University of Arizona****Tucson, AZ 85721****April 9, 1992****Sample 78020-001, Bucket 112 (AAL-6538)****Coral (*Desmophyllum cristagalli*) from Orphan Knoll, Canada****Submitted by Alan Ruffman, Geomarine Associates**

Lab-ID	Fraction modern	Age (yr BP)
AA-8724	0.2381 ± 0.0032	$11,525 \pm 105$

Results reported to D.S. Kaufman by A.J.T. Jull on April 1, 1992

The sample was pretreated by removing the outer layer by mechanical grinding then acid leaching in 2 N HCl to remove an additional 33% by weight. The final weight of the sample submitted to the laboratory was 36.2 mg.

The date is based upon the Libby half life of 5570 yr for ^{14}C and corrected to a base of $\delta^{13}\text{C} = -25\text{‰}$. The error is $\pm 1\sigma$ based on the analytical data. The age is referenced to year A.D. 1950 and has not been adjusted for marine reservoir effects.

JUN-24-1991 09:14 FROM U OF T PHYSICS

TO S19024264104 P.02

IsoTrace Radiocarbon Laboratory

Accelerator Mass Spectrometry Facility
 at the University of Toronto

60 St. George Street
 Toronto (Ont) Canada M5S 1A7

Telephone: 416-978-4628
 Fax: 416-978-5848
 Email: isoTrace@utorphys.bitnet

Radiocarbon Analysis Report

June 20, 1991

Submitter: P.J.Mudie, Atlantic Geoscience Centre, Dartmouth NS

The results for samples TO-2392 and TO-2394 are the average of 4 machine-ready targets (high precision) while the result for sample TO-2393 is the average of 2 machine-ready targets (normal precision). All results have been corrected for natural and sputtering fractionation to a base of $\delta^{13}\text{C} = -25\%$. The sample ages are quoted as uncalibrated conventional radiocarbon dates in years before present (BP), using the Libby ^{14}C meanlife of 8033 years. The errors represent 68.3% confidence limits. Before hydrolysis the outer 20-30% of the samples was removed by HCl leaching to ensure that clean, unaltered carbonate material was used.

A reservoir correction of 410 years is equivalent to a fractionation correction to a base of $\delta^{13}\text{C} = 0\%$.

Sample Identification	Description	Weight used (mg)	IsoTrace Lab number	Age (years BP)	Age corrected for a 410 yr reservoir effect (years BP)
78020-001-A	coral, septal tooth	260	TO-2392	11,540 \pm 80	11,130 \pm 80
78020-001-B	coral, 3 calyces	94	TO-2393	460 \pm 70	50 \pm 70
78020-001-C	coral, base of colony	300	TO-2394	12,780 \pm 90	12,370 \pm 90

I would like to hear your comments on these results. If these results are used in a publication, I would appreciate it if you could send me a reprint.



Dr. R. P. Beukens

Appendix 2:
Results of This Study

Coral	B.I.O. Reference	U/Th date Yr BP
1 - Top	Hu78-020- 118-7	13822 ± 49
1 - Bottom	Hu78-020- 118-7	No U collected
20	Hu78-020- 118-8	no Th collected
12	Hu78-020- 112-4	14157 ± 62
35	Hu78-020- 112-1	76628 +422 -417
34	Hu78-020- 112-1	16195 ± 114
10	Hu78-020- 112-3	no Th collected
14	Hu78-020- 112-5	14095 ± 104
25	Hu78-020- 112-1	23191 +149 -148
17	Hu78-020- 112-5	17319 +462 -457
46	Hu78-020- 112-5	13816 ± 51

Coral	B.I.O. Reference	U/Th date Yr BP
21	Hu78-020- 118-8	51635 +1014-995
23	Hu78-020- 118-8	14143 ± 43
27	Hu78-020- 112-1	4093 ± 22
2	Hu78-020- 118-9	25434 +126 -125

Coral 1

Sample	$\delta^{13}\text{C}$	$\delta^{18}\text{O}$
A9	-0.924	2.711
A10	-2.098	2.194
A11	-2.056	2.247
A12	-1.983	2.484
B1	-2.339	2.153
B2	-3.127	2.038
B3	-2.687	0.965
B4	-4.434	0.710
B5	-3.508	1.282
B6	-2.889	2.358
B7	-1.897	2.536
B8	-3.363	1.596
B9	-3.366	1.809
B10	-3.232	1.532
B11	-2.209	1.926
B12	-1.424	2.001
C1	-1.991	2.174
C2	-0.680	2.816
C3	-3.230	1.720
C4 cf	-3.500	1.700
C5	-3.829	1.509
C6	-2.914	1.240
C7	-3.107	1.637
C8	-3.405	1.689
C9	-2.440	2.287
C11	-2.220	2.193

cf = cold finger

Coral 1
cont.

Sample	$\delta^{13}\text{C}$	$\delta^{18}\text{O}$
C12	-2.725	1.903
D1	-2.438	1.935
D2	-2.973	1.592
D3	-4.144	1.154
D4	-3.801	1.121
D5	-4.517	0.664
D6	-3.363	1.454
D7 cf	-4.000	1.300
D8	-4.130	1.154
D9	-3.756	1.379
D10	-3.443	1.539
D11	-3.135	1.560
D12	-3.312	1.395
E2	-3.418	1.337
E3	-3.661	1.298
E4	-3.874	1.111
E6	-3.111	1.520
E7	-3.132	1.476
E8	-3.543	1.361
E9	-3.407	1.242
E10	-4.159	1.076
E11	-4.363	0.891
E12	-4.581	0.701
F1	-4.418	0.916
F2	-4.199	0.800
F3	-4.318	0.779
F4	-4.159	1.002

cf = cold finger

Coral 1
cont.

Sample	$\delta^{13}\text{C}$	$\delta^{18}\text{O}$
F6	-3.654	1.117
F7	-4.372	0.590
F8	-4.035	0.715
F9	-4.367	0.506
G1	-4.020	0.904
G2	-4.594	-0.148
G3	-4.362	0.408
G4	-4.231	1.062
G5	-3.914	1.725
G6	-3.867	0.832
G7	-3.671	0.703
G8	-2.700	1.439
G9	-2.067	1.382
G10	-1.371	2.017
G11	-0.451	2.677
G12	-0.384	2.552

Average	-3.125	1.425
STD	1.144	0.655

Coral 20

Sample	$\delta^{13}\text{C}$	$\delta^{18}\text{O}$
J1	-3.369	1.173
J2	-3.337	1.045
J3	-3.153	1.246
J4	-2.710	1.307
J5	-3.398	1.106
J6	-2.608	1.528
J7	-3.330	1.209
J8	-2.715	1.377
Average	-3.078	1.249
STD	0.318	0.144

Coral 12

Sample	$\delta^{13}\text{C}$	$\delta^{18}\text{O}$
J9	-3.254	1.553
J10	-3.101	1.697
J11	-2.865	1.540
J12	-2.227	1.904
Average	-2.862	1.674
STD	0.392	0.147

Coral 35

Sample	$\delta^{13}\text{C}$	$\delta^{18}\text{O}$
M1	-3.278	2.071
M2	-2.567	2.271
M3	-1.888	2.687
M4	-2.984	1.668
M5	-2.274	2.505
M6 cf	-0.673	2.513

cf = cold finger

Average	-2.598	2.240
STD	0.494	0.354

Coral 34

Sample	$\delta^{13}\text{C}$	$\delta^{18}\text{O}$
L7	-3.655	1.579
L8	-3.264	1.792
L9	-3.904	1.527
L10	-2.019	2.324
L12	-1.836	2.598

Average	-2.936	1.964
STD	0.850	0.424

Coral P

Sample	$\delta^{13}\text{C}$	$\delta^{18}\text{O}$
P1	-3.094	2.462
P2	-3.160	2.138
P3	-3.105	2.310
P4	-4.549	1.795

Average	-3.477	2.176
STD	0.619	0.248

Coral 10

Sample	$\delta^{13}\text{C}$	$\delta^{18}\text{O}$
H3	-3.787	1.569
H4	-3.084	1.916
H5	-2.792	2.051
H6	-3.594	1.340
H7	-3.580	1.316
H8	-3.966	0.920
H9	-3.561	1.384
H10	-3.354	1.387
H11	-3.505	1.109
H12	-3.736	0.982
I1	-3.430	1.501
I2	-3.557	1.749
I3	-3.281	1.368
I4	-2.993	1.831
I5	-2.838	1.859
I6	-2.834	1.817
I7	-2.926	1.878
I8	-2.920	1.814
I9	-2.527	2.076
I10	-1.068	2.472
I11	-2.381	1.828
I12	-2.857	1.807

Average	-2.981	1.564
STD	0.873	0.494

Coral 14

Sample	$\delta^{13}\text{C}$	$\delta^{18}\text{O}$
K1	1.298	3.550
K2	2.011	3.757
K3	1.745	3.709
K4	0.642	3.342
K5	1.909	3.816
K6	1.562	3.709
K7	0.934	3.352
K8	1.243	3.160
Average	1.418	3.549
STD	0.447	0.223

Coral 25

Sample	$\delta^{13}\text{C}$	$\delta^{18}\text{O}$
K9	-2.037	2.455
K10	-2.027	2.704
K11	-0.439	2.885
K12	-0.588	2.899
Average	-1.273	2.736
STD	0.761	0.179

Coral 17

Sample	$\delta^{13}\text{C}$	$\delta^{18}\text{O}$
L1	-0.113	3.271
L2	-0.178	3.193
L3	0.069	3.011
L4	0.729	3.482
L5	-0.107	3.055
L6	-1.328	2.393
Average	-0.155	3.068
STD	0.607	0.338

Coral 46

Sample	$\delta^{13}\text{C}$	$\delta^{18}\text{O}$
O1	-2.799	0.986
O2	-3.356	1.304
O3	-3.124	2.234
O4	-5.059	1.302
O5	-3.716	1.901
O6	-5.603	1.249
Average	-3.943	1.496
STD	1.031	0.429

Coral 21

Sample	$\delta^{13}\text{C}$	$\delta^{18}\text{O}$
O7	-4.248	1.403
O8	-4.026	1.685
O9	-2.803	2.365
O10	-2.484	2.209
O11	-2.381	2.169
O12	-2.592	2.339
Average	-3.089	2.028
STD	0.755	0.359

Coral 23

Sample	$\delta^{13}\text{C}$	$\delta^{18}\text{O}$
N7 cf	-1.381	-2.579
N8	-1.781	2.606
N9	-2.611	1.515
N10	-3.573	1.946
N11	-3.693	1.786
N12	-4.906	1.524
Average	-3.313	1.875
STD	1.057	0.400

cf = cold finger

Coral 27

Sample	$\delta^{13}\text{C}$	$\delta^{18}\text{O}$
N1	-4.086	0.477
N2	-4.447	0.708
N3	-5.065	0.879
N4	-5.281	0.388
N5	-5.545	0.292
N6	-5.312	0.809
Average	-4.956	0.592
STD	0.518	0.219

Coral 2

Sample	$\delta^{13}\text{C}$	$\delta^{18}\text{O}$
M7	-5.226	0.885
M8	-5.109	0.627
M9	-5.245	0.870
M10	-5.208	0.983
M11	-4.521	1.359
M12	-4.438	1.640
Average	-4.958	1.061
STD	0.342	0.338

References

- Aharon, P. (1991) Recorders of reef environment histories: Stable isotopes in corals, giant clams and calcareous algae. Coral Reefs 10: 71 - 90.
- Anderson, T.F. and Arthur, M.A. (1983) Stable isotopes of oxygen and carbon and their application to sedimentologic and paleoenvironmental problems. In: Arthur, M.A., ed. Stable Isotopes in Sedimentary Geology. SEPM Short Course No. 10, Dallas: 1 - 151.
- Bard, E., Arnold, M., Duprat, J., Moyes, J. and Duplessy, J.C. (1987) Bioturbation effects on abrupt climatic changes recorded in deep-sea sediments. Correlation between $\delta^{18}\text{O}$ profiles and accelerator ^{14}C dating. In: Berger, W.H. and Labeyrie, L.D. eds. Abrupt Climatic Change. D. Reidel Publishing Company: 263 - 278.
- Bard, E., Hamelin, B., Fairbanks, R.G., and Zindler, A. (1990) Calibration of the ^{14}C timescale over the past 30,000 years using mass spectrometric U - Th ages from Barbados corals. Nature 345: 405 - 410.
- Benton, M.J. (1986) More than one event in the late Triassic mass extinction. Nature 321: 857 - 861.
- Boyle, E.A., and Keigwin, L. (1987) North Atlantic thermohaline circulation during the past 20,000 years linked to high-latitude surface temperature. Nature 330: 35 - 40.
- Broecker, W.S. (1966) Absolute dating and the astronomical theory of glaciation. Science 151: 299 - 304.
- Broecker, W.S. (1974) Chemical Oceanography. Harcourt Brace Jovanovich, Inc., New York: 214 pp.
- Broecker, W.S. (1982) Glacial to interglacial changes in ocean chemistry. Progress in Oceanography 11: 151 - 197.
- Broecker, W.S. (1992) The strength of the Nordic heat pump. In: Bard, E. and Broecker, W.S., eds. The Last Deglaciation: Absolute and Radiocarbon Chronologies. NATO ASI Series, Vo. 12. Springer-Verlag, Berlin: 173 - 181.
- Broecker, W.S., Thurber, D.L., Goddard, J., Ku, T.H., Matthews, R.K. and Mesolella, K.J. (1968) Milankovitch hypothesis supported by precise dating of coral reefs and deep-sea sediments. Science 159: 297 - 300.
- Broecker, W.S., Andree, M., Wolfli, W., Oeschger, H., Bonani, G., Kennett, J. and Peteet, D. (1988) The chronology of the last deglaciation: Implications to the cause of the Younger Dryas event. Paleoceanography 3: 1 - 19.

- Broecker, W.S. and Denton, G.H. (1989a) The role of ocean-atmosphere reorganizations in glacial cycles. Geochimica et Cosmochimica Acta 50: 2465 - 2501.
- Broecker, W.S., Kennett, J.P., Flower, B.P., Teller, J.T., Trumbore, S., Bonani, G. and Wolfli, W. (1989b) Routing of meltwater from the Laurentide Ice Sheet during the Younger Dryas cold episode. Nature 341: 318 - 321.
- Buddemeier, R.W., Maragos, J.E. and Knutson, D.W. (1974) Radiographic studies of reef coral exoskeletons: Rates and patterns of coral growth. Journal of Experimental Marine Biology and Ecology 14: 179 - 200.
- Caims, S.D. (1982) Antarctic and Subantarctic Scleractinia. Antarctic Research Series 34: 1 - 74.
- Carriquiry, J.D., Risk, M.J., and Schwarcz, H.P. (1988) Timing and temperature record from stable isotopes of the 1982 - 1983 El Niño warming event in eastern Pacific corals. Paleos 3: 359 - 364.
- Cowen, R. (1983) Algal symbiosis and its recognition in the fossil record. In: Tevesz, M.J.S. and McCall, P.L., eds. Biotic Interactions in Recent and Fossil Benthic Communities. Plenum Press, New York: 431 - 478.
- Dawson, A.G. (1992) Ice Age Earth. Routledge Publishers, London: 293 pp.
- Denton, G.H. (1974) Quaternary glaciations of the White River Valley, Alaska, with a regional synthesis for the Northern St. Elias Mountains, Alaska and Yukon Territory. Geological Society of America Bulletin 85: 871 - 892.
- Duplessy, J.C., Moyes, J. and Pujol, C. (1980) Deep water formation in the North Atlantic Ocean during the last ice age. Nature 286: 479 - 482.
- Duplessy, J.C., Shackleton, N.J., Fairbanks, R.G., Labeyrie, L., Oppo, D. and Kallel, N. (1988) Deepwater source variations during the last climatic cycle and their impact on the global deepwater circulation. Paleoceanography 3: 343 - 360.
- Fairbanks, R.G. (1989) A 17,000-year glacio-eustatic sea level record: Influence of glacial melting rate on the Younger Dryas event and deep-ocean circulation. Nature 342: 637 - 642.
- Fairbanks, R.G. and Matthews, R.K. (1978) The marine oxygen isotope record in Pleistocene coral, Barbados, West Indies. Quaternary Research 10: 181 - 196.
- Fitzgerald, R.A., Winters, G.V. and Buckley, D.E. (1987) Evaluation of a Sequential Leach Procedure for the Determination of Metal Partitioning in Deep Sea Sediments. Geological Survey of Canada. Open File Report 1701: 21 pp.
- Friedman, G.M. (1959) Identification of carbonate materials by staining methods. Journal of Sedimentary Petrology 29: 87 - 97.

- Goreau, T.F. (1959) The physiology of skeleton formation in corals. 1. A method for measuring the rate of calcium deposition by corals. Biological Bulletin 117: 239 - 250.
- Hudson, J.H., Shinn, E.A., Halley, R.B. and Lidz, B. (1976) Sclerochronology: A tool for interpreting past environments. Geology 4: 361 - 364.
- Imbrie, J., Hays J.D., Martinson, D., Mix, A., Morley, J., Pisias, N., Prell, W. and Shackleton, N.J. (1984) The orbital theory of Pleistocene climate: Support from a revised chronology of the marine $\delta^{18}\text{O}$ record. In: Berger, A.L., Imbrie, J., Hays, J.I., Kunkin, G. and Saltzman, B. eds. Milankovitch and Climate, Part 1. D.Reidel, Hingham, Mass: 269 - 305.
- Isdale, P. (1984) Fluorescent bands in massive corals record centuries of coastal rainfall. Nature 310: 578 - 579.
- Keith, M.L. and Weber, J.N. (1965) Systematic relationships between carbon and oxygen isotopes in carbonates deposited by modern corals and algae. Science 150: 498 - 501.
- Knutson, D.W., Buddemeier, R.W. and Smith, S.V. (1972) Coral chronometers: Seasonal growth bands in reef corals. Science 177: 270 - 272.
- Laughton, A.S., Berggren, W.A., Benson, R.N., Davies, T.A., Franz, U., Musich, L.F., Perch-Nielsen, K., Ruffman, A.S., van Hinte, J.E., Whitmarsh, R.B., Nelson, H.W., Pocock, S.A.J., Hacquebard, P.A., Jeletzky, J.A., Bloxam, T.W., Kelling, G., James, N.P., Hopkins, J.C., Pessagno, Jr., E.A., Longoria, T.J.F., and Bukry, D. (1972) Site 111. In: Davies, T.A., ed. Part 1: Shipboard Reports: Initial Reports of the Deep Sea Drilling Project. Volume XII: 33 - 159.
- Manabe, S. and Stauffer, R.J. (1988) Two stable equilibria of a coupled ocean-coupled ocean-atmosphere model. Journal of Climatology 1: 841 - 866.
- Matsch, C.L. (1976) North America and the Great Ice Age. McGraw-Hill, Inc., New York: 131 pp.
- McConnaughey, T. (1989a) ^{13}C and ^{18}O isotopic disequilibrium in biological carbonates: 1. Patterns. Geochimica et Cosmochimica Acta 53: 151 - 162.
- McConnaughey, T. (1989b) ^{13}C and ^{18}O isotopic disequilibrium in biological carbonates: 2. *In vitro* simulation of kinetic isotope effects. Geochimica et Cosmochimica Acta 53: 163 - 171.
- McCrea, J.M. (1950) On the isotope chemistry of carbonates and a paleotemperature scale. Journal of Chemical Physics 18: 849 - 857.

- Mullins, H.T., Newton, C.R., Heath, K., and Van Buren, H.M. (1981) Modern deep-water coral mounds north of Little Bahama Bank: Criteria for recognition of deep-water bioherms in the rock record. Journal of Sedimentary Petrology 51: 999 - 1013.
- Nozaki, Y., Rye, D.M., Turekian, K.K. and Dodge, R.E. (1978) A 200 year record of carbon-13 and carbon-14 variations in a Bermuda coral. Geophysics Research Letters 5: 825 - 828.
- Oliver, Jr., W.A. and Coates, A.G. (1987) Phylum Cnidaria. In: Boardman, R.S., Cheetham, A.H. and Rowell, A.J. eds. Fossil Invertebrates. Blackwell Scientific Publications: 140 - 193.
- Parson, L.M., Masson, D.G., Rothwell, R.G. and Grant, A.C. (1984) Remnants of a submerged pre-Jurassic (Devonian?) landscape on Orphan Knoll, offshore eastern Canada. Canadian Journal of Earth Sciences 21: 61 - 66.
- Porter, S.C. (1981) Pleistocene glaciation the southern Lake District of Chile. Quaternary Research 16: 263 - 321.
- Reed, J.K. and Jones, R.S. (1982) Deep water coral. Oceans 15: 38 - 41.
- Rooth, C. (1982) Hydrology and ocean circulation. Progress in Oceanography VII: 131 - 149.
- Ruddiman, W.F. and McIntyre, A. (1981) The North Atlantic Ocean during the last deglaciation. Paleogeography, Paleoclimatology, Paleoecology 35: 145 - 214.
- Ruddiman, W.F., Cline, R.M.L., Hays, J.D., Prell, W.L., Moore, T.C., Kipp, N.G., Molfino, B.E., Denton, G.H., Hughes, T.J., Balsam, W.L., Brunner, C.A., Duplessy, J.C., Esmay, A.G., Fastook, J.L., Imbrie, J., Keigwin, L.D., Kellogg, T.B., McIntyre, A., Matthews, R.K., Mix, A.C., Morley, J.J., Shackleton, N.J., Streeter, S.S., Thompson, P.R. (CLIMAP) (1984) The last interglacial ocean. Quaternary Research 21: 123 - 224.
- Ruffman, A. and van Hinte, J.E. (1989) Devonian Shelf-depth Limestone Dredged from Orphan Knoll: A 1971 Discovery and a Reassessment of the HUDSON 78-020 Dredge Hauls from Orphan Knoll. Canada Department of Energy, Mines and Resources, Geological Survey of Canada, Atlantic Geoscience Centre, Open File No. 2065: 119 pp.
- Rye, D.M. and Sommer, M.A. (1980) Reconstruction of paleotemperature and paleosalinity regimes with oxygen isotopes. In: Rhodes, D.C. and Lutz, R.H., eds. Skeletal Growth of Aquatic Organisms. Plenum Press, New York: 169 - 202.
- Schnitker, D. (1979) The deep waters of the western North Atlantic during the past 24,000 years, and the reinitiation of the Western Boundary Undercurrent. Marine Micropaleontology 4: 265 - 280.

- Schwarcz, H.P. and Blackwell, B. (1985) Uranium series disequilibrium dating. In: Rutter, N.W., ed. Dating Methods of Pleistocene Deposits and Their Problems. Geological Association of Canada: 9 - 17.
- Shackleton, N.J. (1987) Oxygen isotopes, ice volume and sea level. Quaternary Science Reviews 6: 183 - 190.
- Squires, D.F. (1964) Fossil coral thickets in Wairarapa, New Zealand. Journal of Paleontology 38: 904 - 915.
- Stanley, Jr., G.D. (1981) Early history of scleractinian corals and its geological consequences. Geology 9: 507 - 518.
- Stanley, Jr., G.D. and Cairns, S.D. (1988) Constructional azooxanthellate coral communities: An overview with implications for the fossil record. Palaios 3: 233 - 242.
- Weber, J.N. (1973) Deep-sea ahermatypic scleractinian corals: Isotopic composition of the skeleton. Deep-Sea Research 20: 901 - 909.
- Wells, J.W. (1956) Scleractinia. In: Moore, R.C., ed. Treatise on Invertebrate Paleontology. Part F, Coelenterata. University of Kansas Press, Lawrence, Kansas: F328 - F344.
- Wheeler, C.W. and Aharon, P. (1991) Mid-oceanic carbonate platforms as oceanic dipsticks: Examples from the Pacific. Coral Reefs 10: 101 - 114.

to 1.3°C (Duplessy et al., 1980). A change of $\pm 1^{\circ}\text{C}$ is reflected by only a 0.25‰ alteration in $\delta^{18}\text{O}$, so it seems apparent that most of the isotopic fluctuations displayed in Figure 3.3-1 are due to salinity changes.

Figure 3.2-1 shows that from at least 12.8 ky BP, the $\delta^{18}\text{O}$ of the coral skeletons steadily decreased: presumably this is a result of an ameliorating climate which warmed the oceanic waters and facilitated the gradual return of isotopically-light meltwater to the Atlantic basin. At the lower boundary of the Younger Dryas, however, the oxygen-isotope curve steepens abruptly in response to the sudden return to intense glacial conditions. The increase of skeletal $\delta^{18}\text{O}$ may be partially attributed to cooling water, but primarily reflects the increasing salinity of the seawater as a result of readvancing ice sheets. The large magnitude of the salinity change ($\sim 2\text{‰}$) supports Broecker's (1992) theory that the salt accumulation in the North Atlantic was exacerbated by the shutdown of the Gulf Stream Conveyor, with concurrent cessation of excess salt export. He contends that when the salinity of the Atlantic was high enough to overcome the effects of the fresh-water pooling on the ocean surface, the redirection of meltwater back to the Mississippi acted to push the system 'over the brink', triggered reinitiation of the conveyor and brought the Younger Dryas event to an abrupt end.

The bulk of the data points on Figure 3.2-1 were derived from the seventy samples taken from Coral 1 along a line of continuous growth. If one assumes an approximately constant coral-growth rate, the points are about 18 years apart, since the bottom of the coral was dated at 12,370 y BP, and the top at 11,130 y BP. Actual growth rate would have been ca. 0.2 mm/yr . This detailed chronology allows the rapidity of the onset of the Younger Dryas event to be assessed: the switch from interglacial to glacial conditions appears to have occurred within 150 years. In order to evaluate the validity of this growth rate assumption, a modern specimen from a similar environment was examined. Dr. Barbara Hecker of Lamont-Doherty Geological